OREGON STATE UNIVERSITY
TRIGA® REACTOR
LICENSE NO. R-106
DOCKET NO. 50-243

SAFETY ANALYSIS REPORT
FOR
THE CONVERSION OF THE
OREGON STATE UNIVERSITY
TRIGA® REACTOR
FROM HEU TO LEU FUEL

REDACTED VERSION

SECURITY-RELATED INFORMATION REMOVED

REDACTED TEXT AND FIGURES BLACKED OUT OR DENOTED BY BRACKETS

OSU
Oregon State
UNIVERSITY

Radiation Center
Oregon State University, 100 Radiation Center, Corvallis, Oregon 97331-5903
T 541-737-2341 | F 541-737-0480 | http://ne.oregonstate.edu/facilities/radiation_center

November 6, 2007

Mr. Alexander Adams
U. S. Nuclear Regulatory Commission
Research and Test Reactors Branch A
Office of Nuclear Reactor Regulation
Mail Stop O12-G13
One White Flint North
11545 Rockville Pike
Rockville, MD 20852-2738

Reference: Oregon State University TRIGA Reactor (OSTR)
Docket No. 50-243, License No. R-106

Subject: Safety Analysis Report for the Conversion of the OSTR from High Enriched Uranium (HEU) Fuel to Low Enriched Uranium (LEU) Fuel

Mr. Adams:

Enclosed with this letter you will find four copies of the Safety Analysis Report for the conversion of the OSTR from HEU fuel to LEU fuel. The format of the report follows the guidelines described in NUREG-1537, *Guidelines for Preparing and Reviewing Applications for the Licensing of Non-Power Reactors*, particularly chapter 18. License amendments needed for this conversion can be found in sections 14 and 15.2.

If you have any questions, please call me at the number above. I declare under penalty of perjury that the foregoing is true and correct.

Executed on: 11/6/07.

Sincerely,

Steve Reese
Director

Enclosure

cc: John Cassady, OSU
Rich Holdren, OSU
Todd Palmer, OSU (w/o enclosure)
Todd Keller, OSU (w/o enclosure)

A020

SAFETY ANALYSIS REPORT
FOR
THE CONVERSION OF THE OREGON STATE TRIGA® REACTOR
FROM HEU TO LEU FUEL

DOCKET NUMBER 50-243

FACILITY LICENSE NO. R-106

SUBMITTAL REPORT
Documentation of Analyses of Conversion
of the Oregon State University TRIGA® Reactor
from HEU to LEU Fuel

Submitted By:

Radiation Center
Oregon State University
Corvallis, Oregon

November 2007

TABLE OF CONTENTS

LIST OF TABLES

LIST OF FIGURES

1 GENERAL DESCRIPTION OF THE FACILITY

1.1 Introduction

This report contains the results of the design, safety and accident analyses performed by the Radiation Center for the conversion of the Oregon State University TRIGA® Reactor (OSTR) from the use of Highly Enriched Uranium (HEU) fuel to Low Enriched Uranium (LEU) fuel. This study investigates the performance and safety margins of the proposed LEU core under normal and accident conditions. The objectives of this study were to: 1) design an LEU core having operational capabilities similar to the original OSTR HEU FLIP core, and 2) demonstrate acceptable reactor performance and safety margins for the LEU core under normal and accident conditions.

The design and safety analyses in this report provide comparisons of reactor parameters and safety margins for the original OSTR HEU FLIP core and the proposed LEU 30/20 core. Neutronic and thermal-hydraulic behaviors of the LEU core are analyzed under normal and accident conditions. The only facility change required for conversion from HEU to LEU fuel is removal of the old HEU FLIP fuel and installation of TRIGA® LEU 30/20 fuel. In conjunction with conversion, all graphite reflector elements will be replaced with stainless steel clad graphite reflector elements and the annular reflector assembly may be replaced with a new annular reflector.

The proposed LEU core contains an initial loading of 88 fuel elements, including one Instrumented Fuel Element (IFE) and three fueled control rod followers. The LEU core is shown to maintain throughout its lifetime: 1) acceptable reactivity coefficients, 2) fuel integrity under all operating conditions, and 3) dose to the public from the Maximum Hypothetical Accident (MHA) well below applicable limits. With proper fuel inventory management, the LEU core also maintains acceptable shutdown margin and excess reactivity characteristics throughout core lifetime.

1.2 Summary and Conclusions of Principal Safety Considerations

The conclusion of this conversion proposal is that the new LEU core for the OSTR meets or exceeds all safety requirements as specified in this Conversion Analysis Safety Analysis Report (CA SAR). Discussion and analysis of all significant changes are located in the following sections. Differences in the reactor characteristics due to fuel conversion are described in Chapter 4, Reactor Description. The reload and startup plan for the new core is included in Chapter 12, Conduct of Operations. Differences in hypothetical accident characteristics and consequences are described in Chapter 13, Accident Analysis. Changes to the technical specifications are described in Chapter 14, Technical Specifications. Other topics covered by this CA SAR represent minor changes from the existing OSTR HEU Safety Analysis Report (HEU SAR).[1]

1.3 Summary of Reactor Facility Changes

The new LEU fuel assemblies are very similar to HEU FLIP elements with the exception of the composition of the fuel meat. Fuel element dimensions, upper and lower end fittings and clad are identical to FLIP fuel elements. LEU 30/20 fuel has been approved by the Nuclear Regulatory Commission (NRC) for use in non-power reactors.[2] A detailed description of the proposed LEU fuel is provided in Chapter 4, Reactor Description. A new annular reflector may be installed to replace the old reflector in order to increase neutron fluxes in the beam ports. Graphite reflector elements will also be replaced with stainless steel clad graphite reflector elements in an effort to reduce reflector element swelling over time.

1.4 Summary of Operating License, Technical Specifications, and Procedural Changes

The OSTR operating license will be amended to allow possession of the HEU and LEU core inventories during the conversion period. Guidelines governing the new core loading procedure and initial startup are provided in Chapter 12.6, Reactor Reload and Startup Plan.

Changes to the Technical Specifications are located in Chapter 14, Technical Specifications. Significant Technical Specification and license changes include:

- Changing all references to fuel or fuel type from HEU FLIP fuel to LEU 30/20 fuel in the Technical Specifications, and
- Changing the pulse limit from \$2.55 to \$2.15 in the Technical Specifications, and
- Updating the license to include the new fuel, possession only for the HEU FLIP fuel, and changing the pulse limit from \$2.55 to \$2.15.

1.5 Comparison with Similar Facilities Already Converted

The Texas A&M University 1 MW TRIGA® research reactor was successfully converted to LEU fuel. Like the OSTR, they converted from HEU FLIP fuel to LEU 30/20 fuel. However the TAMU reactor consists of fuel arranged in four-rod clusters, and therefore their neutronic and thermal-hydraulic characteristics differ from those of the OSTR. No other reactors utilizing a circular gridplate with HEU FLIP fuel have been previously converted.

2 SITE CHARACTERISTICS

The site characteristics of the OSTR are described in the OSTR HEU SAR. The conversion from HEU to LEU fuel does not impact the site characteristics.

3 DESIGN OF STRUCTURES, SYSTEMS AND COMPONENTS

The design of structures, systems and components of the OSTR is described in the OSTR HEU SAR. In conjunction with conversion, the annular reflector assembly may be replaced with a new annular reflector and all graphite reflector elements will be replaced with stainless steel clad graphite reflector elements. The conversion from HEU to LEU fuel does not impact the design of structures, systems or components.

4 REACTOR DESCRIPTION

4.1 Summary Description

The conversion of the OSTR from HEU to LEU only affects the design of the fuel elements themselves. No other design changes to the facility are necessary to accommodate the conversion. In conjunction with conversion, the annular reflector assembly will be replaced with a new annular reflector and all graphite reflector elements will be replaced with stainless steel clad graphite reflector elements.

4.2 Reactor Core

The conversion of the OSTR from HEU to LEU will necessitate removal of the HEU FLIP fuel and installation of the LEU 30/20 fuel. The core components present in the reference HEU FLIP core and the replacement LEU 30/20 core are detailed in Table 4-1.

Table 4-1 Core Components for HEU FLIP and LEU 30/20 Cores.

Core Configuration	HEU FLIP	LEU 30/20
Standard Fuel Elements	81	84
Instrumented Fuel Assemblies	1	1
Fuel-Followed Control Rod	3	3
Void-Followed Transient Rod	1	1
Aluminum Clad Reflector Elements	21	---
Stainless steel clad graphite reflector elements	---	34

As will be further discussed in Chapter 4.5, the original HEU FLIP core had a lifetime of ~ 3800 MWd, while the replacement LEU 30/20 core has a similar lifetime of ~3600 MWd. Hence, the conversion from HEU to LEU will not adversely impact the long-term operation of the OSTR. Specific details regarding the configuration of the reference HEU FLIP core and the replacement LEU 30/20 core are presented in Chapter 4.5.1 and 4.5.2, respectively.

4.2.1 Reactor Fuel

The design of the HEU fuel utilized in the OSTR is shown in Figure 4-1. The LEU 30/20 fuel proposed for use in the OSTR will be manufactured to the same dimensions as those of the HEU FLIP fuel. The only changes to the fuel exist in the fuel alloy compacts themselves. The design features of the HEU FLIP fuel and the LEU 30/20 fuel are compared in Table 4-2. Table 4-2 Comparison of HEU FLIP and LEU 30/20 Fuel Designs.

Table 4-2 Fuel Characteristics for HEU FLIP and LEU 30/20 Cores.

Fuel Type	HEU FLIP	LEU 30/20
Uranium content [mass %]	8.5	30
U-235 enrichment [mass % U]	70	19.75
Erbium content [mass %]	1.6	1.1
Fuel alloy inner diameter [mm]	6.35	6.35
Fuel alloy outer diameter [mm]	36.449	36.449
Fuel alloy length [mm]	381	381
Cladding material	Type 304 SS	Type 304 SS
Cladding thickness [mm]	0.508	0.508
Cladding outer diameter [mm]	37.465	37.465

Figure 4-1 TRIGA® HEU Fuel Element Design Utilized in the OSTR Core

4.2.1.1 TRIGA® Fuel Development

No additional fuel development was necessary to qualify the LEU 30/20 fuel for use in the OSTR. The use of high-uranium content, low-enriched uranium/zirconium hydride fuels in TRIGA® reactors has been previously addressed in NUREG-1282.[3]

4.2.1.2 Dissociation Pressures

The conversion from the HEU FLIP fuel to the LEU 30/20 fuel does not change the hydrogen dissociation pressure associated with the zirconium hydride fuel.

4.2.1.3 Hydrogen Migration

The conversion from the HEU FLIP fuel to the LEU 30/20 fuel does not alter the hydrogen migration properties of the fuel.

4.2.1.4 Hydrogen Retention

The conversion from the HEU FLIP fuel to the LEU 30/20 fuel does not impact the hydrogen retention properties of the fuel elements.

4.2.1.5 Density

The conversion from the HEU FLIP fuel to the LEU 30/20 fuel will result in a change in density of the fuel alloy compacts. The calculated density for the HEU FLIP fuel containing 8.5 mass % uranium, enriched to 70.0 mass % U-235, and 1.6 mass % natural erbium is 6.02 g/cm^3. The calculated density for the LEU 30/20 fuel containing 30 mass % uranium, enriched to 19.75 mass % U-235, and 1.1 mass % natural erbium is 7.18 g/cm^3.

4.2.1.6 Thermal Conductivity

Data from the thermal diffusivity measurements taken by General Atomics along with the best available data for density and specific heat showed that the thermal conductivity is both independent of temperature and uranium content. Thermal conductivity is given below in Equation (4.1).[4,5]

$$K(T)_{HEU,LEU-FUEL} = 0.18 \pm 0.009 \quad \text{[W/cm-°C]} \qquad (4.1)$$

4.2.1.7 Volumetric Specific Heat

TRIGA® FLIP fuel has a defined volumetric heat capacity as shown in Equation 4.2.[6]

$$\rho C_P(T)_{HEU,LEU-FUEL} = 2.04 + 4.17 \cdot 10^{-3}(T) \quad [\text{W-sec/cm}^3\text{-°C}] \qquad (4.2)$$

As stated in NUREG-1282,[7] "The performance of uranium-zirconium hydride fuel is substantially independent of uranium content up to 45 w% uranium. The behavior of the proposed 20- and 30-w% uranium fuels is indistinguishable from that of the currently approved 8.5-w% uranium fuel." It is thus assumed that volumetric heat capacity of the LEU fuel is similar to that of the HEU fuel.

4.2.1.8 Chemical Reactivity

The conversion from the HEU FLIP fuel to the LEU 30/20 fuel will not alter the chemical reactivity of the Zr-H/U/Er fuel compacts.

4.2.1.9 Irradiation Effects

The conversion from the HEU FLIP fuel to the LEU 30/20 fuel is not expected to impact the irradiation performance of the Zr-H/U/Er fuel compacts.

4.2.1.10 Erbium Additions

The LEU 30/20 fuel previously approved for use in TRIGA® reactors by NUREG-1282 contained 0.9 mass percent natural erbium, while the proposed LEU 30/20 fuel for the OSTR contains 1.1 mass percent natural erbium. However, Table 1 of NUREG-1282 bounds the erbium content from 0.0 to 1.8 wt% for nominal 20% enriched fuels under varying wt% uranium contents. The conclusion of NUREG-1282 is that fuel performance is substantially independent of uranium content up to 45 wt%. While the analysis concentrated on uranium loading, erbium loading was also varied. A reasonable conclusion can be drawn that if no performance issues were observed, fuel performance is independent of erbium content in this range as well. Additionally, in the Simnad[8] paper referenced in NUREG-1282 it was concluded that, "All available evidence indicates that the addition of erbium to the U-ZrH introduces no deleterious effects to the fuel." The only anticipated effect of the increased erbium content is to decrease reactivity, the entire purpose of which is to reduce the power per element in order to increase the number of fuel elements in the core.

4.2.1.11 Prompt-Temperature Coefficient of Reactivity

The physical mechanisms which combine to give the TRIGA® fuel its large negative prompt-temperature coefficient of reactivity remain the same in the LEU 30/20 fuel. The magnitude of the prompt-temperature coefficient of the LEU 30/20 fuel relative to the HEU FLIP fuel is discussed in greater detail in Chapter 4.5.

4.2.1.12 Fission Product Retention

The conversion from the HEU FLIP fuel to the LEU 30/20 fuel does not adversely impact the fission product retention capability of the fuel.

4.2.2 Control Rods

The LEU 30/20 fuel-followed control rods will be built to the same dimensional specifications as the HEU FLIP control rods. The only changes to the fuel-followed control rods exist in the fuel alloy compacts themselves. The void-followed transient rod is unaffected by the conversion from HEU FLIP to LEU 30/20 fuel. The reactivity worth of the individual rods is discussed in further detail in Chapter 4.5.

4.2.3 Neutron Moderator and Reflector

The design of the OSTR reflector assembly is unaffected by the conversion from HEU FLIP to LEU 30/20 fuel. All graphite reflector elements will be replaced during the conversion process and the annular reflector assembly may be replaces as well. The new annular reflector will be identical to the old reflector. The only difference between new and old reflector elements is that the new elements will be stainless steel clad instead of aluminum clad.

4.2.4 Neutron Startup Source

The neutron startup source is unaffected by the conversion of the fuel from HEU FLIP to LEU 30/20. The same source used in the HEU core will be used in the LEU core. The source will be located in the G-ring during regular operation, although it may be moved to other locations to support other reactor operations.

4.2.5 Core Support Structure

The LEU 30/20 fuel elements will have the same dimensional specifications as the HEU FLIP fuel elements. Thus, no changes to the design of the core support structure are necessary for the conversion from HEU FLIP to LEU 30/20 fuel.

4.3 Reactor Tank or Pool

The conversion from HEU FLIP to LEU 30/20 fuel does not require any changes to the reactor tank.

4.4 Biological Shield

The conversion from HEU FLIP to LEU 30/20 fuel does not require any changes to the biological shield.

4.5 Nuclear Design

4.5.1 HEU FLIP core

To assess the impact of the conversion from HEU FLIP fuel to LEU 30/20 fuel, detailed neutronic analyses were undertaken. The OSTR core was modeled using MCNP5.[9] MCNP5 is a general purpose Monte Carlo transport code which permits detailed neutronics calculations of complex 3-dimensional systems, and it is well suited to explicitly handle the material and geometrical heterogeneities present in the OSTR core. In the model developed to describe the OSTR, facility drawings, provided by the manufacturer at the time of construction of the facility, were used to define the geometry of the core and surrounding structures. The geometry of the standard fuel elements, instrumented fuel element (IFE), and fuel-followed control rods (FFCR) were based upon the manufacturing drawings for the assemblies, TOS210D210 Rev. R, TOS210J220 Rev. T, and TOS250D225 Rev. A, respectively. Cross-sectional views of the MCNP5 model are shown in Figures Figure 4-2 and Figure 4-3.

Figure 4-2 Horizontal Cross-section of the MCNP5 Model used to Perform Neutronic Analyses of the OSTR HEU FLIP Core (taken at the core mid-plane)

Figure 4-3 Vertical Cross-section of the MCNP5 Model used to Perform Neutronic Analyses of the OSTR HEU FLIP Core (taken at the core mid-plane)

Extensive start-up testing data is available for the original HEU FLIP core. To demonstrate the capability of MCNP5 to accurately predict core neutronic parameters, the MCNP5 model depicted in Figure 4-2 and Figure 4-3 was modified to simulate core conditions present during start-up testing (the initial critical core and the initial operational core were simulated), and the calculational results of the model were compared to the experimentally determined values. The core loading arrangement for the initial HEU FLIP core is shown in Figure 4-4 and Figure 4-5. The number densities for the fuel and the mass fractions of the other major components in the MCNP5 model used to simulate the HEU FLIP core are summarized in Table 4-3 and Table 4-4, respectively. The number densities for the fuel were obtained from the fuel receipt data provided with the HEU FLIP fuel with an assumed H:Zr ratio of 1.6 and erbium loading of 1.6 mass percent natural erbium. An additional amount of erbium was added to the fuel as Er-166 (labeled "Er-16x") to account for the presence of erbium isotopes other than Er-166 and Er-167. This technique was required to accurately model the natural erbium in the fuel due to the fact that the only erbium cross sections available in MCNP5 are Erbium-166 and Erbium-167.

Thirty-eight critical cases taken from the initial calibration of the HEU FLIP control rods were modeled to establish the bias of the MCNP5 model, and it was found that the model exhibited a bias of +0.0045 $\Delta k/k$ +/- 0.0010 $\Delta k/k$. During the start-up testing of the HEU FLIP core, a value of 0.0070 was used for β_{eff} to convert measured reactivity to units of dollars [$]. To be consistent with the start-up data, in the analyses that follow, reactivity was converted to dollars using $\beta_{eff} = 0.0070$, but as will be shown later, the best-estimate value of β_{eff} for the HEU FLIP core during start-up testing was actually $\beta_{eff} = 0.0076$. In units of dollars, the bias for the beginning of life core was [+0.0045 $\Delta k/k$ +/- 0.0010 $\Delta k/k$] / 0.0070 = +$0.64 +/- $0.14. All reactivity values stated in this CA SAR are the calculated values compensated for the +0.0045 $\Delta k/k$ +/- 0.0010 $\Delta k/k$ model bias.

All MCNP5 simulations of the HEU and LEU cores included an annular ring representing the rotating rack sample holder. In these models, this annulus was modeled as solid aluminum. The actual rotating rack sample holder is an aluminum shell containing mostly air or nitrogen. Calculations indicate that modeling the annulus as 100% air instead of solid aluminum reduces the model bias by 0.00095 $\Delta k/k$ ($0.13) from +0.0045 $\Delta k/k$ to +0.00355 $\Delta k/k$ (+$0.47).

Table 4-3 Number Densities for the As-Received HEU FLIP Fuel

	Standard Fuel Elements and Instrumented Fuel Element	**Fuel-Followed Control Rod**
Nuclide	Number Density [1/(barn-cm)]	Number Density [1/(barn-cm)]
H	5.5519E-02	5.5648E-02
C	-----	----
Zr	3.4699E-02	3.4780E-02
Er-166	1.1505E-04	1.1537E-04
Er-16x	2.9918E-05	3.0001E-05
Er-167	7.8491E-05	7.8711E-05
U-234	-----	----
U-235	8.9251E-04	8.9953E-04
U-236	-----	----
U-238	3.7801E-04	3.8101E-04
Hf	2.0820E-06	2.0868E-06
Sum	9.1714E-02	9.1935E-02

Table 4-4 Physical Densities and Mass Fractions for Selected Core Components in the MCNP5 Model of the OSTR (HEU Fuel)

Material	Physical Density [g/cm^3]	Nuclide	Mass Fraction
Type 304 SS (Fuel Clad)	7.857	C-12	7.993E-04
		Natural Cr	1.900E-01
		Natural Ni	1.000E-01
		Natural Fe	7.092E-01
Graphite Reflector (Fuel)	1.560*	C-12	1.0000
Graphite Segments (FFCR)	1.750	C-12	1.0000
Graphite Reflector Elements	1.620*	C-12	1.0000
Graphite Reflector (Core)	1.698	C-12	1.0000
Zr Fuel Pin	6.398	Natural Zr	1.0000
Stainless Steel + Water Mix	3.056	C-12	6.165E-04
		Natural Cr	1.465E-01
		Natural Ni	7.713E-02
		Natural Fe	5.470E-01
		H-1	2.560E-02
		O-16	2.032E-01
Pure Aluminum	2.700	Al-27	1.0000
Aluminum 6061-T6	2.700	Al-27	0.9793
		Natural Cr	1.900E-03
		Natural Cu	2.800E-03
		Natural Mg	1.000E-02
		Natural Si	6.000E-03
		B-10	1.475E-06
Water	1.000	H-1	0.1119
		O-16	0.8881
Air	1.29E-03	N-14	0.7671
		O-16	0.2329

* Smeared density, accounting for graphite to clad gap. True physical density is 1.75 g/cm^3.

Figure 4-4 Schematic Illustration of the OSTR Upper Grid Plate Showing the Arrangement of Core Components for the HEU FLIP Core.

Figure 4-5 Horizontal Cross-Section of the MCNP5 Model of the HEU FLIP Core, Demonstrating the Arrangement of Core Components within the Model (taken at the core mid-plane).

The calculated excess reactivity of the HEU FLIP core at beginning-of-life (BOL) was \$7.10 which compares very favorably with the measured value of \$7.17. The reactivity worths of the individual control rods were calculated using the rod positions from the initial rod calibrations. The results of the MCNP5 calculations are compared to the measured values in Figure 4-6 through Figure 4-9. The integral rod worths are tabulated in Table 4-5. The calculated values are in reasonable agreement with the empirically determined values.

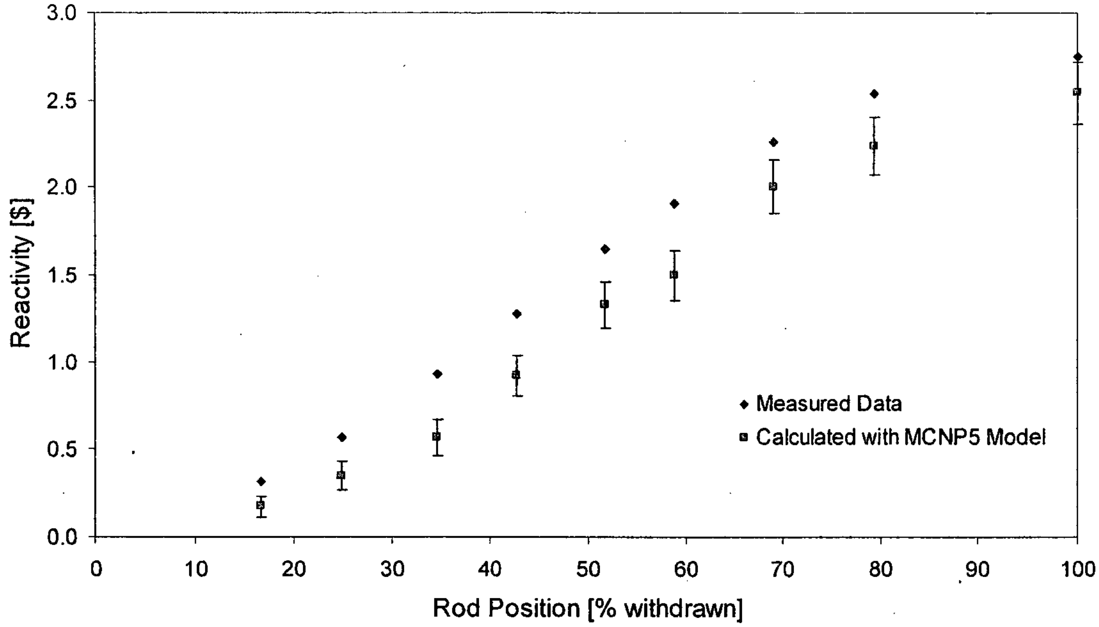

Figure 4-6 Shim Rod Calibration for HEU FLIP Core at BOL ($\beta_{eff} = 0.0070$).

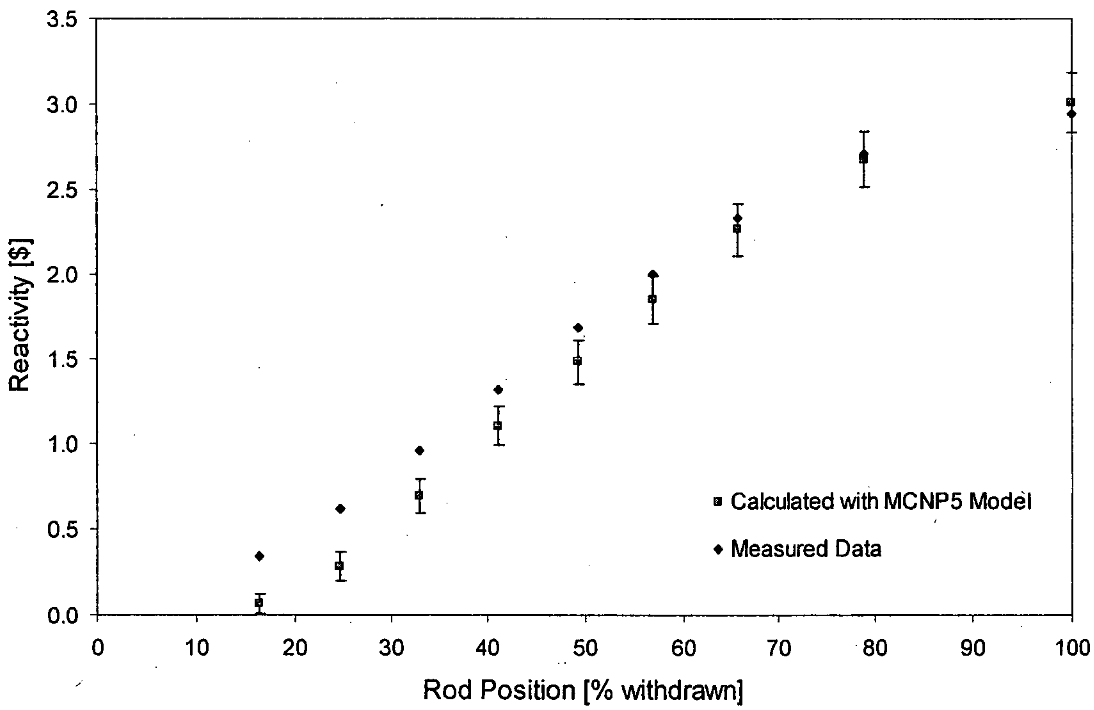

Figure 4-7 Safety Rod Calibration for HEU FLIP Core at BOL ($\beta_{eff} = 0.0070$).

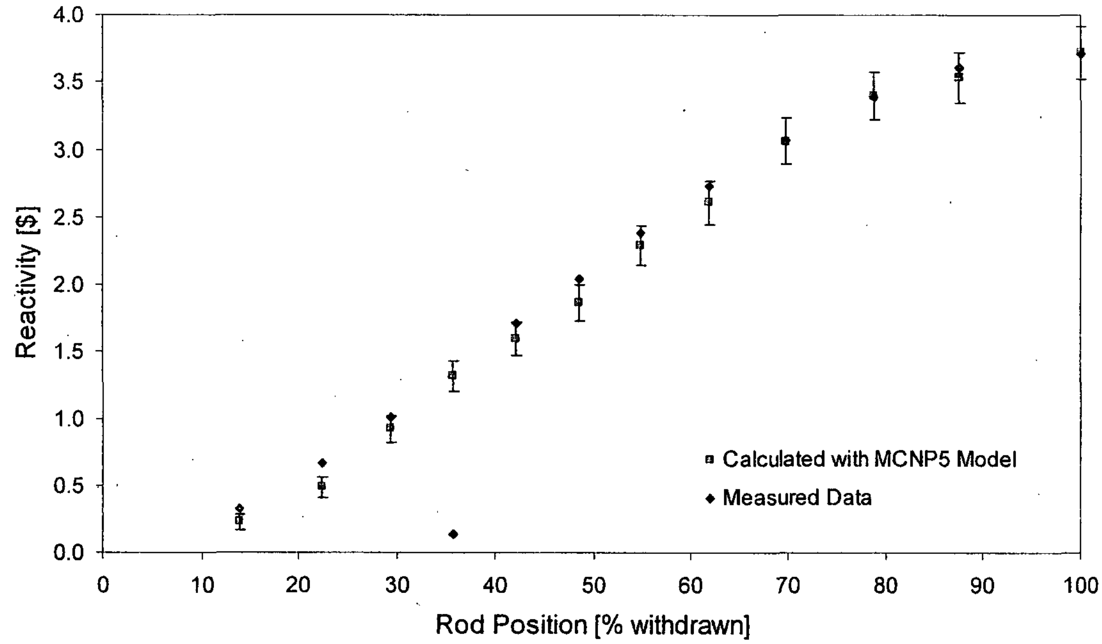

Figure 4-8 Regulating Rod Calibration for HEU FLIP Core at BOL ($\beta_{eff} = 0.0070$).

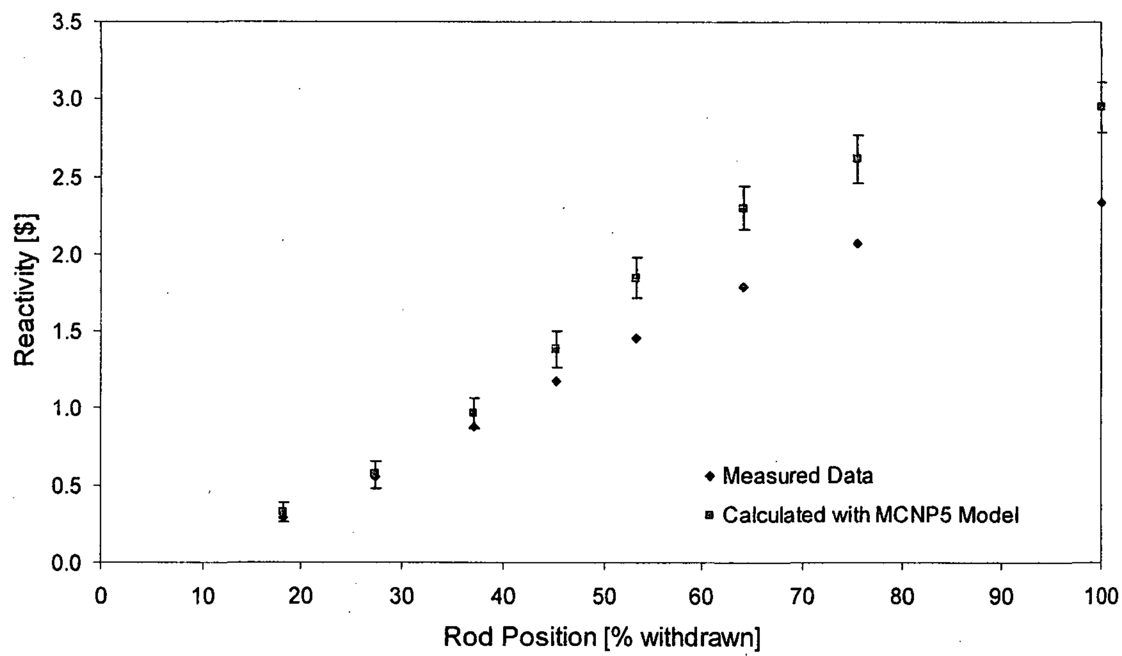

Figure 4-9 Transient Rod Calibration for HEU FLIP Core at BOL ($\beta_{eff} = 0.0070$).

Table 4-5 Summary of Measured and Calculated Integral Control Rod Worth for the HEU FLIP Core at BOL ($\beta_{eff} = 0.0070$)

Control Rod	Measured Rod Worth [$]	MCNP5 Calculated Rod Worth [$]
Shim Rod	2.75	2.54 +/- 0.17
Safety Rod	2.94	3.01 +/- 0.17
Regulating Rod	3.71	3.72 +/- 0.20
Transient Rod	2.33	2.95 +/- 0.16
Sum of all Rods	11.73	12.22 +/- 0.35

Shutdown margins for the HEU FLIP core were calculated using the MCNP5 model by fully inserting three rods with the remaining rod fully withdrawn. The results of the shutdown margin calculation are presented in Table 4-6. The calculated shutdown margin met the required Technical Specification shutdown margin (at the time of the start-up testing) of $-0.57 with the exception of the regulating rod which has a calculated shutdown margin of $-0.20. It should be emphasized that the empirically determined shutdown margin, determined during the initial start-up testing of the HEU FLIP core, met the required Technical Specification shutdown margin of $-0.57 for all rods at all times. The apparent discrepancy between the measured and calculated shutdown margins is inherent to the difference in the evaluation techniques. The theoretical shutdown margin with one rod fully removed was calculated directly using MCNP5, but the measured shutdown margin was inferred from control rod calibration curves and the cold, clean critical rod heights. This measurement method has been used throughout the OSTR lifetime and is approved by the NRC.

Table 4-6 Summary of Shutdown Margin Calculations for the HEU FLIP Core at BOL ($\beta_{eff} = 0.0070$)

Control Rod Fully Withdrawn	Shutdown Margin Calculated by MCNP5 model
Shim Rod	-1.11 +/- $0.04
Safety Rod	-0.90 +/- $0.04
Regulating Rod	-0.20 +/- $0.04
Transient Rod	-1.00 +/- $0.04

REBUS-MCNP5 was utilized to perform a depletion analysis of the HEU FLIP core.[10] The depletion analysis was performed by dividing the fuel into five equal-height axial segments, with each axial segment further subdivided into three equal-volume radial rings. The depletion analysis was conducted at a core power of 1.1 MW_{th}, a fuel temperature of 327°C, and a moderator temperature of 50°C. Depletion calculations were performed in a continuous manner, which is a departure from the actual operating tempo of the OSTR which is ~0.3 MWd at 1.0 MW_{th} per operating day. The results of the depletion analysis are shown in Figure 4-10. Based upon the depletion analysis, middle-of-life (MOL) and end-of-life (EOL) for the HEU FLIP core were determined to be 1800 MWd and 3800 MWd, respectively.

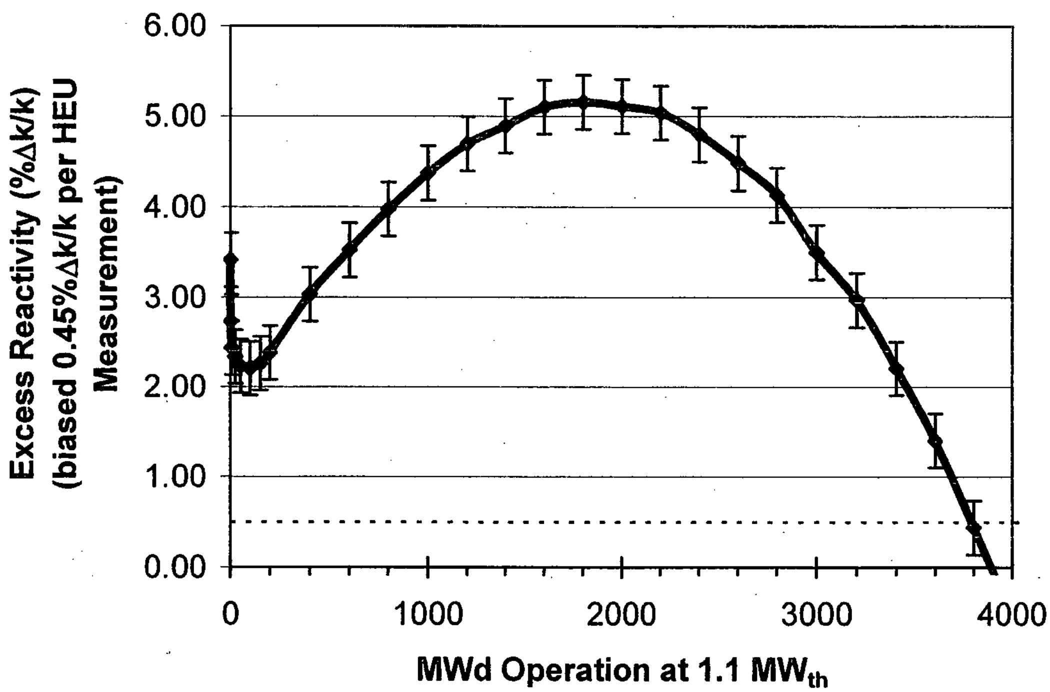

Figure 4-10 REBUS-MCNP5 Depletion Analysis of the HEU FLIP Core.

The prompt-neutron lifetime, l_p, was calculated for the HEU FLIP core at BOL, MOL, and EOL using MCNP5 and the 1/v absorber method, whereby a small amount of boron is distributed homogeneously throughout the reactor.[11] The calculation of l_p is as follows:

$$l_p = \frac{1}{N_{B-10}\sigma_{ao}v_o}\frac{k_{ref}-k_p}{k_p},$$

where: k_{ref} is the eigenvalue of the original system,

k_p is the eigenvalue of the system with trace amounts of B-10,

N_{B-10} = boron-10 number density [atoms/(barn-cm)],

v_o = 220,000 cm/sec, and

σ_{ao} = 3837 barns = σ_a^{B-10} at 220,000 cm/sec.

The limit as N $\rightarrow$ 0 was found by perturbing the system with two different boron concentrations and then linearly extrapolating to N = 0. The boron concentrations utilized were 7.5 x 10^{-8} atoms/(barn-cm) and 1.5 x 10^{-7} atoms/(barn-cm). The results of the prompt-neutron lifetime calculations for the HEU FLIP core are summarized in Table 4-7. A prompt-neutron lifetime of 30 μsec has historically been used for the HEU FLIP core in calculations for the OSTR and in operation of the reactor, and based upon the values presented in Table 4-7, this value is reasonable for the MOL timeframe of the core.

Table 4-7 Summary of Prompt-Neutron Lifetime, l_p, Calculations for the HEU FLIP Core at Various Times in Core Life.

Time in Core Life	Prompt-Neutron Lifetime [μs]
BOL	18.7 +/- 2.8
MOL	32.5 +/- 3.1
EOL	37.1 +/- 2.9

The effective delayed neutron fraction for the HEU FLIP core was calculated with MCNP5 by utilizing the expression

$$\beta_{eff} = 1 - \frac{k_p}{k_{p+d}},$$

where k_p is the system eigenvalue assuming fission neutrons are born with the energy spectrum for prompt neutrons, and k_{p+d} is the system eigenvalue assuming fission neutrons are born with the appropriately weighted energy spectra for both prompt and delayed neutrons. The results of the effective delayed neutron fraction calculations are given in Table 4-8.

Table 4-8 Summary of the Calculated Effective Delayed Neutron Fraction for the HEU FLIP Core at Various Times in Core Life.

Time in Core Life	Effective Delayed Neutron Fraction
BOL	0.0076 +/- 0.0002
MOL	0.0078 +/- 0.0002
EOL	0.0073 +/- 0.0002

The prompt-temperature coefficient associated with the HEU FLIP fuel, α_F, was calculated by varying the fuel temperature while leaving other core parameters fixed. The MCNP5 model was used to simulate the reactor with all rods out at 300, 400, 600, 800, and 1200 K. The prompt-temperature coefficient for the fuel was calculated at the mid-point of the four temperature intervals, and the results were fit to a linear expression. The results are shown in Figure 4-11 and tabulated in Table 4-9. The prompt-temperature coefficient is observed to be a linear function over the given temperature range, and the magnitude of the calculated BOL and EOL prompt-temperature coefficients compare favorably with those of Simnad *et. al.*[12]

The void coefficient of reactivity was also determined using the MCNP5 model. The voiding of the core was introduced by uniformly reducing the density of the liquid moderator in the central region of the core. The center of the core was chosen for two reasons: 1) it is the most likely place to develop a void during reactor operations as this is the region of maximum heat flux, and 2) it is the location with the highest neutron importance in the core, hence also the maximum void coefficient. The calculated void coefficient, using the best-estimate value for β_{eff} of 0.0076, was -\$0.86/% void. Here the calculated core volume was based on the fueled height of the core (38.1 cm), including the volume of the fuel elements themselves. This value is in reasonable agreement with a recent experimental measurement in which the reactivity worth of an irradiation facility placed in the B-1 grid position was found to be -\$0.51/% void. The core average void coefficient was also calculated and found to be -\$0.16/% void.

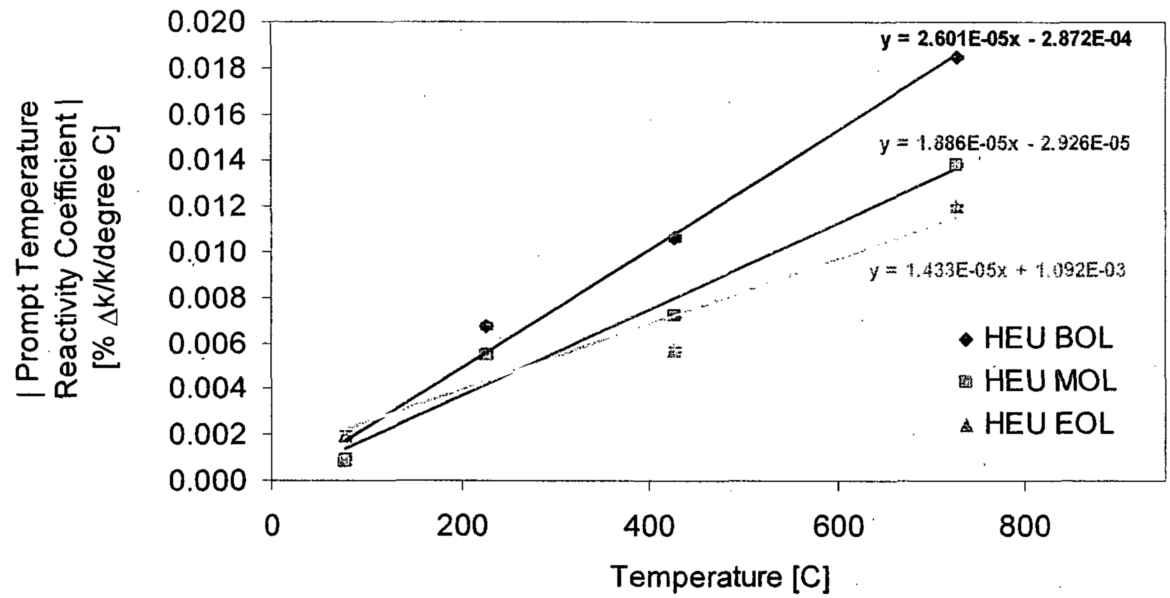

Figure 4-11 Magnitude of the Prompt-Temperature Coefficient, α_F, as a Function of Temperature for the HEU FLIP Fuel at Various Times in Core Life.

Table 4-9 HEU Prompt Temperature Coefficient

Temperature [°C]	Prompt Temperature Coefficient [%Δk/k/°C]		
	HEU BOL	HEU MOL	HEU EOL
77	-9.31E-04 +/- 2.28E-04	-8.47E-04 +/- 1.62E-04	-1.97E-03 +/- 1.71E-04
227	-6.74E-03 +/- 1.23E-04	-5.46E-03 +/- 8.18E-05	-5.53E-03 +/- 8.32E-05
427	-1.06E-02 +/- 1.30E-04	-7.25E-03 +/- 8.10E-05	-5.72E-03 +/- 8.53E-05
727	-1.85E-02 +/- 6.58E-05	-1.38E-02 +/- 4.37E-05	-1.20E-02 +/- 4.71E-05

Figure 4-12 shows a comparison of the magnitude of the prompt reactivity temperature coefficients calculated for the HEU SAR and for the CA SAR. It can be seen from Figure 4-12 that there is a reasonable agreement between the HEU prompt temperature reactivity coefficient used in the HEU SAR, and the HEU prompt temperature reactivity coefficient calculated for use in this conversion SAR.

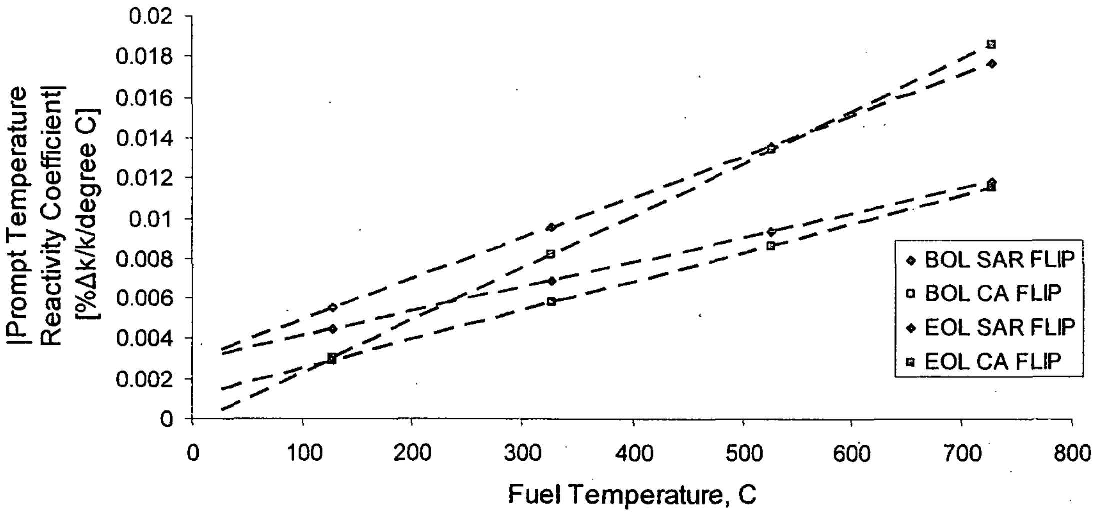

Figure 4-12 Magnitude of the Prompt Temperature Reactivity Coefficient Calculated for the HEU SAR and for the Conversion SAR

The moderator temperature coefficient of reactivity, α_m, was determined by varying the moderator temperature within the MCNP5 model of the HEU FLIP core from 20°C to 60°C. Within this temperature range, the calculated moderator temperature coefficient of reactivity was -0.57¢/°C.

The power coefficient of reactivity and the equilibrium xenon worth for the HEU FLIP core were estimated from the REBUS-MCNP depletion cases. A reactivity loss of $2.05 was observed for an increase of the moderator temperature from 27°C to 50°C coincident with a fuel temperature increase from 27°C to 327°C. These temperatures are characteristic of reactor operation at a power of 1 MW and imply a power coefficient of reactivity of -0.21¢/kW. The equilibrium xenon worth was estimated by calculating the reactivity loss over the course of the first seven days of continuous reactor operation at 1.1 MW. During this time a reactivity loss of $1.28 was observed, which implies an equilibrium xenon poisoning of ~$1.16 at a core power of 1.0 MW.

The behavior of the reactor during a pulse was simulated using the point reactor kinetics function built into RELAP. RELAP calculates the reactivity during the pulse transient using the following equation where $r_{fueltemp}$ represents the fuel temperature reactivity feedback, r_{pulse} represents the reactivity inserted during the pulse and r_b is a bias used by RELAP to ensure that the reactivity is zero prior to the insertion of the pulse. Reactivities in this equation are in dollars.

$$r_t = r_b + r_{pulse} + r_{fueltemp}$$

Both $r_{fueltemp}$ and r_{pulse} are input using user defined tables in RELAP where reactivity is a function of fuel temperature and time respectively. Since the fuel temp at the beginning of the transient is often not at a temperature corresponding to 0.0 reactivity in the $r_{fueltemp}$ table, r_b is used by RELAP to ensure that the transient starts at \$0.0 reactivity. The values used in for the analysis were: bulk coolant temperature (49°C), initial fuel temperature (25°C), number of elements (84 for HEU core and 88 for LEU core), initial power (1kW), β/Λ (describe in section 4.5.1 for the HEU core and section 4.5.2 for LEU core), volumetric specific heat (described in section 4.2.1.7), and a the temperature coefficient of reactivity (described in section 4.5.1 for the HEU and section 4.5.2 for the LEU core).

4.5.2 LEU 30/20 CORE

The analysis of the LEU 30/20 core was performed by modifying the MCNP5 model to reflect the new arrangement of core components within the LEU 30/20 core. Number densities for the LEU 30/20 fuel containing 1.1 mass percent of natural erbium were calculated by the fuel manufacturer using the NUCDEN code and are listed in Table 4-10. As was done for the HEU FLIP core, an additional amount of erbium (labeled "Er-16x") was added as Er-166 to account for erbium isotopes other than Er-166 and Er-167. This additional Er-16x was treated as non-depleting to prevent it from depleting to Er-167 which would artificially increase the magnitude of the prompt temperature coefficient. In addition to the change in the fuel alloy, the LEU 30/20 core will also utilize stainless steel clad graphite reflector elements rather than the aluminum clad graphite reflector elements that were present in the HEU FLIP core. The physical dimensions of the graphite reflector elements remain the same. Only the cladding material is altered in an attempt to eliminate the swelling that was experienced with the aluminum clad elements.

The LEU 30/20 core will have three distinct steady-state operational modes referred to as NORMAL, ICIT, and CLICIT. In the NORMAL mode, a standard fuel element is placed in grid position B-1 and there is a water-filled location in grid position F-23. In the ICIT mode, an in-core irradiation tube (ICIT) is placed in the B-1 grid position, and the standard fuel element that would otherwise be located in the B-1 position is moved to F-23. In the CLICIT mode, a cadmium-lined in-core irradiation tube (CLICIT) is placed in the B-1 grid position, and the standard fuel element that would otherwise be located in the B-1 position is moved to F-23. The arrangement of core components in the NORMAL core is shown in Figure 4-13, while the arrangement of core components in the ICIT or CLICIT core is shown in Figure 4-14. A horizontal cross-section of the MCNP5 model for the LEU 30/20 core in the NORMAL mode is shown in Figure 4-15.

Table 4-10 Number Densities for the LEU 30/20 Fuel

	Standard Fuel Elements, Instrumented Fuel Element, and Fuel-Followed Control Rod
Nuclide	Number Density [1/(barn-cm)]
H	4.9131E-02
C	1.7885E-03
Zr	3.2213E-02
Er-166	9.4400E-05
Er-16x	2.4548E-05
Er-167	6.4820E-05
U-234	8.2400E-06
U-235	1.0829E-03
U-236	1.2110E-05
U-238	4.3250E-03
Hf	1.9328E-06
Sum	8.8746E-02

The ICIT and CLICIT configurations will be used extensively in the LEU core. In the HEU core at BOL, only the NORMAL configuration was used. The ICIT was modeled as a simple air filled tube extending from 32.39 cm. above the core mid-plane to 27.86 cm. below the core mid-plane (even with the bottom of the fuel element lower graphite reflectors). The ICIT aluminum wall has an inner diameter (ID) of 3.2766 cm. and an outer diameter (OD) of 3.7465 cm. The CLICIT is modeled with the same exterior dimensions as the ICIT, but it is composed of a thin layer of cadmium sandwiched between two layers of aluminum. The inner aluminum has ID 2.88036 cm. and ID 3.1750 cm. The cadmium has ID 3.1750 cm. and OD 3.2766 cm. The outer aluminum has ID 3.2766 cm. and OD 3.7465 cm. The CLICIT model also includes thin aluminum and cadmium disks comprising the bottom of the tubes. The thickness of the cadmium disk is 0.0508 cm. The thickness of the aluminum disk is 0.0889 cm.

REBUS-MCNP5 was utilized to perform a depletion analysis of the LEU 30/20 core in the NORMAL mode[10]. The depletion analysis was performed by dividing the fuel into five equal-height axial segments, with each axial segment further subdivided into three equal-volume radial rings. The depletion analysis was conducted at a core power of 1.1 MW_{th}, a fuel temperature of 327°C, and a moderator temperature of 50°C. The results of the depletion analysis are compared with that of the HEU FLIP core in Figure 4-16. Based upon the depletion analysis, middle-of-life (MOL) and end-of-life (EOL) for the LEU 30/20 core were determined to be 1600 MWd and 3600 MWd, respectively. From Figure 4-16, it can be seen that the lifetime of the LEU 30/20 core is nearly as long as the HEU FLIP core (3800 MWd), and the reactivity swing which occurs during the operation of the core due to depletion of the erbium is not nearly as pronounced for the LEU 30/20 core.

Figure 4-13 Schematic Illustration of the OSTR Upper Grid Plate Showing the Arrangement of Core Components for the LEU 30/20 Core in the NORMAL Configuration.

Figure 4-14 Schematic Illustration of the OSTR Upper Grid Plate Showing the Arrangement of Core Components for the LEU 30/20 Core in the ICIT or CLICIT Configuration.

Figure 4-15 Horizontal Cross-Section of the MCNP5 Model of the LEU 30/20 Core in the NORMAL Mode, Demonstrating the Arrangement of Core Components within the Model (taken at the core mid-plane).

Operational experience with the OSTR has shown that core excess reactivity is greatest in the NORMAL mode. The excess reactivity of the LEU 30/20 core in the NORMAL configuration was calculated at various times throughout core life, and the results are presented in Table 4-11. Reactivity was converted to units of dollars using a value of β_{eff} of 0.0075, which, as will be shown later, is the appropriate value for the LEU 30/20 core. In addition, the MCNP5 model bias of 0.0045 $\Delta k/k$ has been taken into account for the reported results. The \$5.48 BOL core excess reactivity for the LEU 30/20 core is lower than the \$7.17 that was measured at BOL for the HEU FLIP core, but it will be sufficient to permit all modes of operation while minimizing the need to alter the core configuration to accommodate the reactivity swing due to the depletion of erbium as the core is depleted.

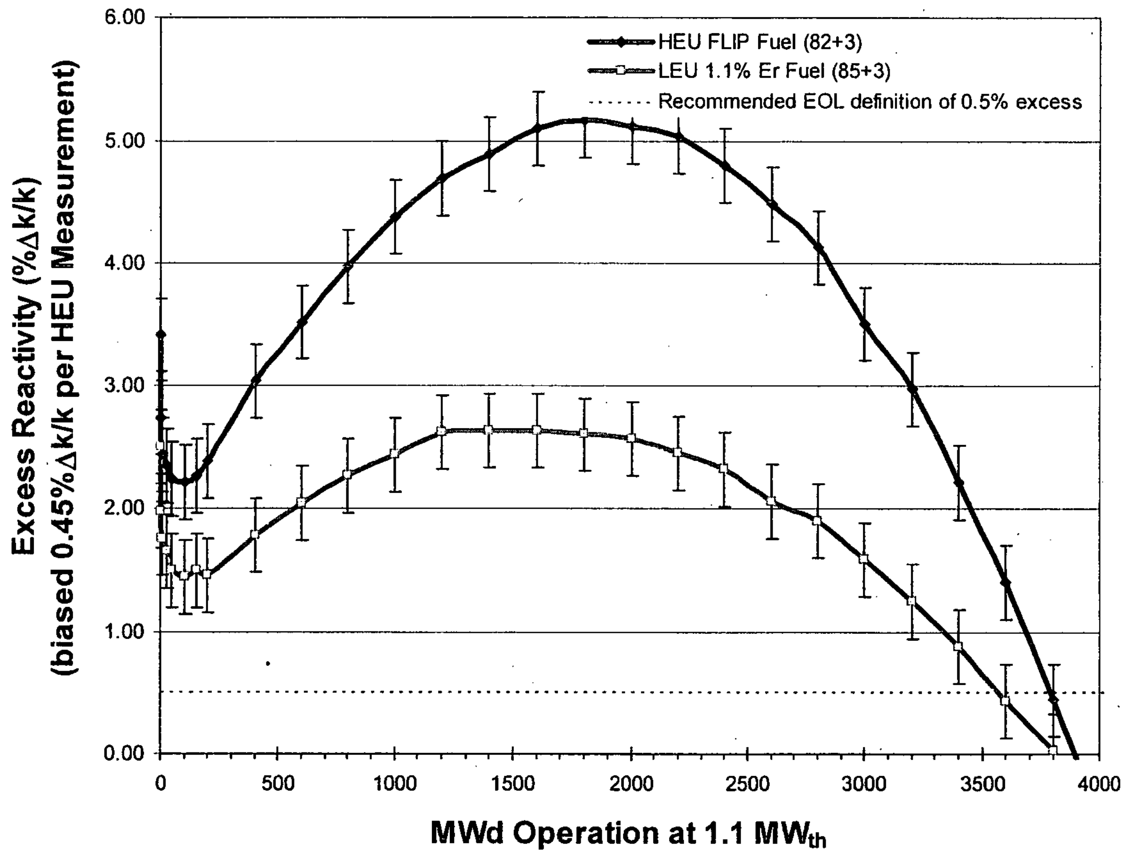

Figure 4-16 REBUS-MCNP5 Depletion Analysis Results for the LEU 30/20 Core and the HEU FLIP Core.

Table 4-11 Summary of Core Excess Reactivity for the LEU 30/20 Core at Various Times in Core Life.

Time in Core Life	k_{eff} from MCNP5 Calculations	Core Excess Reactivity [$]
BOL	1.04776 +/- 0.00009	5.48 +/- 0.012
MOL	1.05634 +/- 0.00012	6.51 +/- 0.016
EOL	1.03384 +/- 0.00012	3.76 +/- 0.016

The reactivity worths of the individual control rods in the LEU 30/20 core at BOL were calculated in the same manner as described for the HEU FLIP core. The results of the MCNP5 calculations are presented in Figure 4-17, Figure 4-18, Figure 4-19 and Figure 4-20. The integral rod worths are tabulated in Table 4-12.

Table 4-12 Summary of Calculated Integral Control Rod Worth for the LEU 30/20 core at BOL

Control Rod	MCNP5 Calculated Rod Worth [$]
Shim Rod	2.55 +/- 0.16
Safety Rod	2.60 +/- 0.16
Regulating Rod	3.36 +/- 0.19
Transient Rod	2.86 +/- 0.15
Sum of all Rods	11.37 +/- 0.33

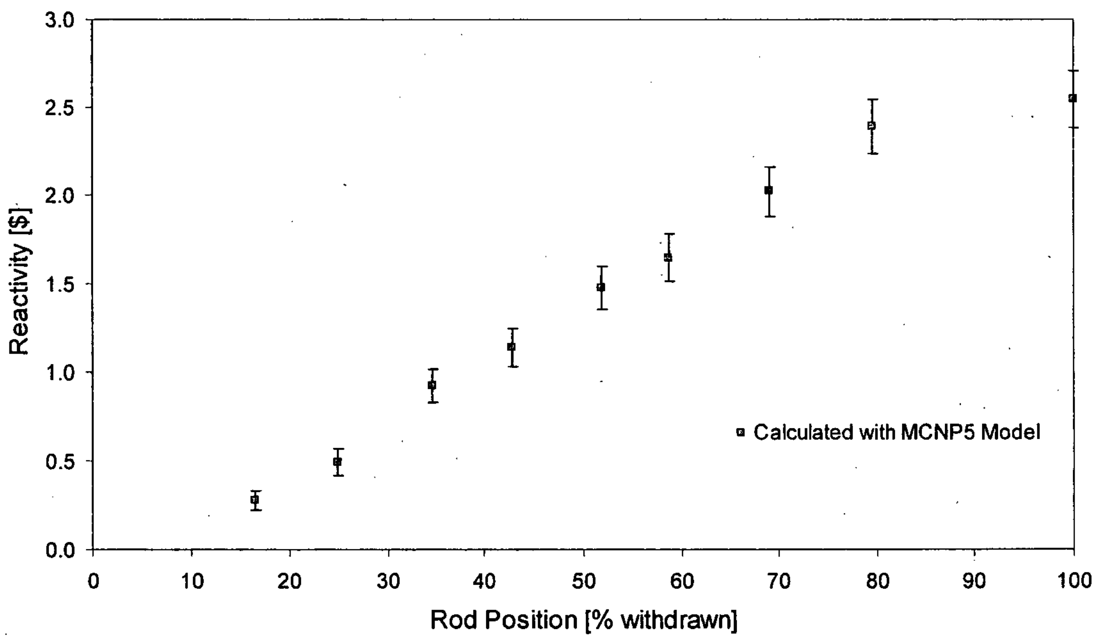

Figure 4-17 Shim Rod Calibration for the LEU 30/20 Core at BOL.

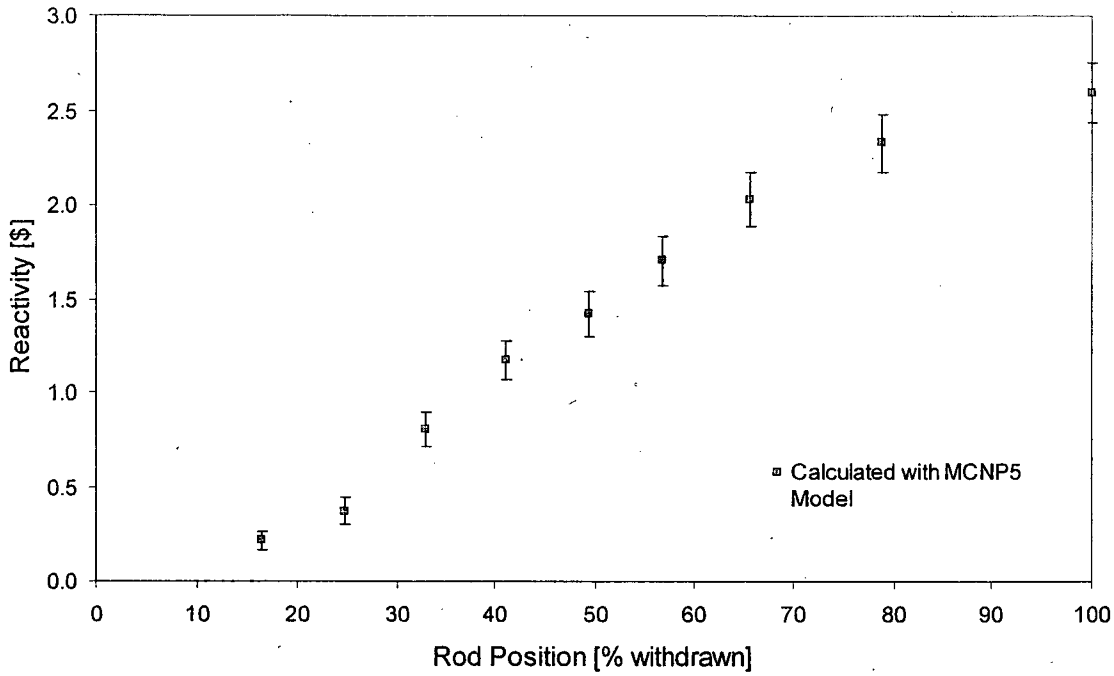

Figure 4-18 Safety Rod Calibration for the LEU 30/20 Core at BOL.

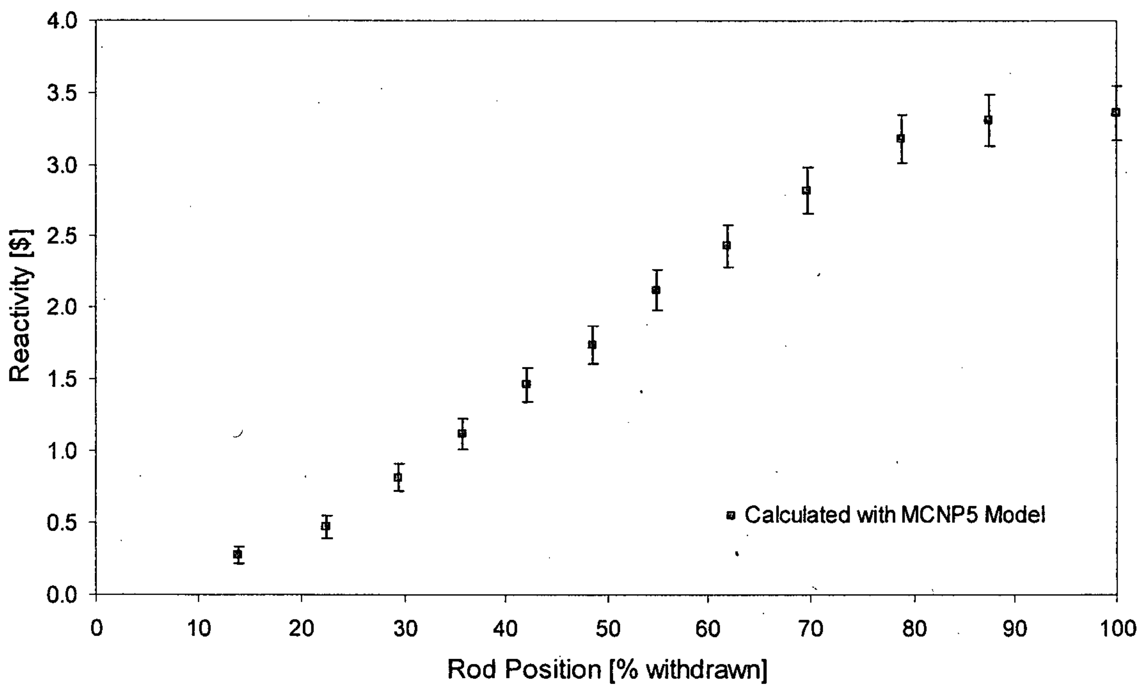

Figure 4-19 Regulating Rod Calibration for the LEU 30/20 Core at BOL.

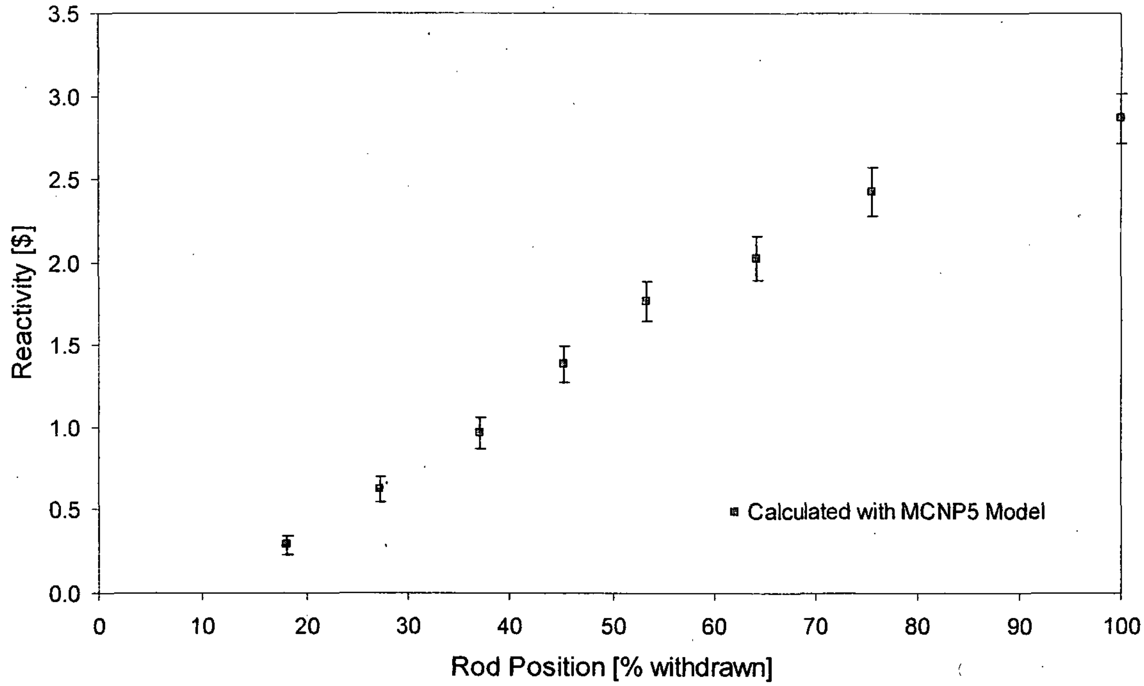

Figure 4-20 Transient Rod Calibration for the LEU 30/20 Core at BOL.

Shutdown margins for the LEU 30/20 core at various times in core life were calculated and compared to the Technical Specification required value of -$0.55. The results of the calculations are summarized in Table 4-13. Inspection of this table shows that the LEU 30/20 core meets the shutdown requirements for all rods at all times in core life with the exception of the regulating rod at MOL which has a shutdown margin of only -$0.37. Operationally, this means that there may be a need to remove one or two fuel elements from the F-ring near MOL to ensure that the regulating rod meets its required shutdown margin. Such modifications to the core will be minor in comparison to those that were necessary to accommodate the reactivity swing that was experienced with the HEU FLIP core.

Table 4-13 Summary of Shutdown Margin Calculations for the LEU 30/20 Core.

Control Rod	BOL [$]	MOL [$]	EOL [$]
Shim Rod	-1.92 +/- $0.03	-1.05 +/- $0.02	-4.04 +/- $0.02
Safety Rod	-1.90 +/- $0.04	-0.97 +/- $0.02	-4.00 +/- $0.02
Regulating Rod	-1.21 +/- $0.04	-0.37 +/- $0.02	-3.46 +/- $0.02
Transient Rod	-1.87 +/- $0.04	-0.96 +/- $0.02	-3.98 +/- $0.02

Prompt-neutron lifetimes for the LEU 30/20 core were calculated using the methodology outlined in Chapter 4.5.1, and the results are summarized in Table 4-14.

Table 4-14 Summary of Prompt-Neutron Lifetime, l_p, Calculations for the LEU 30/20 Core at Various Times in Core Life.

Time in Core Life	Prompt-Neutron Lifetime [μs]
BOL	22.6 +/- 2.9
MOL	19.0 +/- 1.9
EOL	30.7 +/-2.8

Values for the effective delayed neutron fraction of the LEU 30/20 core were calculated at various times in core life as summarized in Table 4-15. Based upon the results presented in Table 4-15, a value for the effective delayed neutron fraction of 0.0075 is a reasonable approximation of its value throughout core life and will be used in calculations in support of the LEU 30/20 core.

Table 4-15 Summary of the Calculated Effective Delayed Neutron Fraction for the LEU 30/20 Core at Various Times in Core Life.

Time in Core Life	Effective Delayed Neutron Fraction
BOL	0.0076 +/- 0.0001
MOL	0.0073 +/- 0.0002
EOL	0.0075 +/- 0.0002

The prompt-temperature coefficient associated with the LEU 30/20 fuel, α_F, was calculated using the methods previously outlined in Chapter 4.5.1, and the results are shown in Figure 4-21 and tabulated in Table 4-16. The variation in the prompt temperature coefficient is similar to that experienced with the HEU FLIP fuel as a function of core life, whereby the coefficient is observed to decrease in magnitude with depletion of the core.

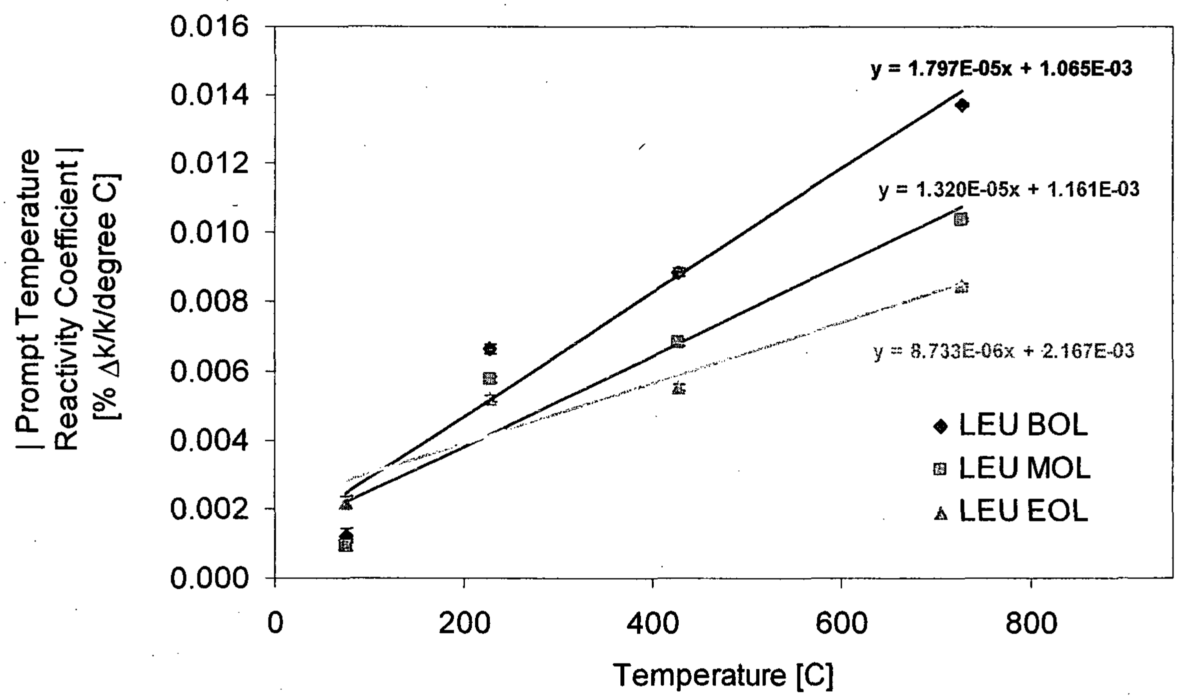

Figure 4-21 Magnitude of the Prompt-Temperature Coefficient, α_F, as a Function of Temperature for the LEU 30/20 Fuel at Various Times in Core Life.

Table 4-16 LEU Prompt Temperature Coefficient

Temperature [°C]	Prompt Temperature Coefficient [%Δk/k/°C]		
	LEU BOL	LEU MOL	LEU EOL
77	-1.23E-03 +/- 2.10E-04	-9.33E-04 +/- 1.65E-04	-2.19E-03 +/- 1.73E-04
227	-6.65E-03 +/- 7.28E-05	-5.75E-03 +/- 9.33E-05	-5.20E-03 +/- 9.07E-05
427	-8.86E-03 +/- 6.08E-05	-6.83E-03 +/- 8.93E-05	-5.54E-03 +/- 9.28E-05
727	-1.37E-02 +/- 3.28E-05	-1.04E-02 +/- 4.19E-05	-8.46E-03 +/- 4.84E-05

The void coefficient of reactivity for the LEU 30/20 core at BOL was calculated by introducing a void into the central region of the core as described in Chapter 4.5.1. The resultant void coefficient of reactivity at the center of the LEU 30/20 core was found to be -\$0.96/% void which is similar to the value of -\$0.86/% void calculated for the HEU FLIP core. The core average void coefficient for the LEU core was also calculated and found to be -\$0.19/% void.

The moderator temperature coefficient of reactivity, α_m, for the LEU 30/20 core at BOL was determined by varying the moderator temperature over a temperature range from 20°C to 60°C. Within this temperature range, the calculated moderator temperature coefficient of reactivity was -0.72¢/°C which is again similar to the value previously determined for the HEU FLIP core at BOL.

The power coefficient of reactivity and the equilibrium xenon worth for the LEU 30/20 core were estimated from the REBUS-MCNP5 depletion cases. A reactivity loss of \$2.16 was observed for an increase of the moderator temperature from 27°C to 50°C coincident with a fuel temperature increase from 27°C to 327°C. These temperatures are characteristic of reactor operation at a power of 1 MW and imply a power coefficient of reactivity of -0.22¢/kW. The equilibrium xenon worth was estimated by calculating the reactivity loss over the course of the first seven days of continuous reactor operation at 1.1 MW. During this time a reactivity loss of \$0.98 was observed, which implies an equilibrium xenon poisoning of ~\$0.89 at a core power of 1MW.

The pulsing performance of the LEU 30/20 core was analyzed using the methodology presented in Chapter 4.5.2, but the appropriate values of β_{eff} and α_F for the LEU 30/20 core, as calculated above, were substituted into the model. The results of the pulse analysis are detailed in Chapter 4.7.

Simulations were also performed to determine the minimum critical core configuration for the LEU 30/20 fuel. With 69 fuel elements arranged as shown in Figure 4-22, the calculated value of core reactivity is $\rho = 0.0010\ \Delta k/k$, or \$0.13. The same core arrangement with the F-10 fuel element removed is calculated to be subcritical. For fuel containing exactly 1.1 mass percent Erbium, the minimum critical core is thus expected to contain 69 fuel elements. If actual erbium content is less than 1.1 mass percent, the minimum critical core may contain fewer than 69 fuel elements. It is also possible that a critical core containing fewer than 69 fuel elements could be obtained if elements in the F-ring were spaced more symmetrically in the F-ring, rather than being placed in the F-1 through F-10 positions. However, since fuel will be loaded clockwise in the F-ring starting from the F-1 position, this analysis is appropriate.

Figure 4-22 Schematic Illustration of the OSTR Upper Grid Plate Showing the Arrangement of Core Components for the LEU 30/20 Core in the Minimum Critical Configuration.

4.6 Functional Design of the Reactivity Control System

No changes are planned for the reactivity control system in conjunction with the HEU-LEU conversion.

4.7 Thermal Hydraulic Design – OSU HEU and LEU Cores

4.7.1 Analysis of Steady State Operation

The following evaluation has been made for a TRIGA® system operating with cooling provided by natural convection water flow around the fuel elements. In this study, the predicted steady state thermal-hydraulic performance of the OSU HEU core at Beginning of Life operating conditions is determined for the reactor operating at 1.1 MW with a water inlet temperature of 49°C. This analysis is conservative since the maximum license power of the OSTR is 1.1 MW, but the reactor is operated at 1.0 MW with a high power SCRAM at 1.06 MW. Per the Technical Specifications, the maximum pool temperature is 49°C. Operational data are used for the benchmark comparisons. The maximum power fuel rod and maximum power heated subchannel were analysed under steady-state and transient conditions. The RELAP5-3D computer code[13] was used to determine the natural convection flow rate, fuel centerline temperature profile, clad temperature profile, axial temperature profile and radial fuel temperature distribution. The power in the hottest rod at which critical heat flux is predicted to occur was calculated with the aid of the RELAP5-3D code. The code was used to calculate coolant flow rate as a function of rod power. The Bernath correlation and the 2006 Groeneveld critical heat flux tables were used to determine the Departure from Nucleate Boiling Ratio (DNBR).

4.7.2 RELAP5 Code Analysis and Results

The thermal hydraulic analysis was conducted using RELAP5-3D. The predicted parameters produced from this code for steady state operation include: channel flow rate, axial fuel centerline temperature distribution, axial clad temperature distribution, axial bulk coolant temperature distribution and axial DNBR. To simplify the RELAP5-3D model, it was assumed that there is no cross flow between adjacent channels. This assumption is conservative since higher values of temperature and lower margins to DNB are predicted when cross flow between adjacent channels is ignored. The parametric inputs into RELAP5-3D include:

1) Inlet coolant temperature
2) System pressure at the top of the core
3) Radial and axial heat source distribution
4) Discretized spacing of heat source nodes
5) Inlet and exit pressure loss coefficients

The analysis was performed using a single flow channel divided into axial segments (nodal distribution is described below). The reactor geometry and hydraulic data for the RELAP5-3D input are given in Table 4-17. Flow channels in the OSTR are triangular, square or irregular, depending on core location. The analysis assumes a triangular rod lattice configuration because the hottest flow channel is shown to occur adjacent to the A and B rings, and in this location, the lattice is triangular.

Table 4-17 RELAP5-3D Input for Reactor and Core Geometry and Heat Transfer.

Hydraulic Data	
Inlet pressure loss coefficient	2.26
Exit pressure loss coefficient	0.63
Absolute pressure at the top of the core [Pa]	1.43E5

A study conducted by General Atomics for the OSTR developed a methodology for calculating each effective subchannel form loss rather than local form losses within the core.[14] These coefficients are shown in Table 4-17. A constant pressure of 1.01E5 Pa (14.7 psia) is assumed to exist at the top of the reactor pool. The OSTR technical specification requires a minimum water column height above the top of the core to be 4.2672 m (168 inches or 14 feet), so this equivalent water column pressure boundary condition is used in the RELAP5-3D model. RELAP5-3D requires that input pressure conditions be entered as absolute pressure, therefore the input RELAP5-3D pressure used in the model at the top of the core is 1.43E5 Pa (20.7717 psia).

A RELAP5-3D thermal hydraulic analysis was performed on the maximum powered channel. The analysis was conducted assuming (conservatively) that the maximum powered channel was also the most restrictive flow channel location found in the OSTR. The flow parameters for the most restrictive flow channel are given in Table 4-18. The geometry of the maximum powered channel is shown in Figure 4-23. It is conservatively assumed that all rods bordering the maximum powered subchannel are operating at the same power as the maximum powered rod as determined for each core configuration.

Table 4-18 Hydraulic Flow Parameters for the Hot Channel.

Parameter	Value
Flow area [m^2]	3.80E-04
Fuel Element Pitch [m]	0.04064
Wetted perimeter [m]	0.117
Hydraulic diameter [m]	1.301E-02
Heated diameter [m]	3.734E-02
Fuel element heated length [m]	0.381
Fuel element surface area [m^2]	4.469E-02
Fuel element surface roughness [m]	2.134E-06

Several hydraulic flow parameters for the hot channel vary during this study from that found in the HEU SAR. The B Ring in the OSTR contains the smallest pitch from fuel rod centerline to centerline, and also contains the smallest subchannel flow area. It is for this reason that the subchannel flow area for the RELAP5-3D model is calculated with reference to the B Ring subchannel flow area. A typical B Ring subchannel is shown in Figure 4-23.

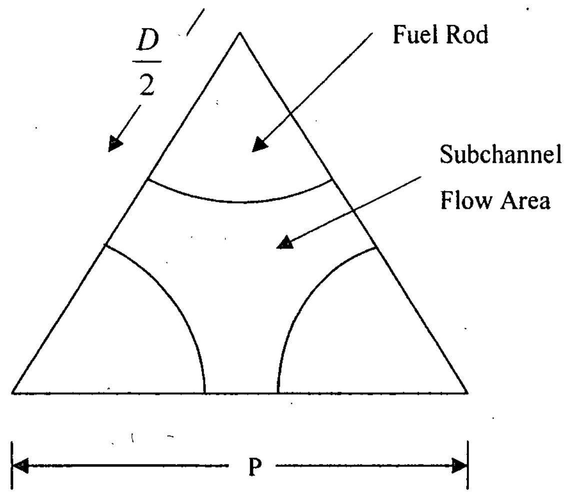

Figure 4-23 Hexagonal Array Axial Average unit subchannel dimensions

The pitch for the B Ring subchannel is 0.04064 m (1.60 in).[15] The fuel rod outer diameter for all OSTR core fuel rods is defined as 0.037 m (1.47 in). Equation (4.3) defines the subchannel flow area for a hexagonal array[16]

$$A_{fi} = \frac{\sqrt{3}}{4}P^2 - \frac{\pi D^2_{\text{outer clad}}}{8} \quad (4.3)$$

where P represents fuel rod pitch and D represents the fuel rod outer diameter. From Equation (4.3) the subchannel flow area is calculated to be 1.90E-4 m^2 (0.295 in^2).

The wetted perimeter for the subchannel only encompasses one half of an entire fuel rod in the figure above. Therefore the total flow area for the subchannel input into the RELAP5-3D model is 3.80E-4 m^2 (0.589 in^2).

The fuel element heated surface area in the RELAP5-3D model was calculated by referring to Figure 4-1. The axial length of the fueled portion of the fuel rod is 0.381 m. (15.0 in) while the diameter of the outer cladding is 0.037 m (1.47 in). The total surface area of the fueled portion of the fuel rod is therefore 4.469E-2 m^2 (69.27 in^2).

The wetted perimeter is defined as $P_{\text{wetted}} = \pi D_{\text{outer clad}}$. This equation produces a value of 0.117 m (4.618 in) for the wetted perimeter of a fuel rod.

The hydraulic diameter is calculated per Equation (4.4). With reference to the previously calculated wetted perimeter and subchannel flow area, the hydraulic diameter is calculated to be 1.301E-2 m (0.512 in).

$$D_h = \frac{4A_{fi}}{P_{wetted}} \tag{4.4}$$

Figure 4-24 Comparison of OSTR Fuel Rod Axial Characteristics and RELAP5-3D Hot Channel

Figure 4-24 shows a direct comparison between a physical OSTR fuel element and the RELAP5-3D discretized subchannel volume. Node dimensions are given in Table 4-19. Nodes 01 and 24 represent the lower and upper grid plates. The lower grid plate is 0.0191 m (0.75 in) thick. The upper gridplate is 0.0159 m (0.625 in) thick. The bottom surface of the upper grid plate is 0.6731 m (26.5 in) above the top surface of the lower grid plate.[17] The fuel element axial nodal dimensions are shown in Figure 4-24.

Node 02 extends from the bottom of the fuelled portion of the fuel rod to the top of the lower gridplate. The equation used to calculate the length of Node 02 (lower unheated node) is:

$$L_{02} = \frac{\left(0.6731 - L_{fuel} - L_{Upper,graphite} - L_{Lower,graphite}\right)}{2} + L_{Lower,graphite} \quad 4.5$$

where L_{02} is the length of Node 02 and $L_{Upper,graphite}$ and $L_{Lower,graphite}$ are the upper and lower graphite lengths of the fuel element.

From Figure 4-24 the fuel nodal lengths must be discretized accordingly and this can be done by use of equation 4.6 for Nodes 03 through 22:

$$L_{03 \to 22} = \frac{L_{fuel}}{n_{fuel}} \quad 4.6$$

$L_{03 \to 22}$ refers to the nodal length for Nodes 03 through 22, n_{fuel} is the number of nodes defined in the fuel region (i.e. 20 nodes).

Equation 4.7 is used to calculate the nodal length for Node 23 (upper unheated node).

$$L_{23} = \frac{\left(0.6731 - L_{fuel} - L_{Upper,graphite} - L_{Lower,graphite}\right)}{2} + L_{Upper,graphite} \quad 4.7$$

Table 4-19 is formulated from Equations 4.5, 4.6, and 4.7.

Table 4-19 Hot Channel Axial Nodal Lengths

Core Volume Axial Nodal Lengths		
Nodal Description	Node Number	Nodal Length [m] (in)
Upper Grid Plate	24	0.01905 (0.75000)
Upper Graphite	23	0.14567 (5.73504)
Fuel	22	0.01905 (0.75000)
	21	0.01905 (0.75000)
	20	0.01905 (0.75000)
	19	0.01905 (0.75000)
	18	0.01905 (0.75000)
	17	0.01905 (0.75000)
	16	0.01905 (0.75000)
	15	0.01905 (0.75000)
	14	0.01905 (0.75000)
	13	0.01905 (0.75000)
	12	0.01905 (0.75000)
	11	0.01905 (0.75000)
	10	0.01905 (0.75000)
	09	0.01905 (0.75000)
	08	0.01905 (0.75000)
	07	0.01905 (0.75000)
	06	0.01905 (0.75000)
	05	0.01905 (0.75000)
	04	0.01905 (0.75000)
	03	0.01905 (0.75000)
Lower Graphite	02	0.14643 (5.76504)
Lower Grid Plate	01	0.01905 (0.75000)

A cross sectional view of a fuel element is shown in Figure 4-25. The radial nodal distribution is shown in Figure 4-26. The fuel portion of the fuel pin consists of an annular U/ZrH/Er casting. The fuel slugs are hydrided and then forced into stainless steel tubes. The central void which aids the hydriding process is backfilled with a zirconium plug. A nominal gap exists between the fuel slug and the stainless steel clad. This gap is initially filled with air, but as burnup of the fuel progresses, hydrogen and fission gasses migrate into the gap.

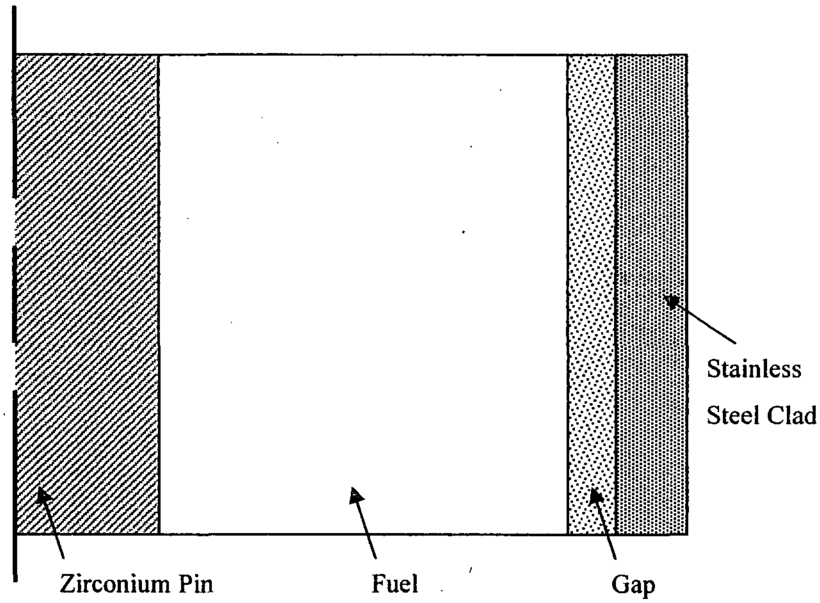

Figure 4-25 Cross Sectional View of Fuel Element

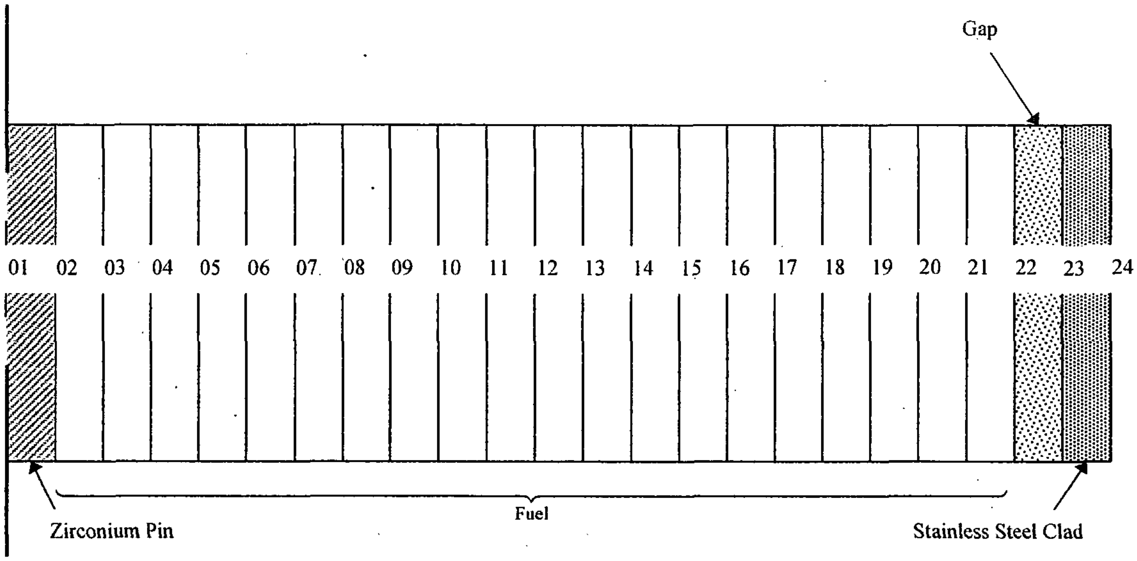

Figure 4-26 Radial Nodal Distribution in a Fuel Element

The mesh points within the fuel region used in the RELAP5-3D model correspond to one node for the central zirconium pin, twenty nodes of equal radial thickness for the fuel meat, one node for the fuel to clad gap and one node for the clad. The radial location of each node is identified in Table 4-20. The outer gap coordinate (Node 22) is varied during this study to simulate different gap widths. Several references for TRIGA® fuel identify that the gap between the stainless steel and the fuel can vary from 1.27E-4 to 1.016E-3 m (0.05 to 0.4 mils). RELAP5-3D input requires that radial mesh points be defined in order to specify all material properties and to calculate temperature gradients within the heat structure.

Table 4-20 Radial Fuel Element Nodal Locations (from fuel center)

Heat Structure Radial Node Lengths		
Nodal Description	Node Number	Node Coordinate [m] (in)
Inner Zirconium Pin	01	0.00000 (0.00000)
	02	0.00318 (0.12500)
Fuel	03	0.00355 (0.13976)
	04	0.00430 (0.16929)
	05	0.00506 (0.19921)
	06	0.00581 (0.22874)
	07	0.00656 (0.25827)
	08	0.00731 (0.28779)
	09	0.00807 (0.31772)
	10	0.00882 (0.34724)
	11	0.00957 (0.37677)
	12	0.01032 (0.40630)
	13	0.01108 (0.43622)
	14	0.01183 (0.46575)
	15	0.01258 (0.49527)
	16	0.01333 (0.52480)
	17	0.01409 (0.55472)
	18	0.01484 (0.58425)
	19	0.01559 (0.61378)
	20	0.01634 (0.64331)
	21	0.01710 (0.67323)
	22	0.01785 (0.70275)
Outer Gap	23	0.01785-0.01786 (0.70285-0.70305)
Outer Stainless Steel Clad	24	0.01873 (0.73750)

Power peaking factors for each core configuration were analyzed using MCNP5. The highest power rod for each configuration was determined by calculating the total power produced in each fuel element present in the configuration. After the highest power rod had been determined, further analyses were performed to find the detailed axial and radial power shapes associated with that rod. The axial and radial power shapes were determined for twenty equally spaced nodes in both the axial and radial directions. The MCNP5 results were used to calculate three peaking factors:

Hot Channel Peak Factor = (maximum fuel rod power)/(core average fuel rod power)

Hot channel Fuel Axial Peak Factor = (maximum axial power in the hot rod)/(average axial power in the hot rod)

Hot Channel Fuel Radial Peak Factor = (maximum radial power in the hot rod)/(average radial power in the hot rod)

It is crucial that average fuel rod power in the core, average axial power in the hot rod and average radial power in the hot rod be properly calculated in order to obtain correct peak factors. The average fuel rod power in the core is calculated by taking the numerical average with each rod weighted equally. The fission rate in the hot rod is then calculated as discussed above and expressed in cylindrical (r,z) coordinates. The average axial power in the hot rod is calculated by taking the numerical average with each of the twenty axial segments weighted equally. Finally the average radial power in the hot rod is calculated at the hottest axial location. In cylindrical coordinates, the average radial power is calculated using the expression

$\bar{f}(z_0) = \dfrac{2\pi \int f(r, z_0) r dr}{2\pi \int r dr}$, where the integral ranges from the inner radius to the outer radius of the fuel meat. This in effect calculates the average radial power weighted by the radial distance from the fuel rod center. This is reasonable since each radial node has the same thickness and thus the volume in each node is proportional to its distance from the fuel rod center.

The effective peak factor for each configuration is the product of these three individual peaking factors. The results of the MCNP5 analyses for the various core configurations, listing the location of the highest power rod along with its associated peaking factors, are summarized in Table 4-21. Note that these peaking factors are calculated for cores with control rods removed. This is conservative since the presence of control rods in the central regions of a core will result in flatter power distributions and lower hot channel peak factors.

The LEU BOL ICIT core has the highest effective power peak factor (3.540) of all the LEU cores, as shown in Table 4-19. The HEU BOL NORMAL core has the highest effective power peak factor (3.399) of the three HEU cores analyzed. All references and results presented for core configurations are based upon the following core life characteristics:

- HEU BOL: ~0 MWdays
- HEU MOL: ~1800 MWdays
- HEU EOL: ~3800 MWdays
- LEU BOL: ~0 MWdays
- LEU MOL: ~1600 MWdays
- LEU EOL: ~3600 MWdays

The HEU BOL NORMAL steady state core is analyzed extensively in section 4.7.4 since it has the highest effective peak factor, and thus represents the bounding HEU core with regard to steady state DNBR analysis. During reactor pulse operation, the HEU core is most limited at EOL since the magnitude of the fuel temperature reactivity coefficient is lowest at EOL, and hence a reactivity insertion of a given magnitude will result in a larger pulse (peak power, temperature end energy) at EOL than at BOL.

For the LEU steady state cores, the ICIT configuration is analyzed in detail. The ICIT core configuration has the highest effective peak factor at BOL, MOL and EOL, and therefore it has the most uneven power distribution. The ICIT cores have the highest peak temperatures, and thus the ICIT core bounds the NORMAL and CLICIT core configurations. For the LEU cores operating in pulse mode, the ICIT core is again analyzed at each stage in life for the same reasons.

Table 4-21 Hot Rod Power Summary

Hot Rod Power Summary						
	Hot Rod Location	Hot Rod Thermal Power [kW]*	Hot Rod Peak Factor [P_{max}/P_{avg}]	Hot Rod Fuel Axial Peak Factor [P_{max}/P_{avg}]	Hot Rod Fuel Radial Peak Factor [P_{max}/P_{avg}]	Effective Peak Factor
HEU-BOL NORMAL Core	B3	18.02	1.376	1.236	1.907	3.243
HEU-MOL NORMAL Core	B6	18.37	1.403	1.209	1.518	2.575
HEU-EOL NORMAL Core	B6	16.48	1.258	1.234	1.708	2.651
LEU-BOL ICIT Core	B6	18.47	1.477	1.221	1.963	3.540
LEU-BOL CLICIT Core	B3	17.03	1.362	1.221	1.943	3.231
LEU-BOL NORMAL Core	B3	17.77	1.422	1.219	1.945	3.371
LEU-MOL ICIT Core	B6	18.52	1.482	1.225	1.846	3.351
LEU-MOL CLICIT Core	B3	17.03	1.363	1.225	1.821	3.040
LEU-MOL NORMAL Core	B3	17.80	1.424	1.222	1.823	3.172
LEU-EOL ICIT Core	B6	17.61	1.409	1.181	1.699	2.827
LEU-EOL CLICIT Core	C7	16.35	1.308	1.212	1.732	2.746
LEU-EOL NORMAL Core	B3	17.02	1.362	1.178	1.707	2.739

* Hot rod thermal power corresponds to core power of 1.1 MW_t.

Two Critical Heat Flux correlations were used in conjunction with this study; the 2006 AECL Groeneveld Look-up Tables,[18] and the Bernath[19] correlation. These correlations were implemented as discussed below.

AECL Groeneveld Look-up Tables:

$$CHF = f\left(G, X_e, P_{abs}, \text{geometry}\right) \tag{4.8}$$

By interpolating in the Groeneveld look-up tables given the mass flux (G), equilibrium quality (X_e) and absolute pressure (P_{abs}) produced in the RELAP5-3D model, a critical heat flux value for the system is produced (CHF_{int}). The appropriate correction factors, K_1 to K_6, must then be multiplied by the interpolated CHF value.

$$CHF = K_1 \cdot K_2 \cdot K_3 \cdot K_4 \cdot K_5 \cdot K_6 \cdot CHF_{int} \tag{4.9}$$

Three correction factors affect the CA SAR: K_1, K_2, and K_4. The other correction factors are assumed to have a value of one.

$$K_1 = \left(\frac{0.008}{D_h}\right)^{\frac{1}{2}}, \tag{4.10}$$

where the hydraulic diameter is measured in meters.

$$K_2 = \min\left[0.8, 0.8\cdot\exp\left(-0.5X_e^{(1/3)}\right)\right], \tag{4.11}$$

where X_e is the equilibrium quality. If X_e is less than zero, it is set to zero.

$$K_4 = \exp\left(\frac{D_H}{L}e^{2\alpha}\right), \tag{4.12}$$

$$\text{where } \alpha = \frac{X_e}{\left[X_e + \frac{\rho_g}{\rho_l(1-X_e)}\right]} \tag{4.13}$$

and L [meters] is the distance from the start of the heated length to the middle of the node. If D_H/L is greater than 0.2, it is set to 0.2. The quantities ρ_l and ρ_g [kg/m^3] are the liquid density and gas density respectively, while D_H is the heated diameter [meters].

The appropriate critical heat flux values from the Groeneveld 2006 Look-up Tables were produced for the CA SAR by applying these correction factors.

The Bernath Correlation:

CHF is defined in units of pound- centigrade per hr-ft^2 per the following equations.

$$CHF = h_{BO}\left(T_{w_{BO}} - T_b\right) \tag{4.14}$$

$$h_{BO} = 10890\left(\frac{D_h}{D_h + D_H}\right) + \Delta v \tag{4.15}$$

$$\Delta = \begin{cases} \dfrac{48}{D_h^{0.6}} & \text{if } D_h \le 0.1 \text{ ft} \\ \dfrac{10}{D_h} + 90 & \text{if } D_h \ge 0.1 \text{ ft} \end{cases} \tag{4.16}$$

$$T_{w_{BO}} = 57\ln\left(P_{abs}\right) - 54\left(\frac{P_{abs}}{P_{abs}+15}\right) - \frac{v}{4} \tag{4.17}$$

Where:

h_{BO}	Limiting film coefficient [p.c.u./hr-ft^2-°C]
T_b	Fluid bulk temperature [°C]
$T_{w_{BO}}$	Wall temperature at CHF [°C]
v	Fluid velocity [ft/sec]
Δ	"slope"
P_{abs}	Absolute pressure [psi]
D_H	Heated diameter [ft]
D_h	Hydraulic diameter [ft]

4.7.3 HEU Power Summary

Figure 4-27 through Figure 4-29 represent the BOL, MOL and EOL core power distribution, respectively. These figures correspond to a core operating at 1.1 MW_{th}. From these, the hot channel peak factor was calculated (see Table 4-21). The MOL core has the highest powered element of the three HEU cores (18.37 KW in position B6). Consequently, the HEU MOL core has a higher hot channel peak factor than the HEU BOL and HEU EOL cores. The HEU BOL NORMAL core has a higher total effective peak factor due to its large radial peak factor, and thus the HEU BOL NORMAL core has the hottest local peak fuel temperature.

Figure 4-27 Core Power Distribution (HEU BOL NORMAL Core).

Figure 4-28 Core Power Distribution (HEU MOL NORMAL Core).

Figure 4-29 Core Power Distribution (HEU EOL NORMAL Core).

4.7.4 HEU Beginning of Life Steady State NORMAL Core Analysis

The axial and radial heat generation distributions are shown in Figure 4-30 and Figure 4-31. Values used in Figure 4-30 and Figure 4-31 were produced from MCNP5 analysis as discussed earlier. From Figure 4-31 it can be seen that the innermost node extends from 0.0 to ~0.37 [cm]. This is because a zirconium pin is located in the radial center of the fuel rod, and during the conversion analysis study no homogenising of the fuel pin was performed. During the thermal hydraulics portion of the conversion analysis, it is assumed that no heat generation occurs within the central zirconium pin, although all thermo-physical properties for the zirconium pin were incorporated into the RELAP5-3D model.

All intra-fuel rod power profiles in the conversion analysis are representative of the hottest rod in the core for the given core configuration. There are 84 FLIP fuel Elements in the initial HEU core including the three control rod fuelled followers. The hot-rod peak factor is 1.376 which corresponds to a hot rod power of 18.02 kW (see Table 4-21) in the 1.1 MW_{th} steady state HEU BOL NORMAL core.

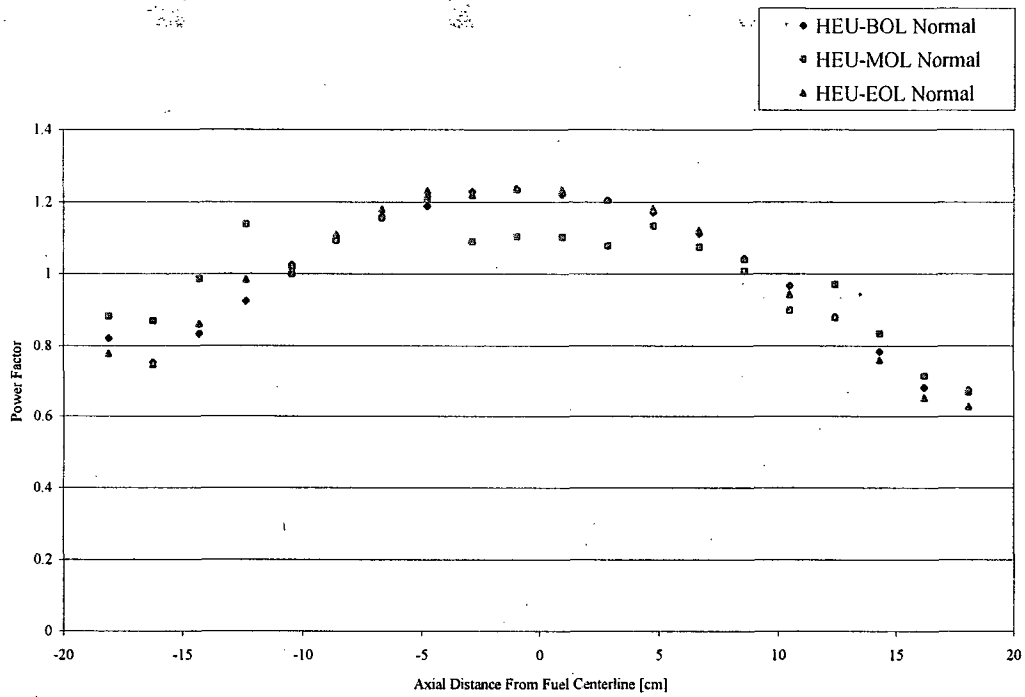

Figure 4-30 OSU HEU NORMAL Core - Axial Power Profile vs. Distance from Fuel Centerline.

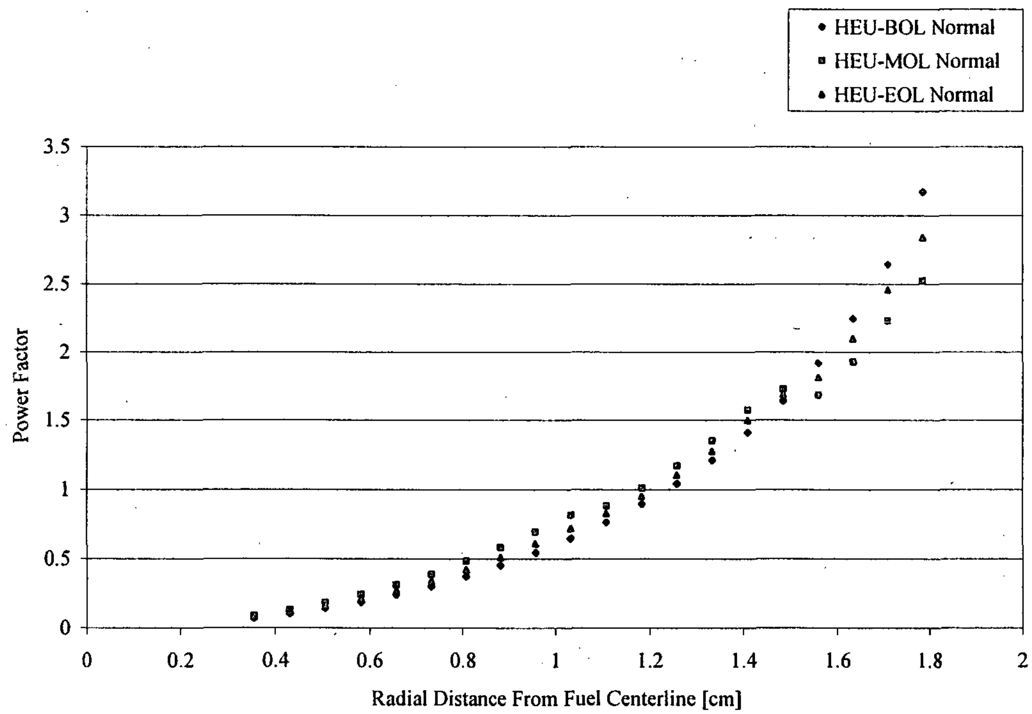

Figure 4-31 OSU HEU NORMAL Core - Radial Power Profile vs. Distance from Fuel Centerline.

The information displayed in Figure 4-31 is a graph of normalized *total power* in a fuel pin as a function of radial distance from fuel centerline. This is different from a graph of normalized *power density* in a fuel pin as a function of radial distance from fuel centerline. The normalized power density distribution in the HEU BOL NORMAL core hot rod is shown in Figure 4-32 for comparison. The total power plot can be obtained from the power density plot since total power distribution is equivalent to power density weighted by radial distance from the fuel centerline. The normalized power density distribution vector is used as a RELAP5-3D input.

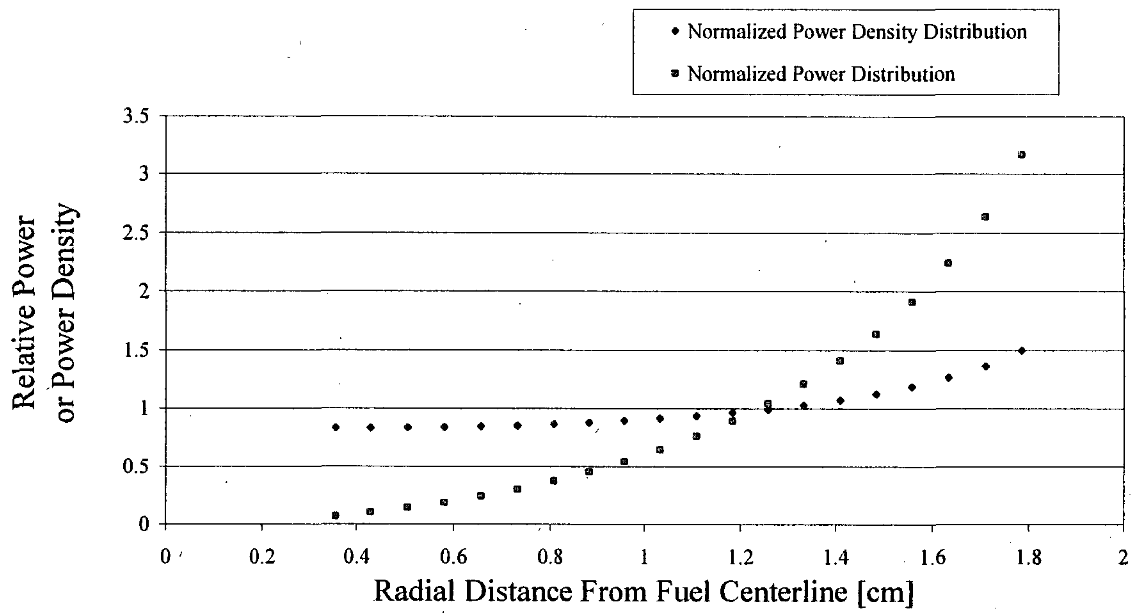

Figure 4-32 Radial Power Profile and Radial Power Density Profile vs. Distance from Fuel Centerline for the Hot Rod in the OSU HEU BOL NORMAL Core.

In Figure 4-30, it can be seen by inspection that the Hot Channel Fuel Axial Peak Factor for the HEU BOL NORMAL core has a value which is slightly higher than 1.2 (exact value = 1.236). The Hot Channel Fuel Axial Peak Factor is defined as the ratio of maximum axial power to average axial power in the hot rod. The curves in the figure have been normalized such that all three have an (unweighted) average equal to 1.0, and therefore the axial power factor can be read from the graph as the highest point on each curve.

In Figure 4-32, both curves have again been normalized such that they both have an unweighted average equal to 1.0. The peak radial power occurs at the outer radius of the fuel and has a value of 105.3 W (normalized to 3.1711). The weighted average of the power distribution curve has a value of 55.21 W (normalized to 1.6627). The Hot Channel Fuel Radial Peak Factor is thus 105.3/55.21 = 1.907. This method was used to calculate Hot Channel Fuel Radial Peak Factors shown in Table 4-21 for each of the twelve cores examined.

The driving force for flow in the OSTR core is supplied by the buoyancy of the heated water in the core. Countering this force are the contraction and expansion losses at the entrance and exits to the channel, and friction losses due to coolant to fuel element interfacial contact. A summary of the RELAP5-3D results for the OSTR HEU beginning of life NORMAL core configuration is given in Figure 4-33 through Figure 4-36. A summary of results from Figure 4-33 through Figure 4-36 is given in Table 4-22.

Table 4-22 Steady State Results for OSU HEU Beginning of life NORMAL Core.

Parameter	**Value**
Flow rate for hottest rod [kg/s]	0.0825
Maximum flow velocity [m/s]	0.2249
Maximum wall heat flux [kW/m^2]	498.28
Maximum fuel centerline temperature [°C]	447.60
Maximum clad temperature [°C]	131.27
Exit clad temperature [°C]	125.64
Exit bulk coolant temperature [°C]	101.18
MDNBR [Groeneveld 2006, Bernath]	4.844, 2.104

Figure 4-33 and Figure 4-34 show the hot channel thermal hydraulic parameters as a function of steady state hot rod power. Using the Bernath Correlation as the bounding MDNBR value, it can be seen in Figure 4-34 that the MDNBR does not reach a value of 2.0 until the hot rod produces a power of ~19.0 kW. This is approximately 105.4 % of the 18.02 kW produced by the theoretical hot rod in the 1.1 MW_{th} HEU BOL NORMAL core.

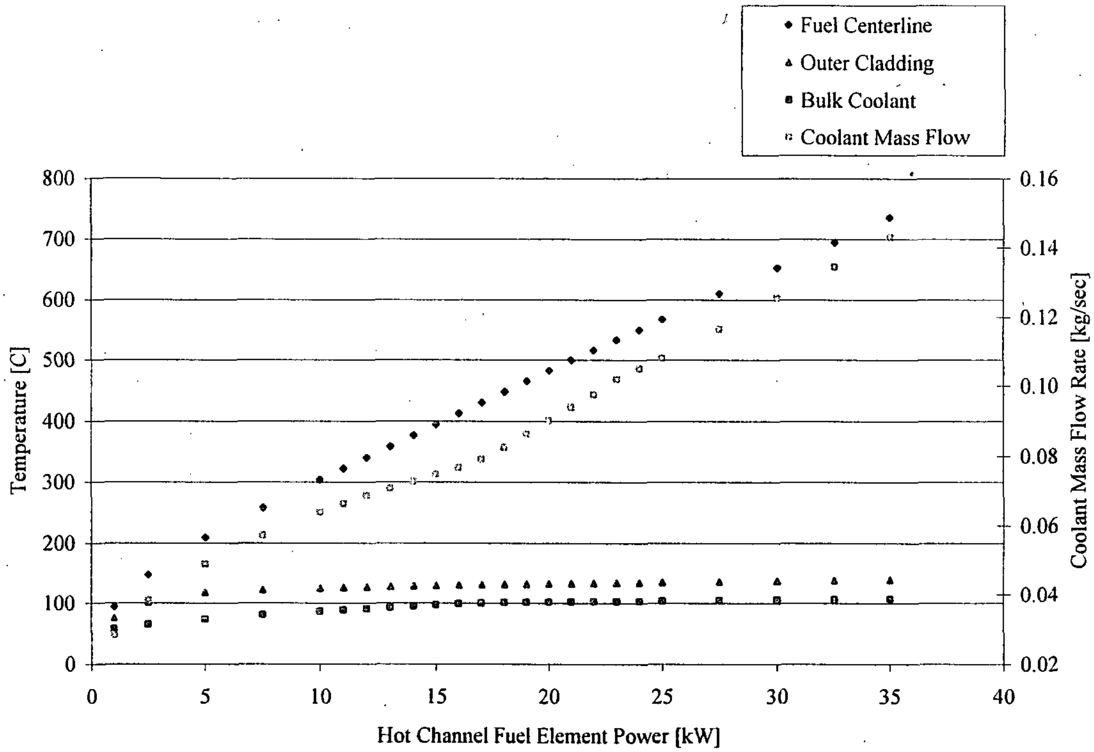

Figure 4-33 Hot Channel Properties (HEU BOL NORMAL Core).

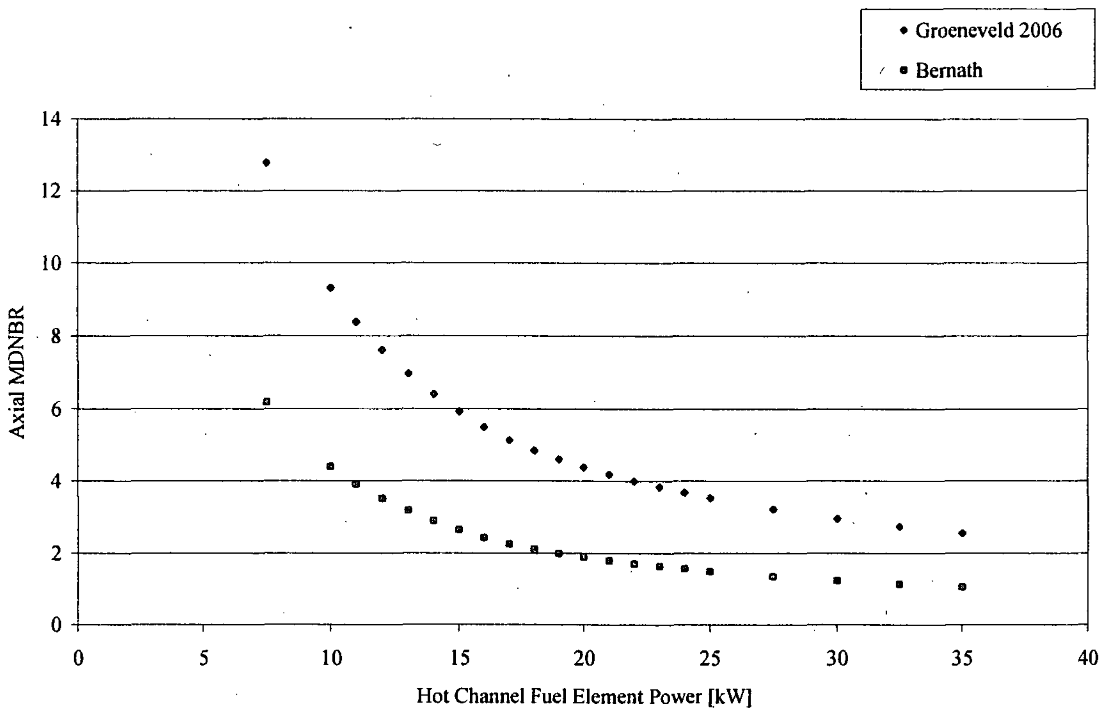

Figure 4-34 Hot Channel MDNBR (HEU-BOL NORMAL Core).

Figure 4-35 shows the axial temperature distribution within the 18.02 kW theoretical hot rod. Figure 4-36 shows the axial DNBR when the hot channel is at 18.02 kW. DNBR is calculated using the results produced from RELAP5-3D with the appropriate correction factors applied (2006 AECL-UO look-up tables or the Bernath Correlation).

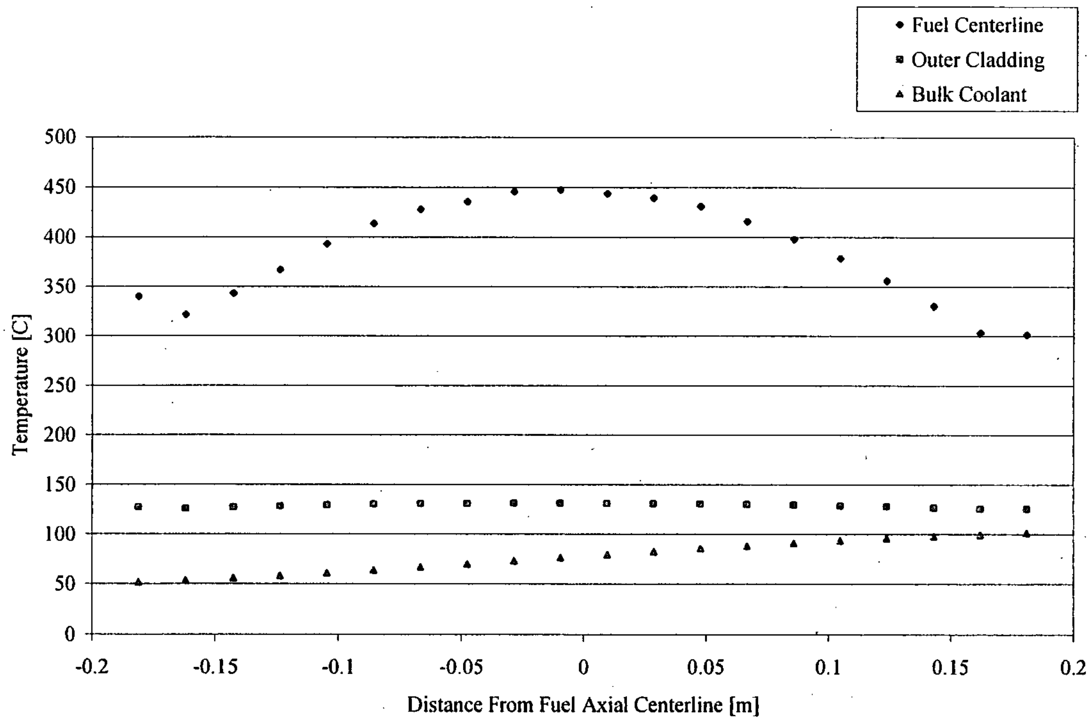

Figure 4-35 Axial Temperature Distribution at 18.02 kW (HEU-BOL NORMAL Core).

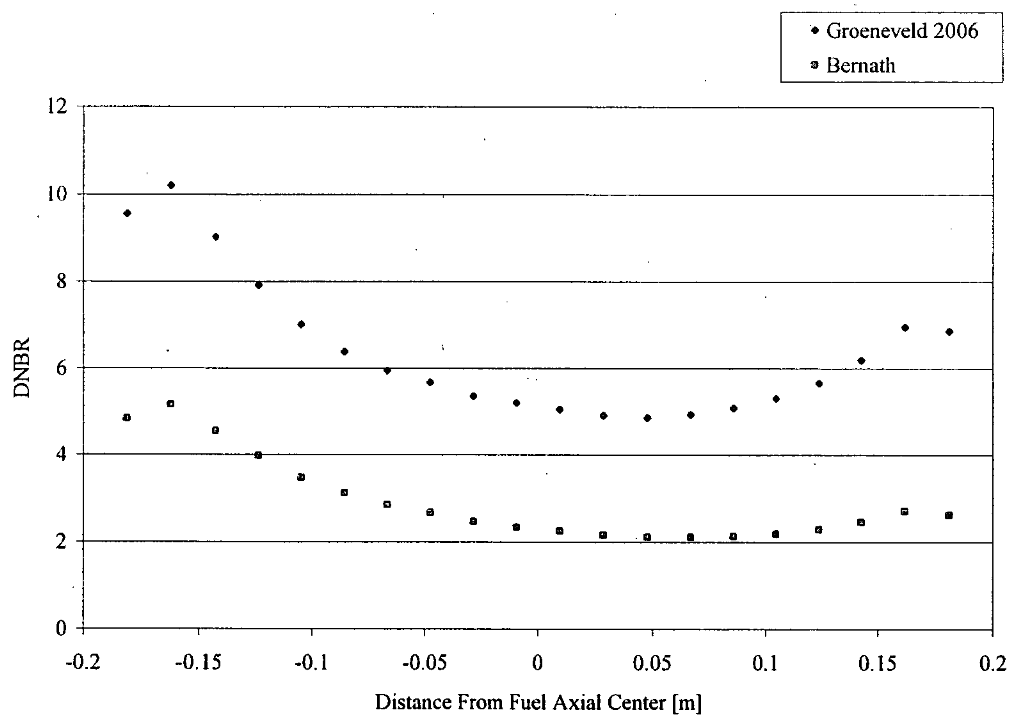

Figure 4-36 Hot Channel Axial DNBR at 18.02 kW (HEU-BOL NORMAL Core).

The OSU HEU TRIGA® fuel contains a central zirconium pin with a diameter of 6.36E-3 m. This pin is surrounded by the U-ZrH fuel meat which has an outer diameter of 0.0357 m. A small gas filled gap exists between the fuel meat and the cladding. The size of this gap is known to vary between 1.27E-6 m and 1.016E-5 m (0.05 and 0.40 mils). The stainless steel cladding thickness is 5.08E-4 m (20 mils). Twenty four radial nodes were defined to map the radial fuel element temperature distribution in the OSTR during this study. The innermost node is located at the fuel centerline and the outermost node is located at the exterior cladding surface.

At 1.1 MW_{th}, the HEU BOL NORMAL core has a corresponding 18.02 kW hot rod in the B3 position. For the HEU Beginning of Life core at a power of 1.0 MW_{th}, the temperature measured at the IFE (B4 position) ranged from 356°C to 373°C. Predicted IFE power at 1.0 MW_{th} is $17.39(1.0/1.1)=15.81$ kW. A RELAP5-3D model was run, simulating the IFE at 15.81kW while using a gap thickness of 0.1 mills and produced Figure 4-37. Predicted steady state IFE temperature is larger than measured steady state IFE temperature by approximately

17°C or 34°C, depending on which IFE temperature is used from Table 4-23. Use of a 0.1 mil gap is thus conservative, and therefore all other core calculations use a gap thickness of 0.1 mills.

The content of the gap gases was chosen to be the default setting for RELAP which assumes a mixture of He, Kr, and Xe at molar fractions of 0.1066, 0.134 and 0.7594, respectively. Although the backfill gas at the BOL for TRIGA® fuel is air, the content at MOL and EOL is unknown. However, because of the difference in thermal conductivity between the gas mixtures is different, the default RELAP mixture will produce higher fuel temperatures and is therefore conservative.

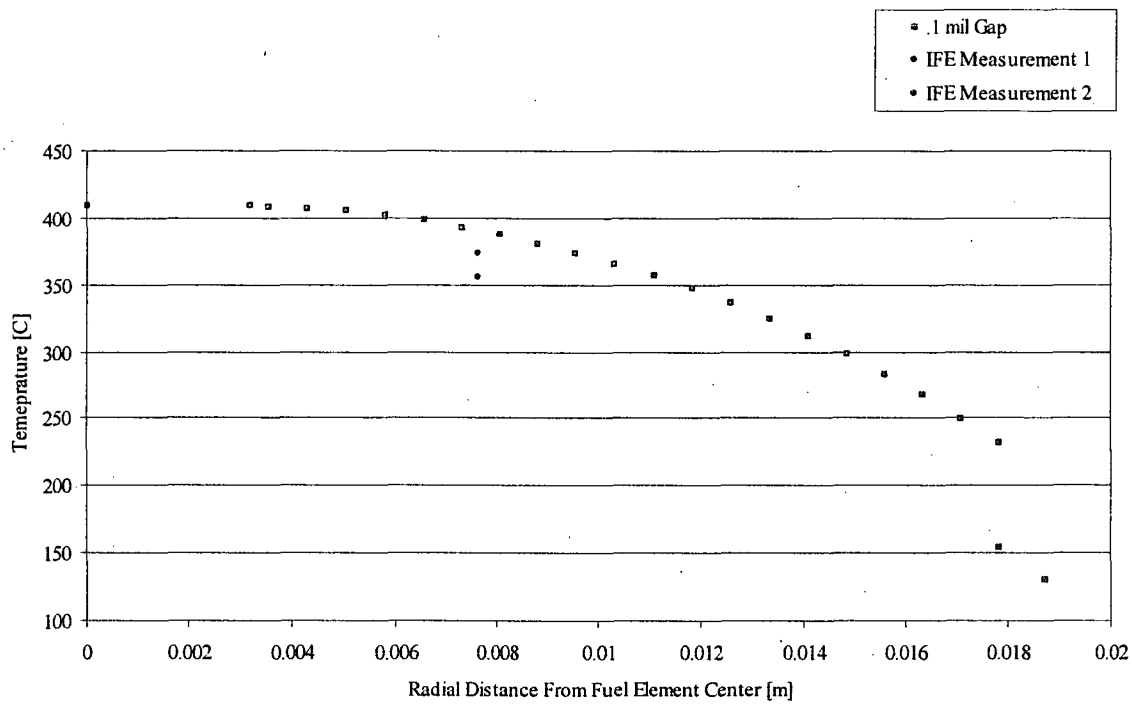

Figure 4-37 IFE Radial Temperature Distribution at 15.81 kW (HEU-BOL NORMAL Core).

The radial temperature distribution in the hot rod at the hottest axial elevation is shown in Figure 4-38. Figure 4-39 shows the radial temperature distribution in the hot rod with a core power of 1.1 MW_{th}. The different curves correspond to different values of the fuel to clad gap ranging from 1.27E-4 to 1.016E-3 m (0.05 to 0.4 mils). The hot rod in the BOL HEU core is located in position B3. The Instrumented Fuel Element (IFE) in the BOL HEU core is located in position B4. A summary of the HEU Beginning of life core temperature results is shown in Table 4-23. These results are based on a 0.1 mil fuel to clad gap.

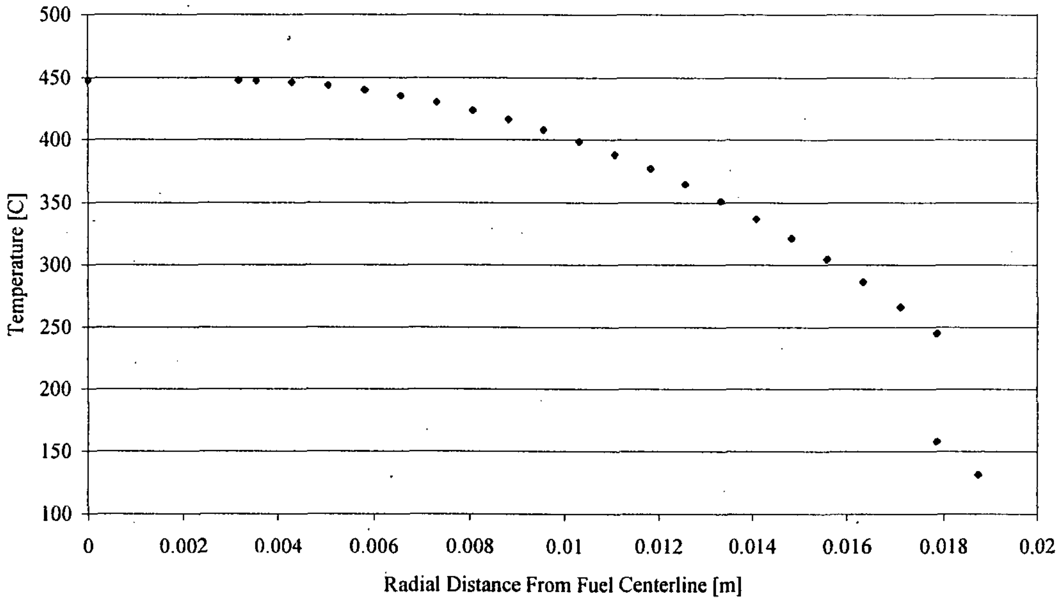

Figure 4-38 Radial Fuel Temperature Distribution at 18.02 kW (HEU-BOL NORMAL Core).

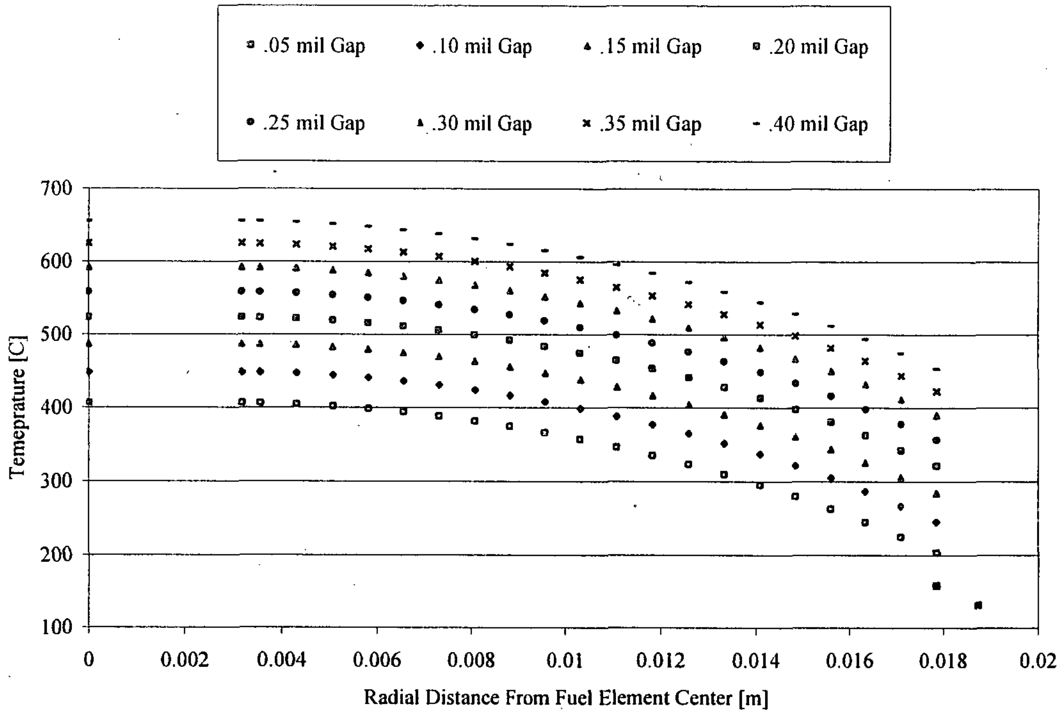

Figure 4-39 Fuel Element Radial Temperature Distribution at 1.1 MW_{th}.

For pulse calculations a 0.1 mil gap is also justified. Pulse characteristics are typically adiabatic and thus insensitive to gap size. Furthermore, at the high fuel temperatures expected during the limiting pulse, differential radial expansion will significantly reduce gap size.

Table 4-23 Calculated and Measured Fuel Temperatures, OSU HEU Beginning of Life Core

$P_{hot\text{-}channel}$ (kW)	Measured [°C]	Calculated [°C]			
	T_{IFE}	T_{max}	$T_{0.3}$	T_{clad}	$T_{coolant}$
14.00	356, 373*	377	360	129	95
16.00		412	394	130	99
18.02		448	427	131	101
20.00		482	459	132	102
22.00		517	491	133	103

* Initial measured values, HEU BOL NORMAL core at 1.0 MW_{th}.

4.7.5 HEU End of Life NORMAL Core Pulse Analysis

The pulse analysis was conducted by implementing the point reactor kinetics model in RELAP5-3D as previously discussed. An adjacent subchannel was modelled next to the hot channel simulating the remaining fuel elements in the HEU End of Life NORMAL Core. All Doppler feedback characteristics calculated by RELAP refer to the core average properties produced by the adjacent subchannel.

While the technical specifications require that the SCRAM after a pulse occurs prior to 15.0 seconds, in reality a high voltage SCRAM occurs ~0.5 seconds after the transient rod is ejected. This analysis assumes that the transient rod remains out of the core for 15.0 seconds and then is fully inserted back into the core, providing the most limiting condition for a pulse. Figure 4-40 presents the prompt total core power and energy trace produced in the RELAP5-3D model after inserting $2.00 of reactivity out to 0.25 seconds.

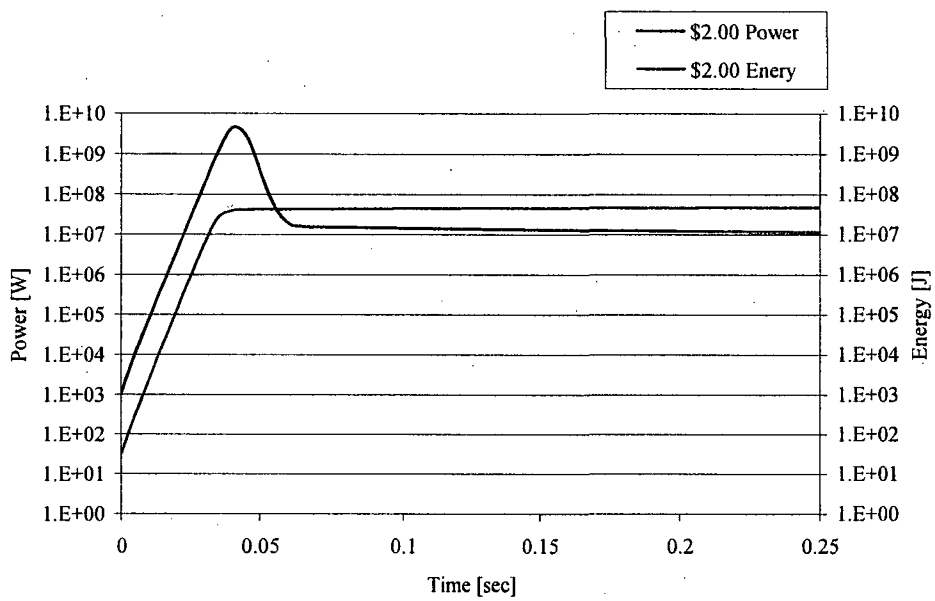

Figure 4-40 HEU EOL NORMAL Core $2.00 Short Power/Energy Trace

The HEU EOL core is analysed in order to allow comparison with data contained in the HEU SAR as seen in Figure 4-41. The HEU core at EOL is considered to be the most limiting HEU core since it has the prompt temperature reactivity coefficient of the smallest magnitude, and thus a pulse due to a given amount of reactivity at EOL will be larger than a pulse due to the same amount of reactivity at other times in core life.

The maximum adiabatic core temperature reached in a pulse is directly related to the energy released during the pulse, which is the integral of core power over the duration of the pulse. Changes in the peak power reached in a pulse have little effect on this maximum temperature, as the reactor is only in the maximum power state for a small fraction of the total pulse duration, particularly for larger reactivity insertions.

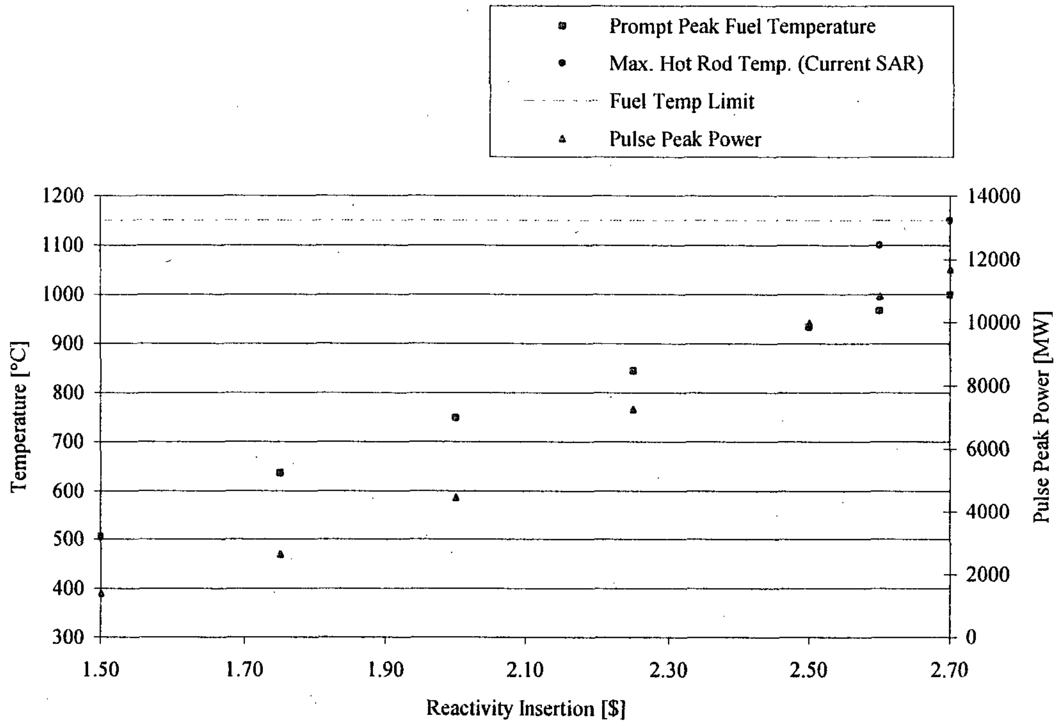

Figure 4-41 Pulse Results Summary (HEU EOL NORMAL Core).

As mentioned, during the pulse analysis the transient rod is held withdrawn from the core for a total of 15.0 seconds. This is the maximum time allowed in the technical specifications. The initial prompt power transient during a pulse produces a peak fuel temperature within ~0.05 seconds after the initial rod motion. This can be seen for the $2.00 pulse in Figure 4-42. The peak fuel temperature is physically located on the outer surface of the fuel. The radial temperature distribution can be seen in Figure 4-43 and clearly shows this at the moment the peak fuel temperature is reached.

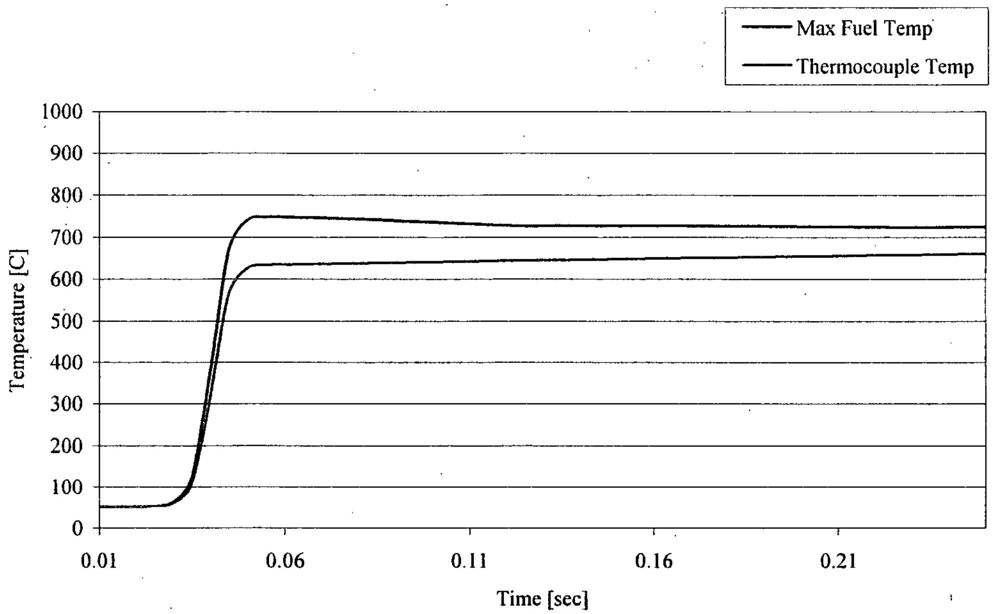

Figure 4-42 HEU End of Life, Hot Channel Pulse Fuel Temperatures ($2.00 Insertion)

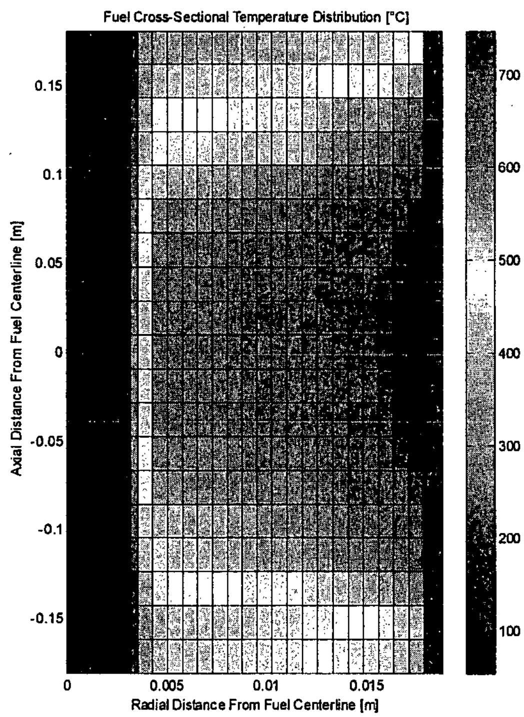

Figure 4-43 HEU EOL Fuel Temperature distribution at Time of Max Fuel Temperature

In the HEU SAR, the peak fuel temperature is identified as 1100°C for a reactivity insertion of $2.59 and 1150°C for a reactivity insertion of $2.70. Peak temperatures predicted by the methods used in this conversion SAR are 966.3°C for a $2.59 pulse and 999.1°C for a $2.70 pulse. The effective hot rod peak factor for the HEU SAR in the HEU EOL core is 3.41, while the effective hot rod peak factor used during this conversion analysis is 2.68 for the HEU EOL core. This difference in effective peak factor is partially responsible for the lower values of maximum fuel temperature produced during this conversion analysis study. Differences between the prompt reactivity coefficient used in the HEU SAR and the coefficient used in the conversion SAR also affect predicted peak temperatures. It should also be noted that the typical peak fuel temperature measured by the IFE during a $2.00 pulse are approximately ~325°C. This suggests that the PRKM in RELAP predicts values that are significantly conservative when compared to measured data.

4.7.6 LEU Power Summary

The LEU Core power distributions, as well as the intra-fuel relative power distribution (radial and axial distribution in the hot rod) are provided in Figure 4-44 through Figure 4-58. Power distribution diagrams are used to derive Hot Channel Peak Factors. Axial hot channel power profiles are used to derive Hot Channel Fuel Axial Peak Factors. Radial hot channel power profiles are used to calculate Hot Channel Fuel Radial Peak Factors. The hot channel peak factor, axial power distribution and radial power distribution are used as RELAP5-3D inputs. All peak factors for HEU and LEU cores at BOL, MOL and EOL are tabulated in Table 4-21.

Figure 4-44 Core Power Distribution (LEU BOL NORMAL Core).

Figure 4-45 Core Power Distribution (LEU MOL NORMAL Core).

Figure 4-46 Core Power Distribution (LEU EOL NORMAL Core).

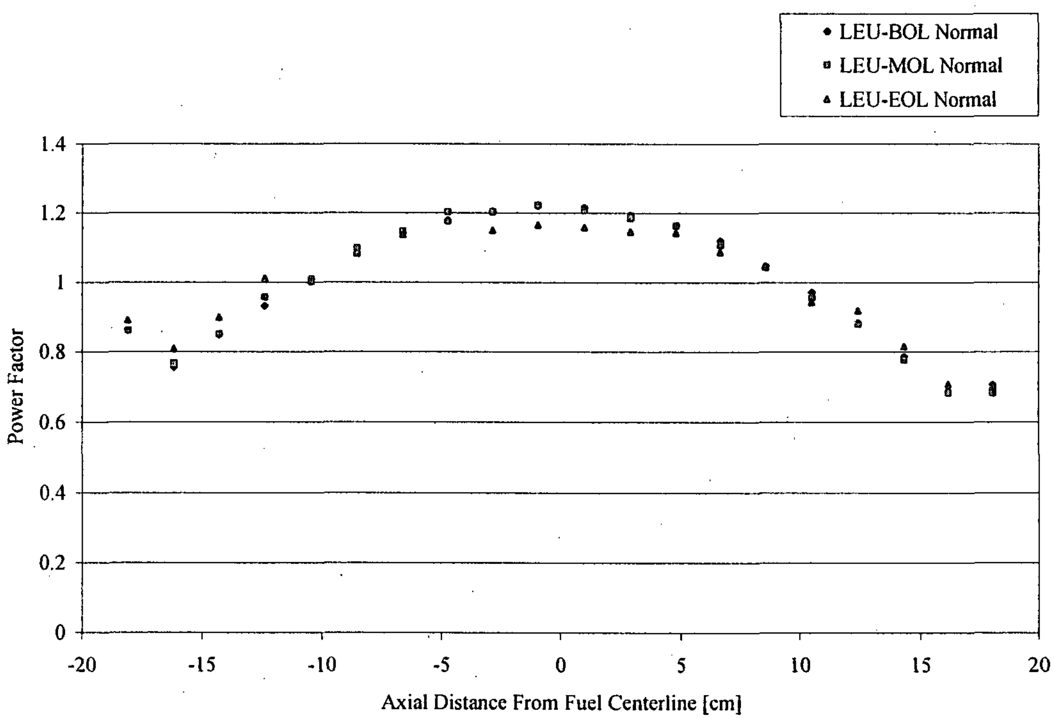

Figure 4-467 OSU LEU - Axial Power Profile vs. Distance from Fuel Centerline.

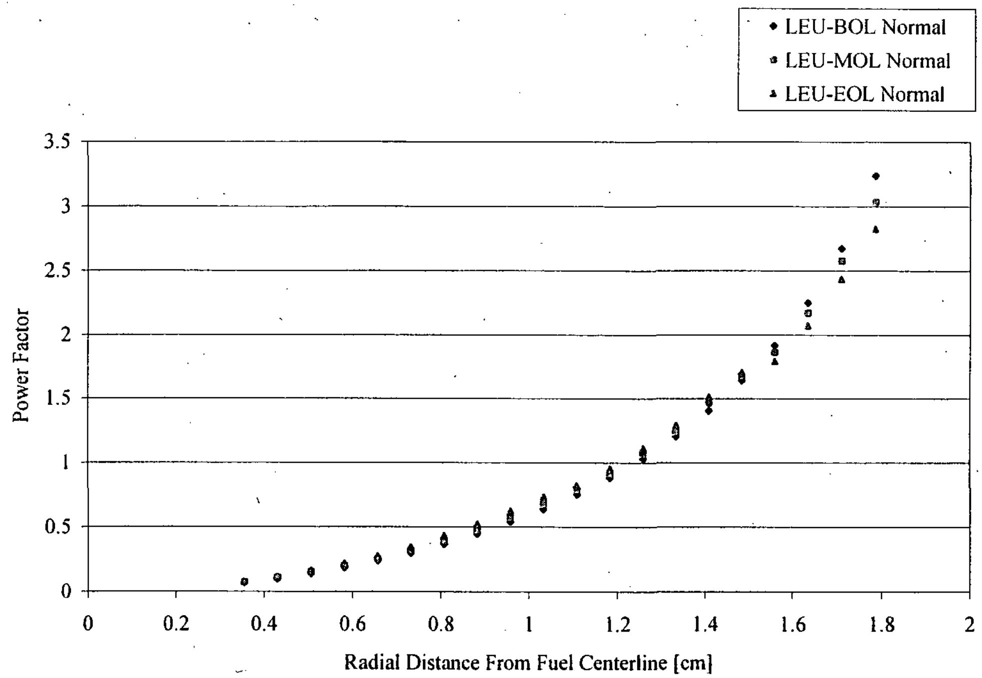

Figure 4-48 OSU LEU -Radial Power Profile vs. Distance from Fuel Centerline.

Figure 4-49 Core Power Distribution (LEU BOL ICIT Core).

Figure 4-50 Core Power Distribution (LEU MOL ICIT Core).

Figure 4-51 Core Power Distribution (LEU EOL ICIT Core).

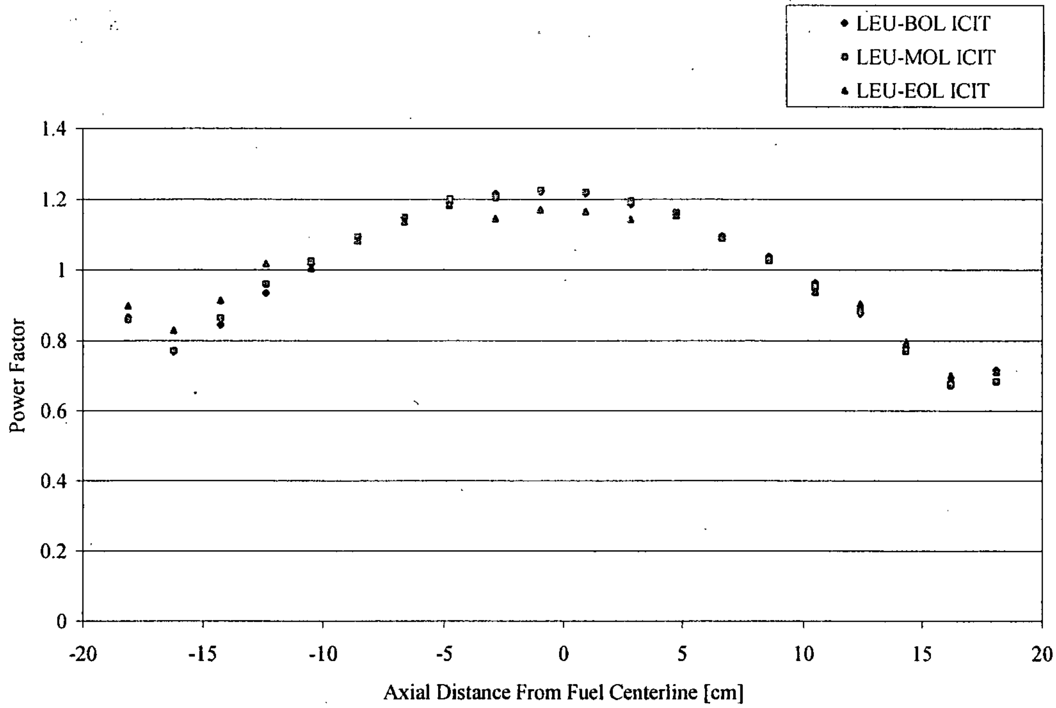

Figure 4-52 Axial Power Factor (LEU ICIT Core).

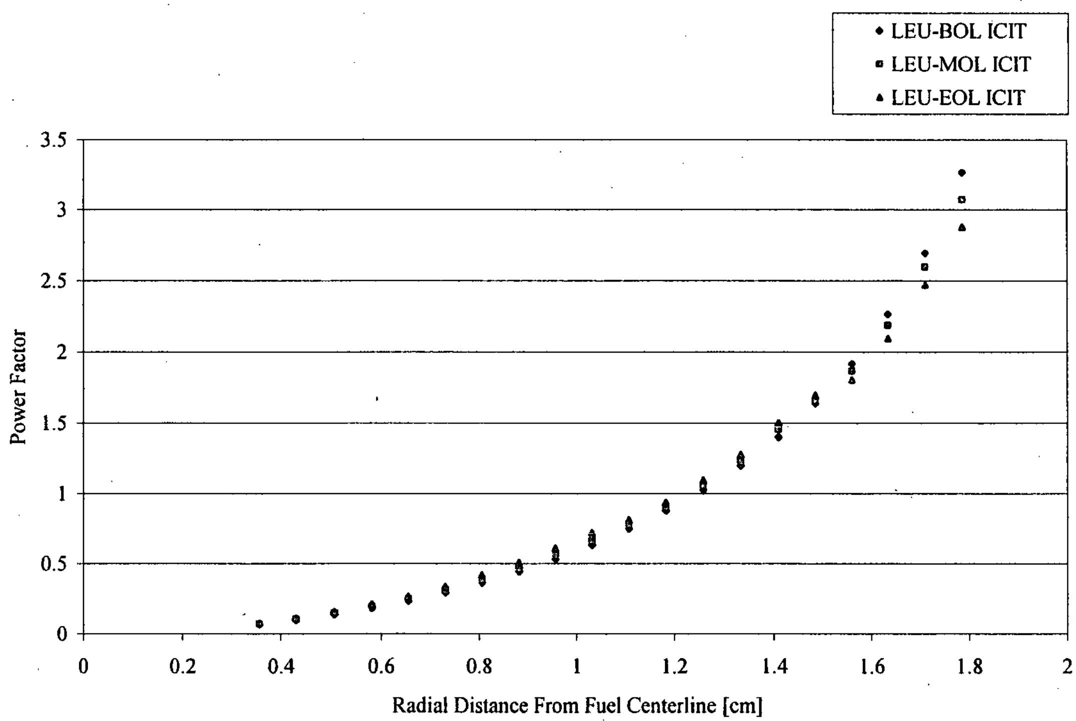

Figure 4-53 Radial Power Factor (LEU ICIT Core).

Figure 4-54 Core Power Distribution (LEU BOL CLICIT Core).

Figure 4-55 Core Power Distribution (LEU MOL CLICIT Core).

Figure 4-56 Core Power Distribution (LEU EOL CLICIT Core).

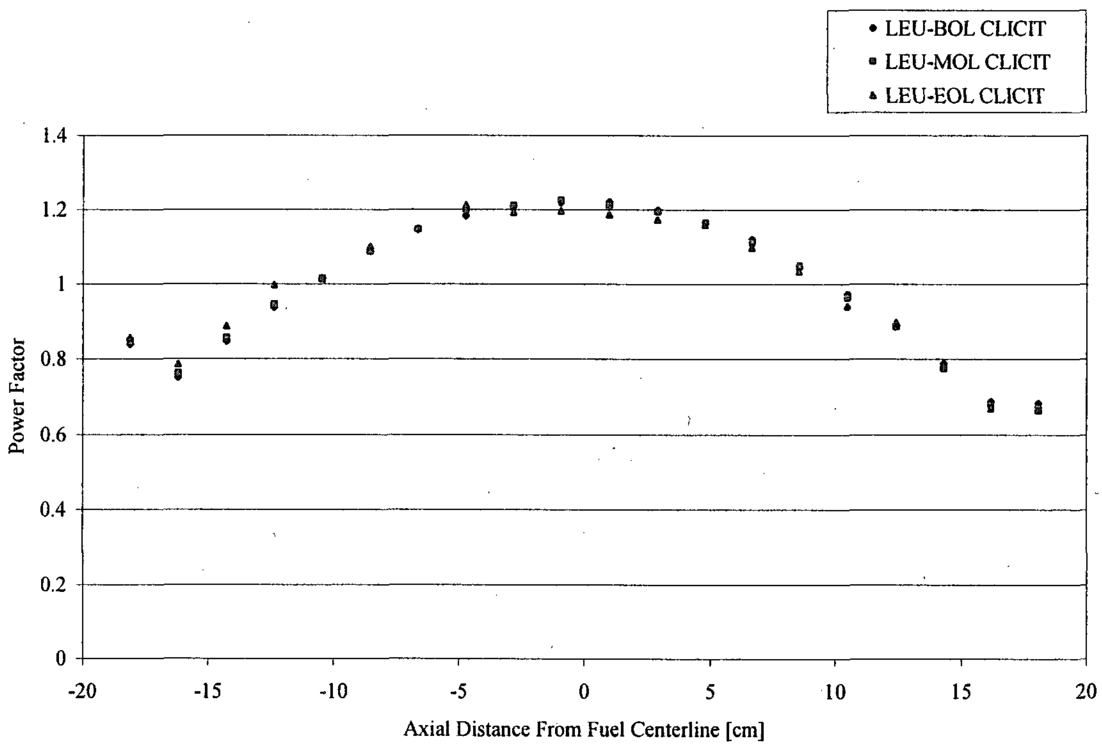

Figure 4-57 Axial Power Factor (LEU CLICIT Core).

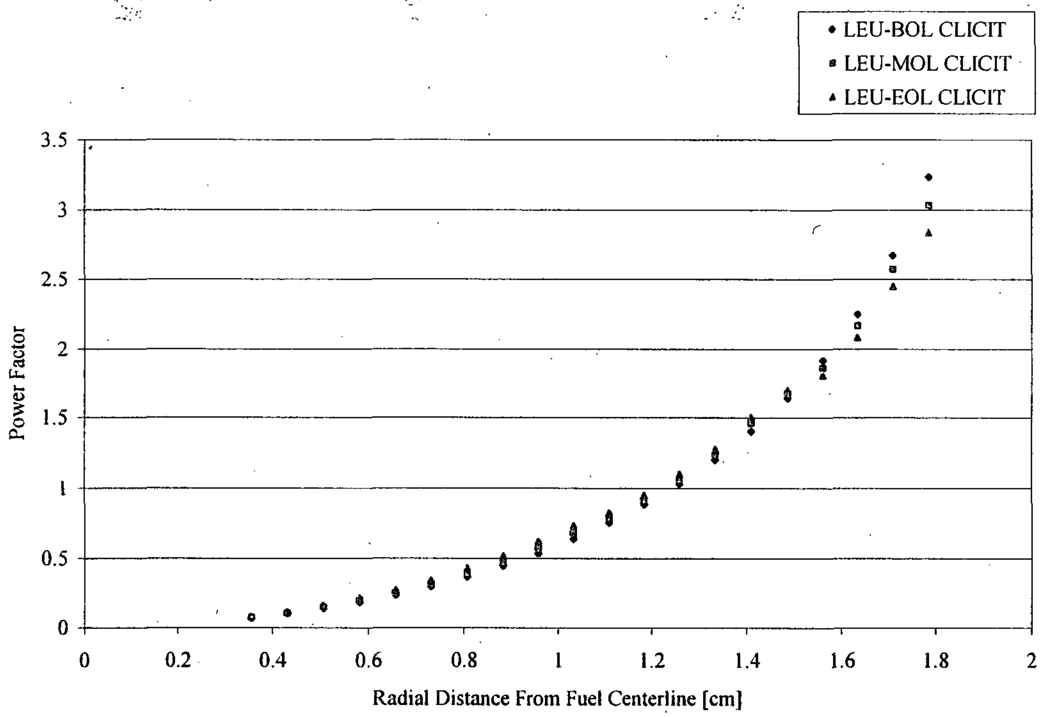

Figure 4-58 Radial Power Factor (LEU CLICIT Core).

4.7.7 LEU Beginning of Life ICIT Core Analysis

All LEU core configurations (NORMAL, ICIT and CLICIT) contain fuel elements that are geometrically similar and therefore the hot channel geometric parameters (i.e. hydraulic diameter, length, etc.) do not change from those defining the HEU Core (Table 4-17 and Table 4-18). The hot channel power summary in terms of parameters and results are given in Table 4-24 andTable 4-25, respectively. Figure 4-46752 and Figure 4-4853 represent the axial and radial intra-fuel power profiles for the LEU beginning, middle, and end of life ICIT core configurations. Figures 4-59 through 4-63 graphically illustrate the results of the analysis on the LEU ICIT BOL core.

Table 4-24 Steady State Results for LEU BOL ICIT core at 1.1 MW_{th}.

Parameter	**Value**
Flow rate for hottest rod [kg/s]	0.0843
Maximum flow velocity [m/s]	0.2339
Maximum wall heat flux [kW/m^2]	504.49
Maximum fuel centerline temperature [°C]	448.13
Maximum clad temperature [°C]	131.93
Exit clad temperature [°C]	126.36
Exit bulk coolant temperature [°C]	101.32
MDNBR [Groeneveld 2006, Bernath]	4.796, 2.083

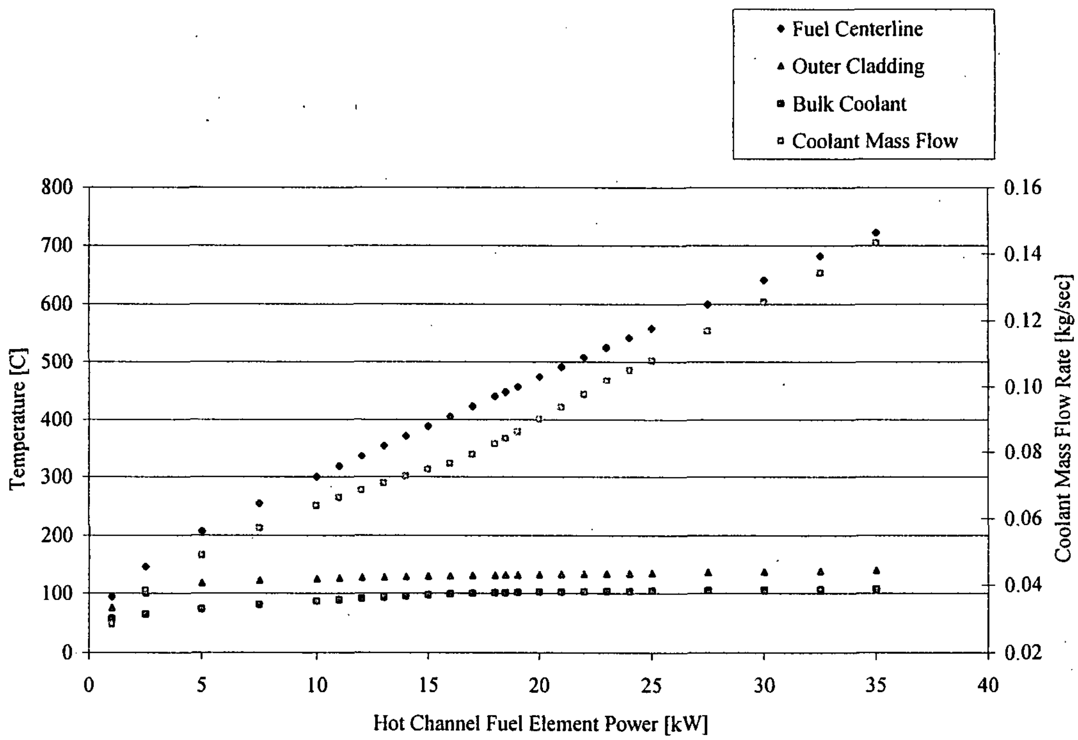

Figure 4-59 Hot Channel Properties (LEU BOL ICIT Core).

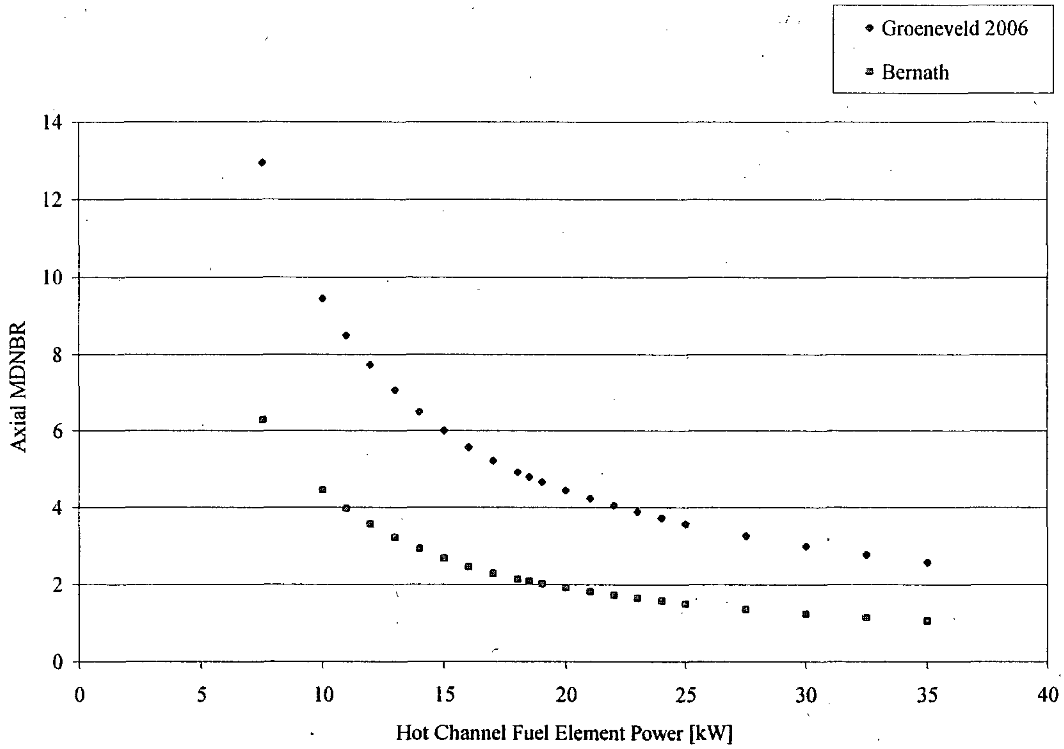

Figure 4-60 Hot Channel MDNBR (LEU BOL ICIT Core).

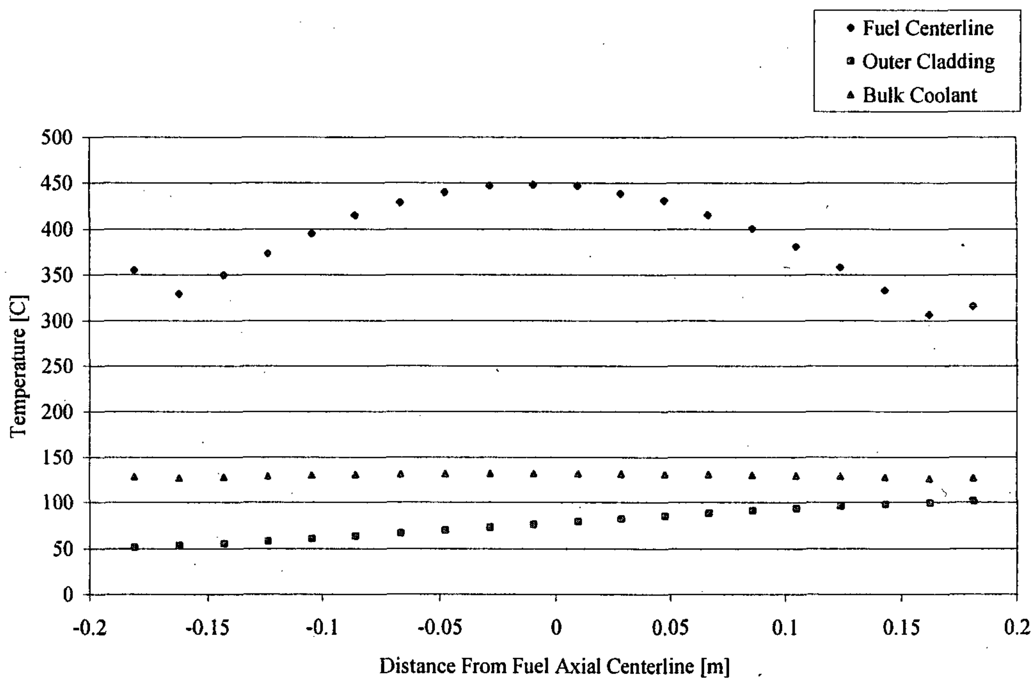

Figure 4-61 Axial Temperature Distribution at 18.47 kW (LEU BOL ICIT Core)

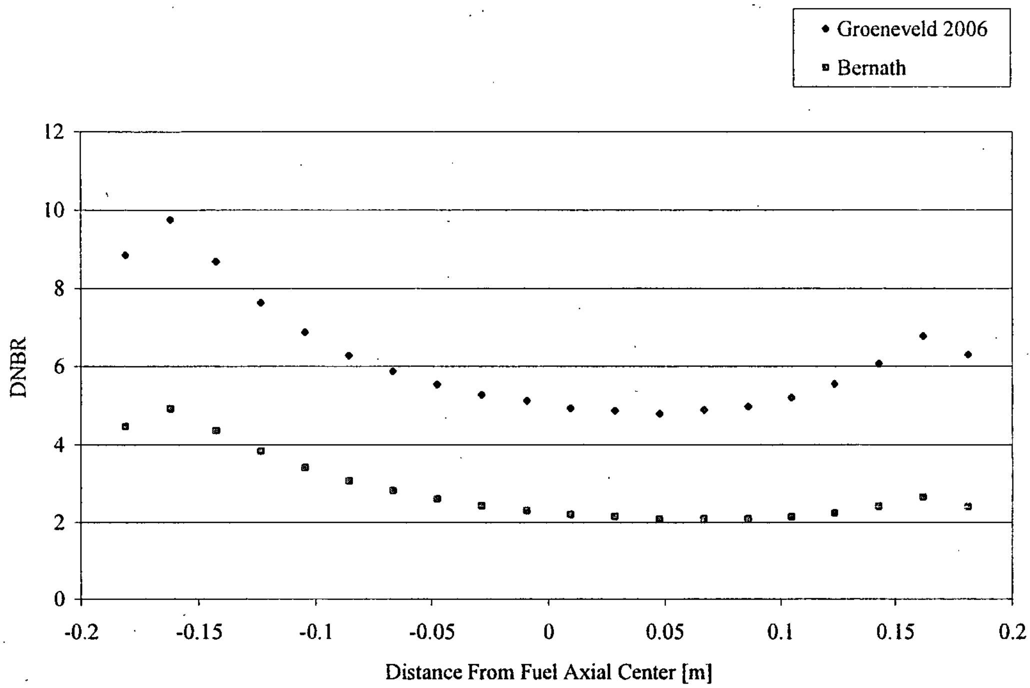

Figure 4-62 Hot Channel Axial DNBR at 18.47 kW (LEU BOL ICIT Core).

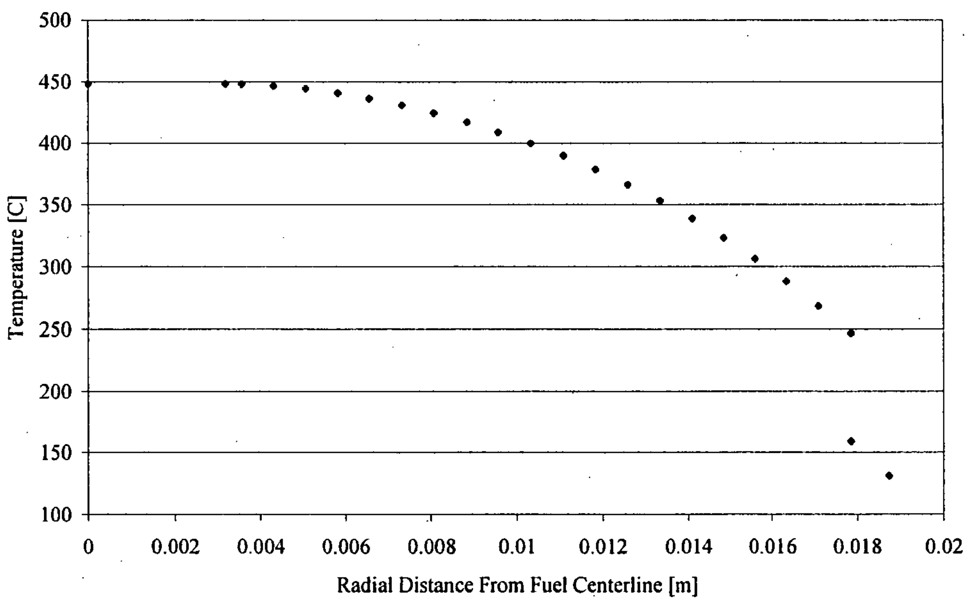

Figure 4-63 Radial Temperature Distribution at 18.47 kW (LEU BOL ICIT Core).

Table 4-25 Calculated Fuel Temperatures for Various Channel Powers in the LEU BOL ICIT Core.

$P_{hot\text{-}channel}$ (kW)	Calculated [°C]			
	T_{max}	$T_{0.3}$	T_{clad}	$T_{coolant}$
14.00	371	358	129	95
16.00	406	391	130	99
18.47	448	431	131	101
20.00	474	455	132	102
22.00	508	487	133	103

The LEU steady state results shown above are for the ICIT core configuration. The LEU BOL ICIT core has a higher effective peaking factor than the LEU BOL CLICIT core or the LEU BOL NORMAL core, and thus is the bounding core for steady state operation. The ICIT core configuration has a MDNBR of 2.083 at 1.1 MW_{th} steady state using the Bernath Correlation. Figure 4-60 shows that the MDNBR in the hot channel will reach a value of 2.00 at approximately 20.0 kW hot channel steady state power. This is 108.3% of the 18.47 kW produced in the hot channel of the LEU BOL ICIT core operating at 1.1 MW_{th}. Using either the Bernath or the Groeneveld 2006 correlations, the LEU BOL ICIT core is operating at power well below that required for departure from nucleate boiling.

4.7.8 LEU Middle of Life ICIT Core Analysis

The results for the LEU Middle of Life ICIT Core Analysis are presented in this section. Hot rod temperature profiles are shown in Figures 4-64, 4-66 and 4-68. The hot channel peak factors used in this analysis are shown in Table 4-21. The hot channel power summary of parameters and results are given in Tables 4-26 and 4-27.

Table 4-26 Steady State Results for LEU MOL ICIT core at 1.1 MW_{th}

Parameter	Value
Flow rate for hottest rod [kg/s]	0.0844
Maximum flow velocity [m/s]	0.2352
Maximum wall heat flux [kW/m^2]	507.74
Maximum fuel centerline temperature [°C]	457.66
Maximum clad temperature [°C]	131.46
Exit clad temperature [°C]	125.98
Exit bulk coolant temperature [°C]	101.40
MDNBR [Groeneveld 2006, Bernath]	4.754, 2.06

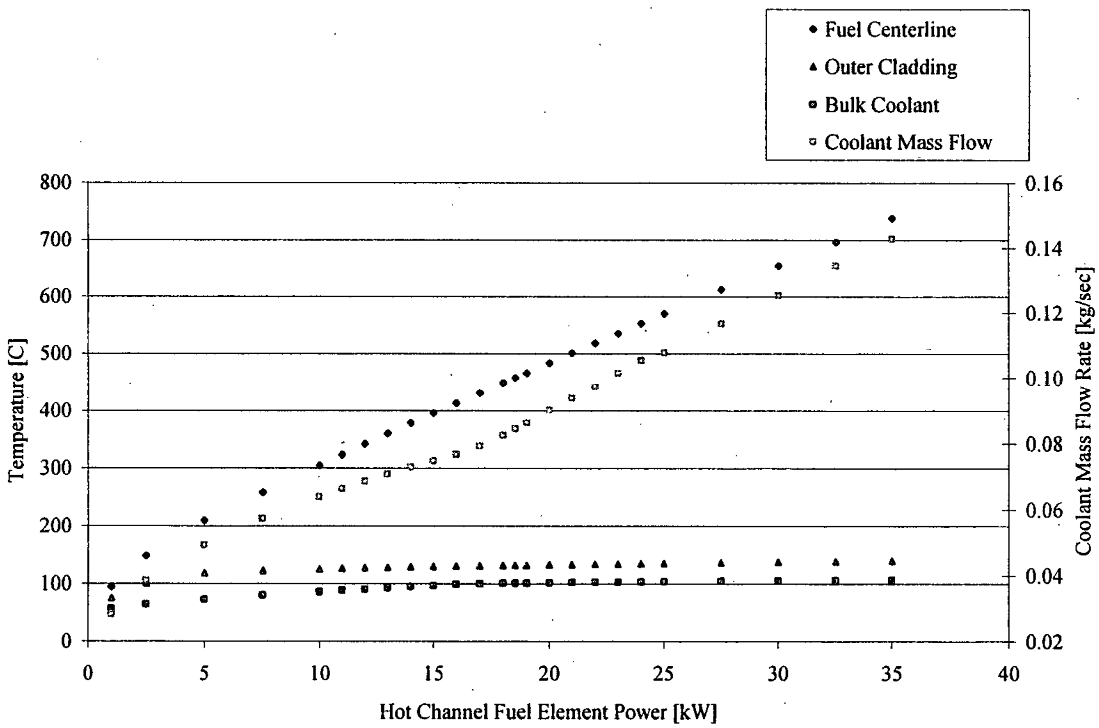

Figure 4-64 Hot Channel Properties (LEU MOL ICIT Core).

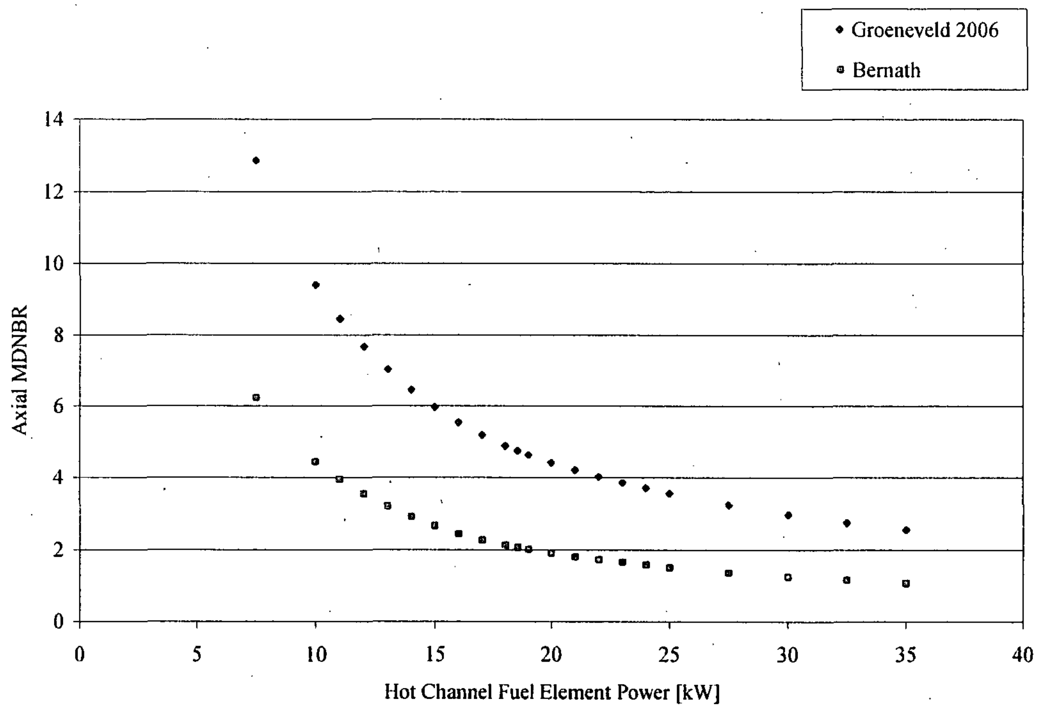

Figure 4-65 Hot Channel MDNBR (LEU MOL ICIT Core).

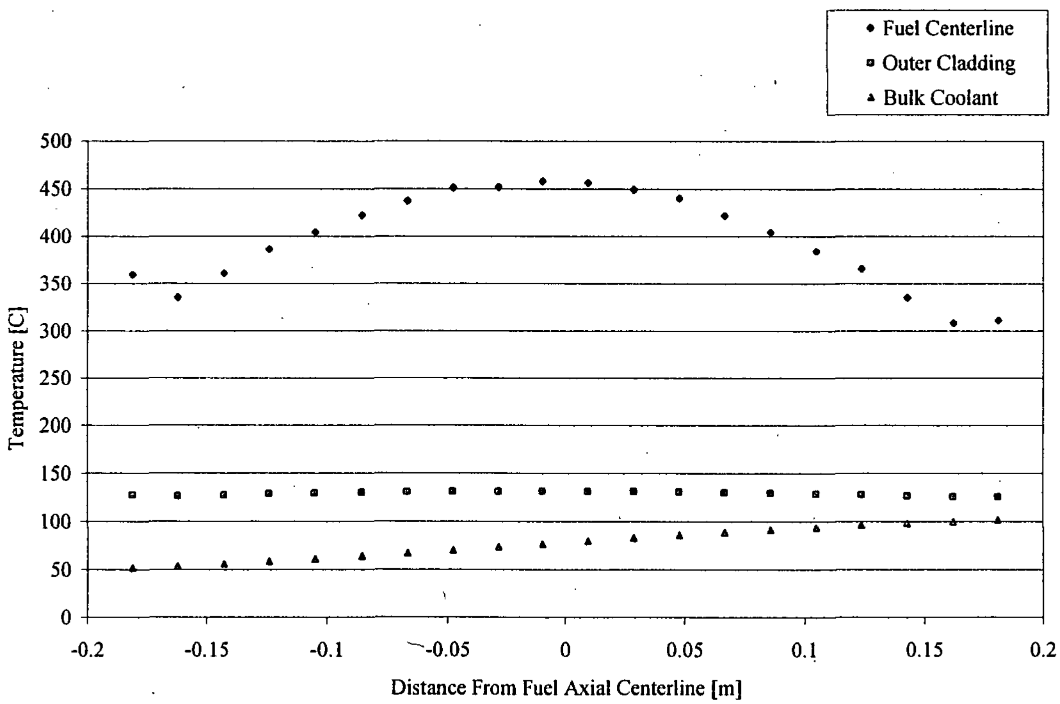

Figure 4-66 Axial Temperature Distribution at 18.52 kW (LEU MOL ICIT Core).

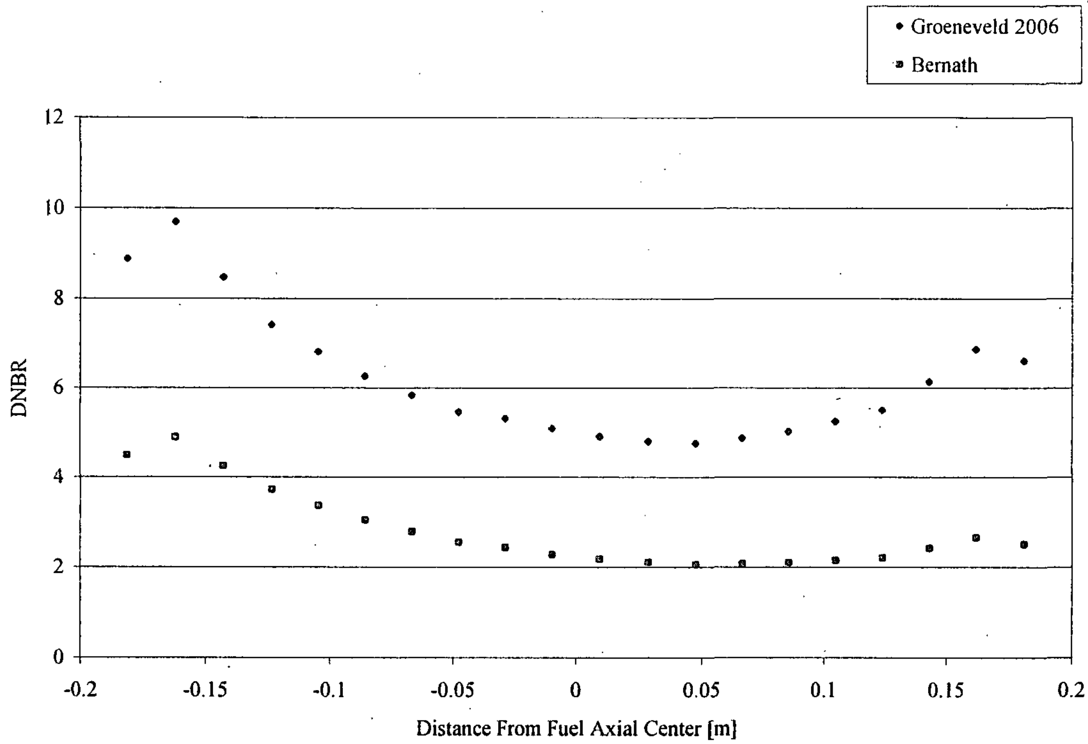

Figure 4-67 Hot Channel Axial DNBR at 18.52 kW (LEU MOL ICIT Core).

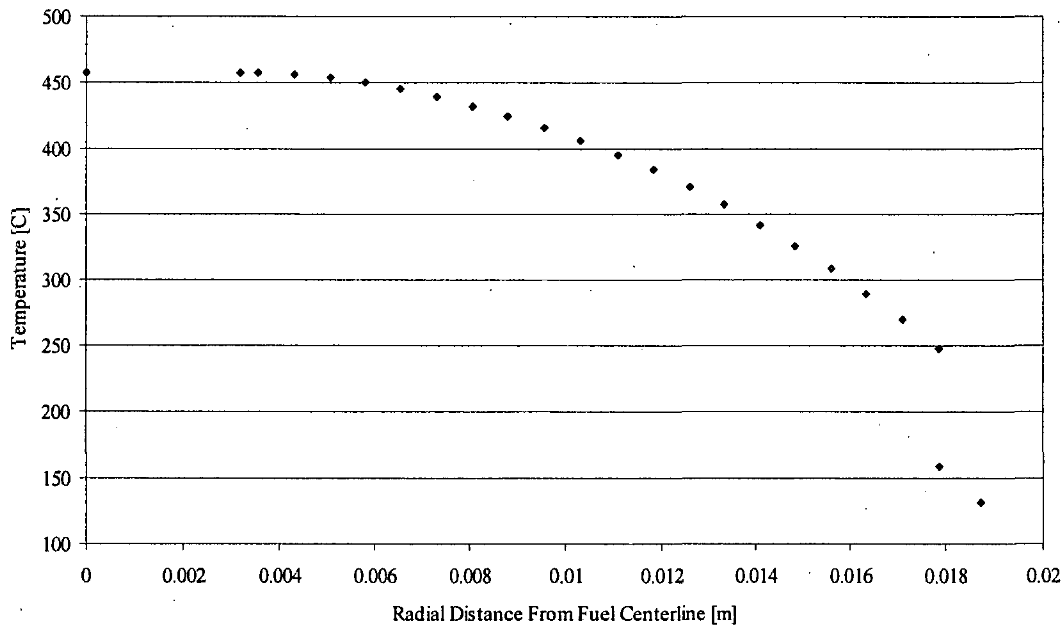

Figure 4-68 Radial Fuel Temperature Distribution at 18.52 kW (LEU MOL ICIT Core).

Table 4-27 Calculated Fuel Temperatures for Various Channel Powers in the LEU MOL ICIT Core.

$P_{hot\text{-}channel}$ (kW)	Calculated Temperature[°C]			
	T_{max}	$T_{0.3}$	T_{clad}	$T_{coolant}$
14.00	378	361	129	95
16.00	413	394	130	99
18.52	458	436	131	101
20.00	483	460	132	102
22.00	518	492	133	103

The LEU steady state results shown above are for the ICIT core configuration. The LEU BOL ICIT core has a higher effective peaking factor than the LEU BOL CLICIT core or the LEU BOL NORMAL core, and thus is the bounding core for steady state operation. The ICIT core configuration has a MDNBR of 2.06 at 1.1 MW_{th} steady state using the Bernath Correlation. Figure 4-67 shows the axial DNBR at the predicted hot rod power. Figure 4-65 shows that the MDNBR in the hot channel will reach a value of 2.00 at approximately 19.85 kW hot channel steady state power. This is 107.2% of the 18.52 kW produced in the hot channel of the LEU BOL ICIT core operating at 1.1 MW_{th}. Using either the Bernath or the Groeneveld 2006 correlations, the LEU BOL ICIT core is operating at power well below that required for departure from nucleate boiling.

4.7.9 LEU End of Life ICIT Core Analysis

The results for the LEU Middle of Life ICIT Core Analysis are presented in this section. Hot rod temperature profiles are shown in Figure 4-7169, 4-71 and Figure 4-7373. The hot channel peak factors used in this analysis are shown in Table 4-21. The hot channel power summary of parameters and results are given in Table 4-28 and Table 4-29.

Table 4-28 Steady State Results for LEU EOL ICIT core at 1.1 MW_{th}.

Parameter	Value
Flow rate for hottest rod [kg/s]	0.0812
Maximum flow velocity [m/s]	0.2245
Maximum wall heat flux [kW/m²]	465.55
Maximum fuel centerline temperature [°C]	438.39
Maximum clad temperature [°C]	130.57
Exit clad temperature [°C]	125.87
Exit bulk coolant temperature [°C]	100.78
MDNBR [Groeneveld 2006, Bernath]	5.048, 2.202

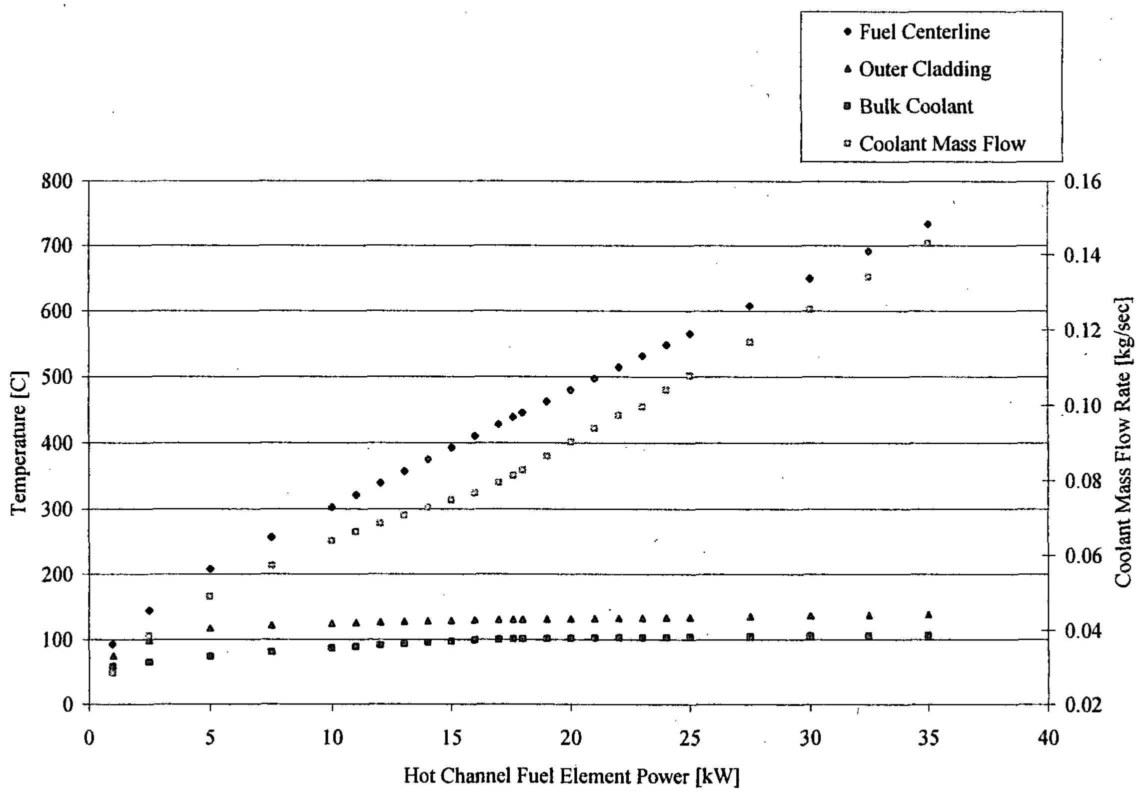

Figure 4-69 Hot Channel Properties (LEU EOL ICIT Core).

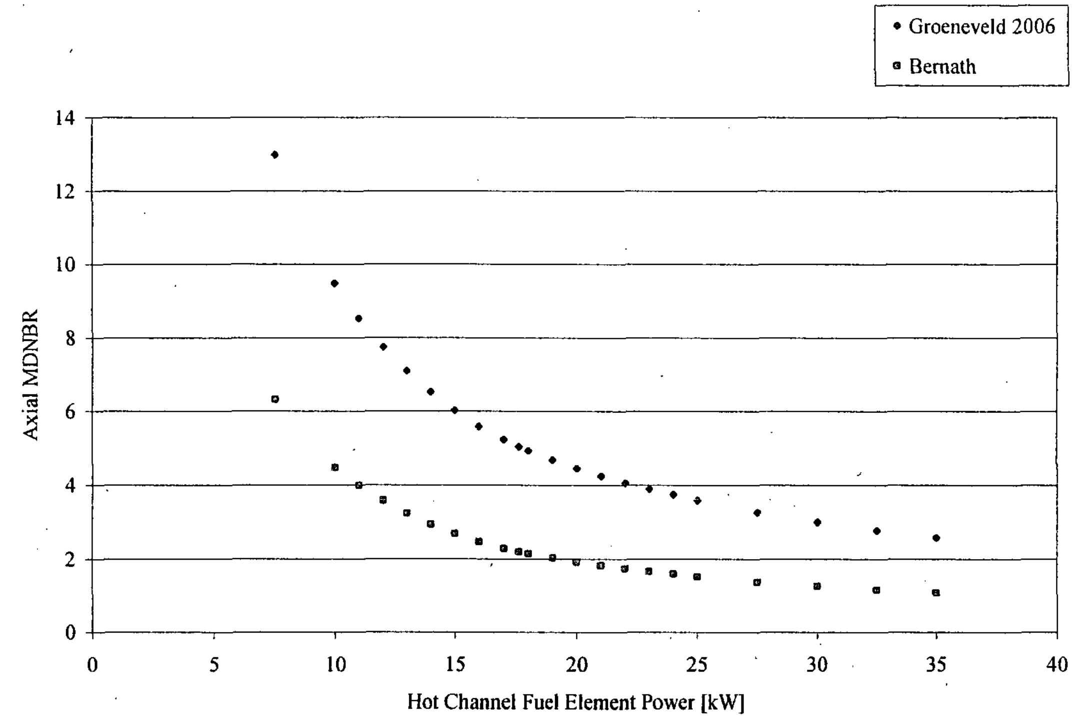

Figure 4-70 Hot Channel MDNBR (LEU EOL ICIT Core).

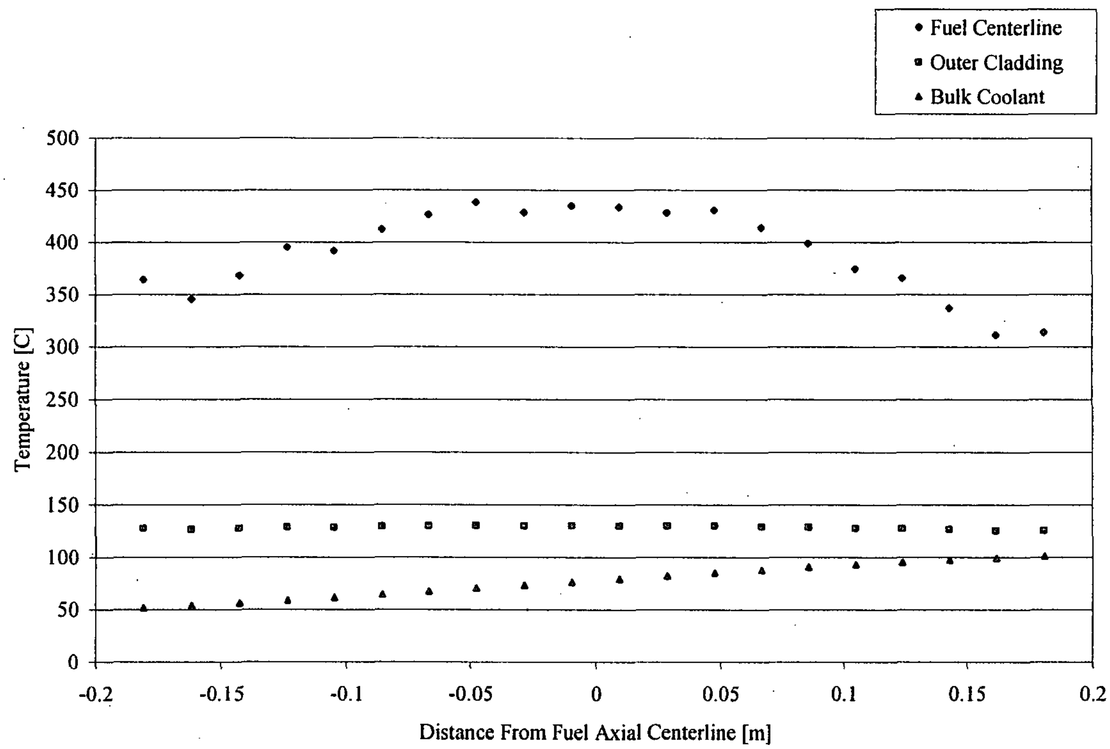

Figure 4-71 Axial Temperature Distribution at 17.61 kW (LEU EOL ICIT Core)

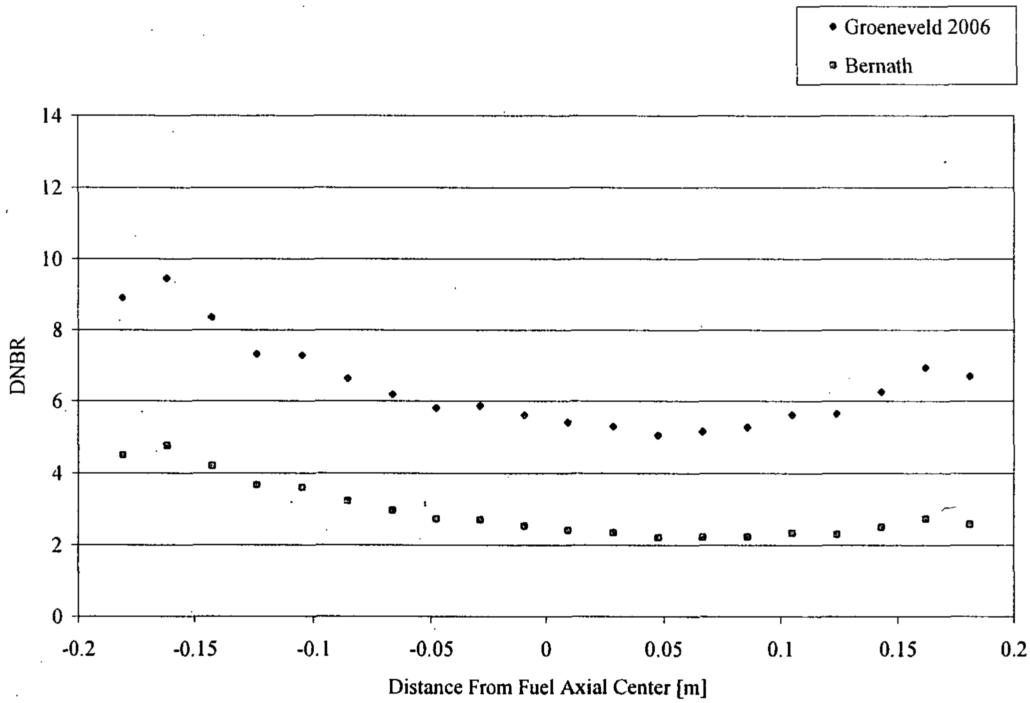

Figure 4-72 Hot Channel Axial DNBR at 17.61 kW (LEU EOL ICIT Core).

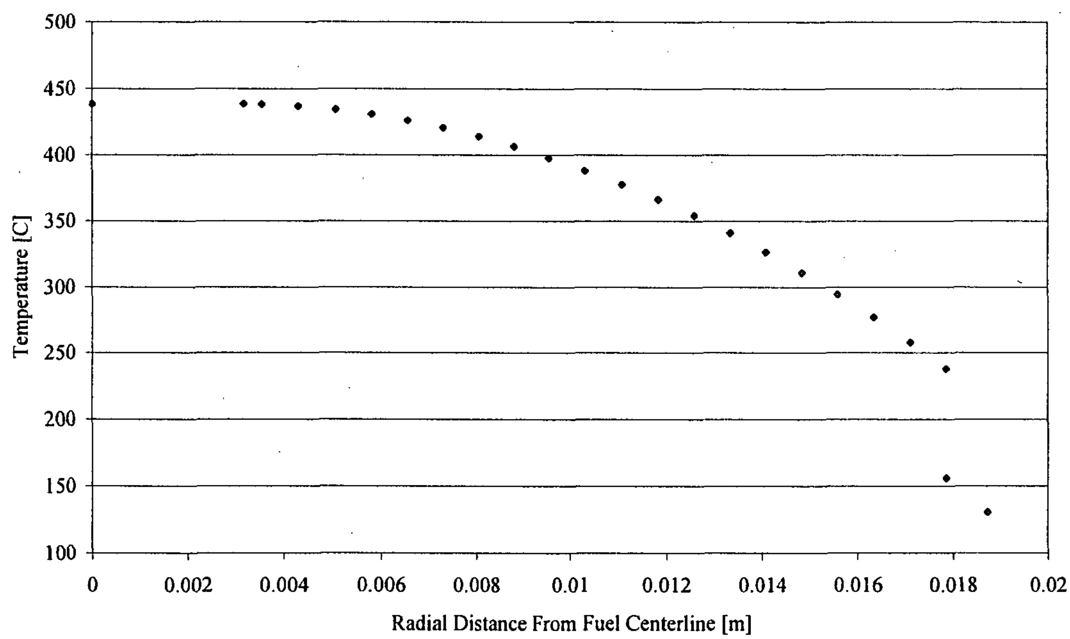

Figure 4-73 Radial Fuel Temperature Distribution at 17.61 kW (LEU EOL ICIT Core).

Table 4-29 Calculated Fuel Temperatures for Various Channel Powers in the LEU EOL ICIT Core.

$P_{hot\text{-}channel}$ (kW)	Calculated [°C]			
	T_{max}	$T_{0.3}$	T_{clad}	$T_{coolant}$
14.00	375	358	128	95
16.00	410	391	130	99
17.61	438	417	131	101
20.00	480	456	132	102
22.00	514	488	133	103

The LEU steady state results shown above are for the ICIT core configuration. The LEU BOL ICIT core has a higher effective peaking factor than the LEU BOL CLICIT core or the LEU BOL NORMAL core, and thus is the bounding core for steady state operation. The ICIT core configuration has a MDNBR of 2.20 at 1.1 MW_{th} steady state using the Bernath Correlation. Figure 4-72 shows the axial DNBR at the predicted hot rod power. Figure 4-70 shows that the MDNBR in the hot channel will reach a value of 2.00 at approximately 20.0 kW hot channel steady state power. This is 113.6% of the 17.61 kW produced in the hot channel of the LEU BOL ICIT core operating at 1.1 MW_{th}. Using either the Bernath or the Groeneveld 2006 correlations, the LEU BOL ICIT core is operating at power well below that required for departure from nucleate boiling.

4.7.10 LEU Core Pulse Analysis

At each stage of core life, the LEU ICIT core has the highest effective peak factor (Table 4-21). Since the core operating mode does not impact the core prompt temperature reactivity coefficient, the ICIT Core was used to conduct the LEU pulse analysis at each stage in core life. The intra-fuel power factor profiles (radial and axial) for the ICIT cores at BOL, MOL and EOL are given in Figure 4-52 and Figure 4-53.

Figure 4-74 shows power and energy as a function of time for the entire LEU ICIT core during a $2.00 pulse. These graphs are produced according to the methodology described in section 4.5.1 using the BOL, MOL, and EOL fuel fissile characteristics found in chapter 4.5.2. This figure shows the hot rod power trace obtained by applying the hot rod peak factors to the nominal channel in each ICIT core

For the following, three figures are given for each stage of core life. These include the fuel temperature as a function of time, the temperature distribution as the moment the peak temperature is observed and a summary of the temperatures as a function of reactivity. Values of important parameters are summarized in a table for each stage on core life.

The pulse summary figures graphically display the following information for a series of pulses of different magnitudes:

1. the peak power of the core during the pulse
2. the prompt maximum value of the fuel in the hot channel
3. the maximum thermocouple temperature during the pulse, assuming that the IFE is located in the hot rod position

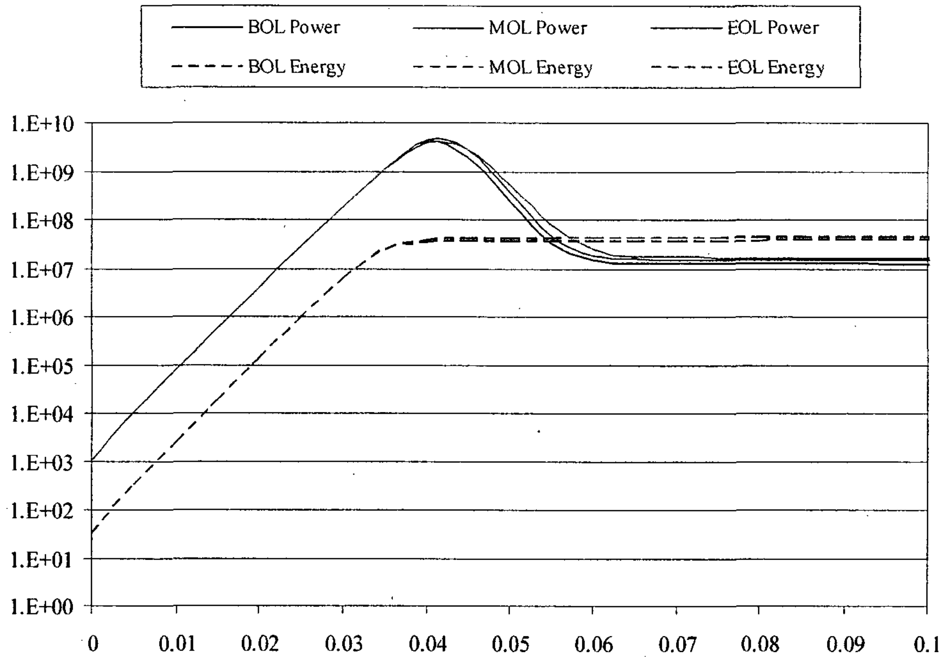

Figure 4-74 Integral Core Pulse Power Trace ($2.00 Pulse, LEU ICIT Core).

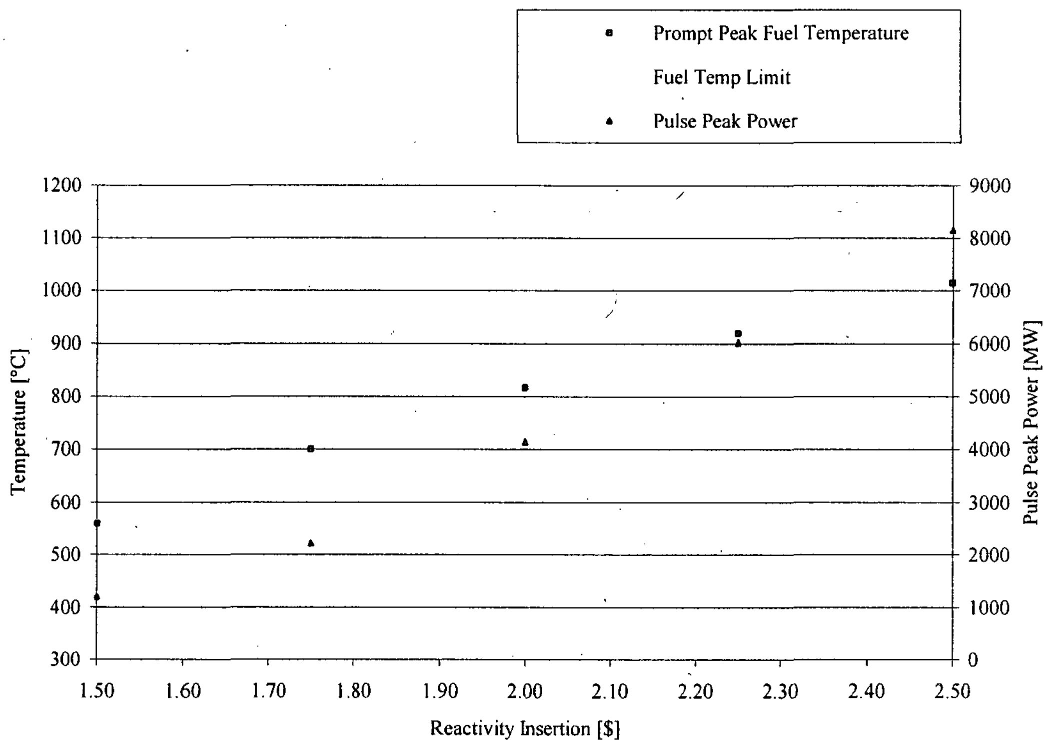

Figure 4-75 Pulse Summary (LEU BOL ICIT Core).

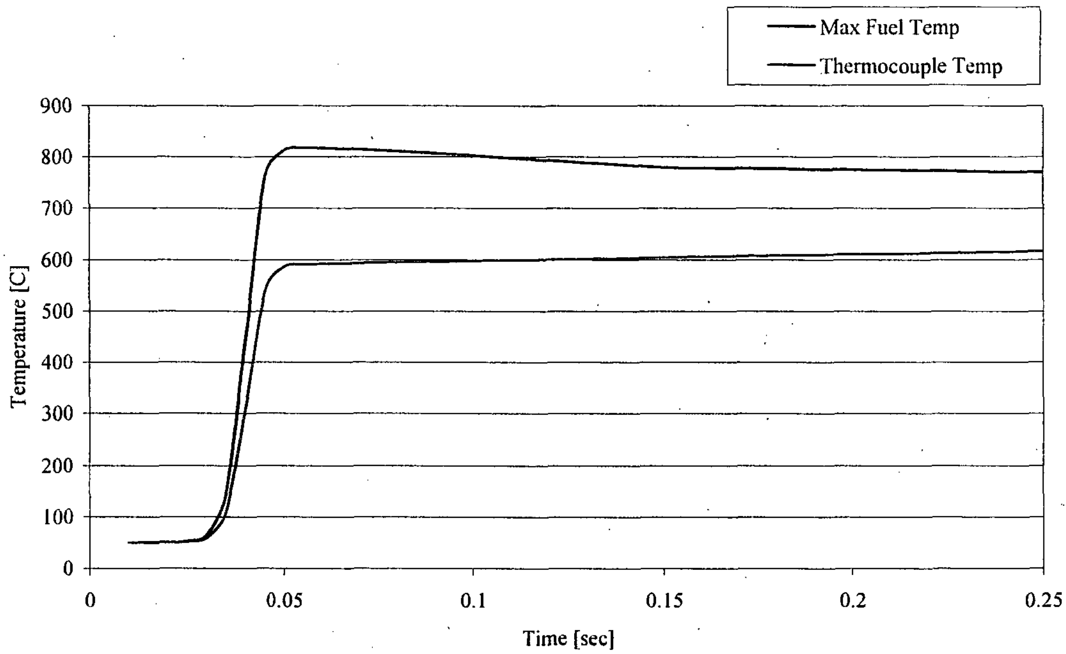

Figure 4-76 LEU BOL ICIT, Hot Channel Fuel Temperatures ($2.00 Pulse)

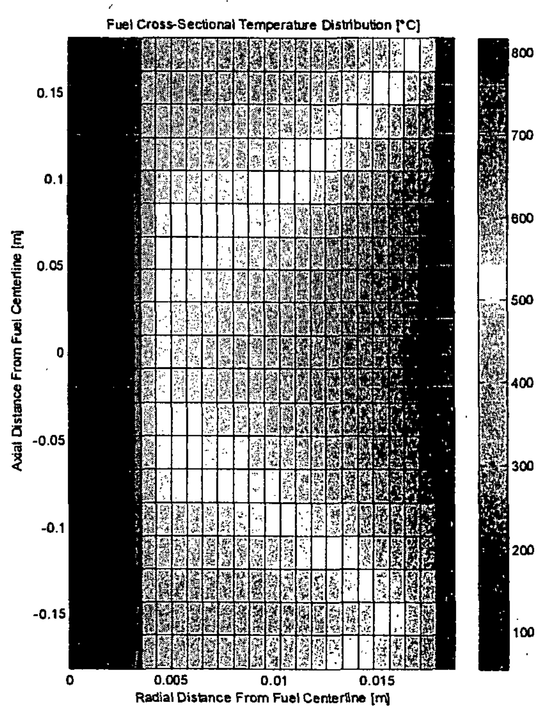

Figure 4-77 LEU BOL ICIT, Fuel Temperature Distribution at Time of Prompt Max Fuel Temperature ($2.00 Pulse)

Table 4-30 Summary of LEU BOL ICIT Pulse Behavior

LEU-BOL ICIT Core Configuration Pulse Results Summary					
Reactivity Insertion [$]	1.50	1.75	2.00	2.25	2.50
Peak Total Core Power [MW]	1216	2222	4138	6022	8138
Prompt Peak Fuel Temperature [°C]	560	701	817	920	1015
Max. Thermocouple Temperature [°C]	433	532	618	692	759

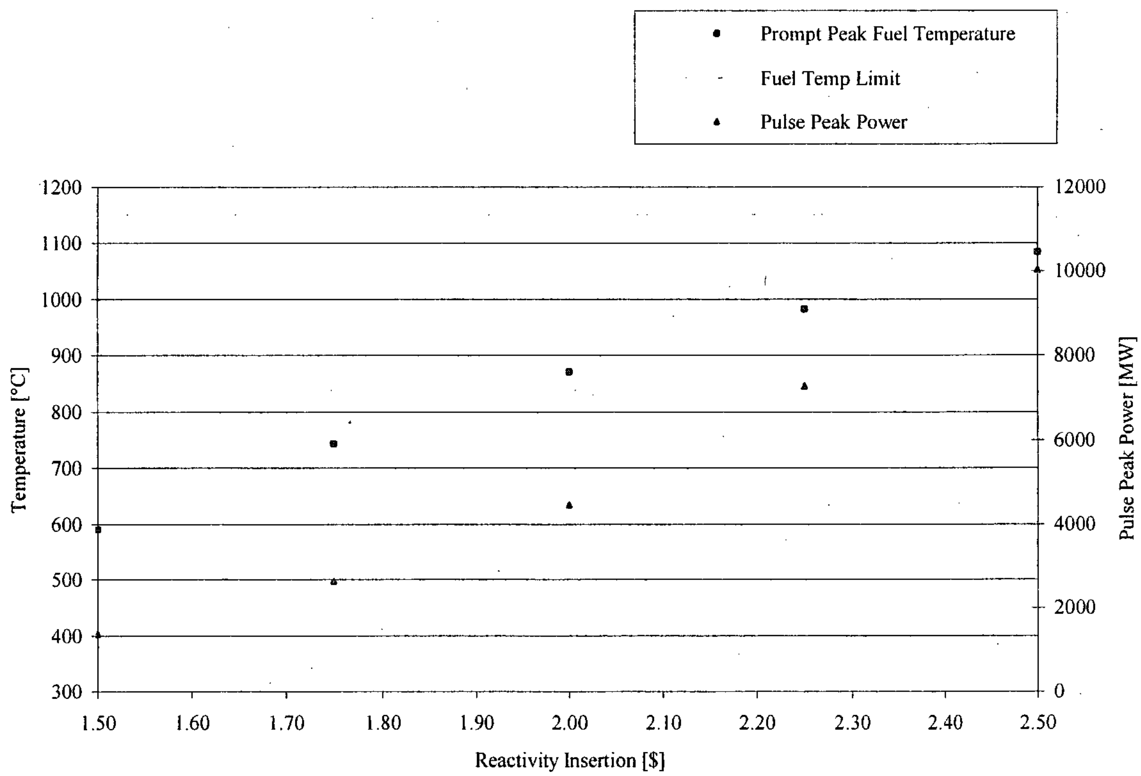

Figure 4-78 Pulse Summary (LEU MOL ICIT Core).

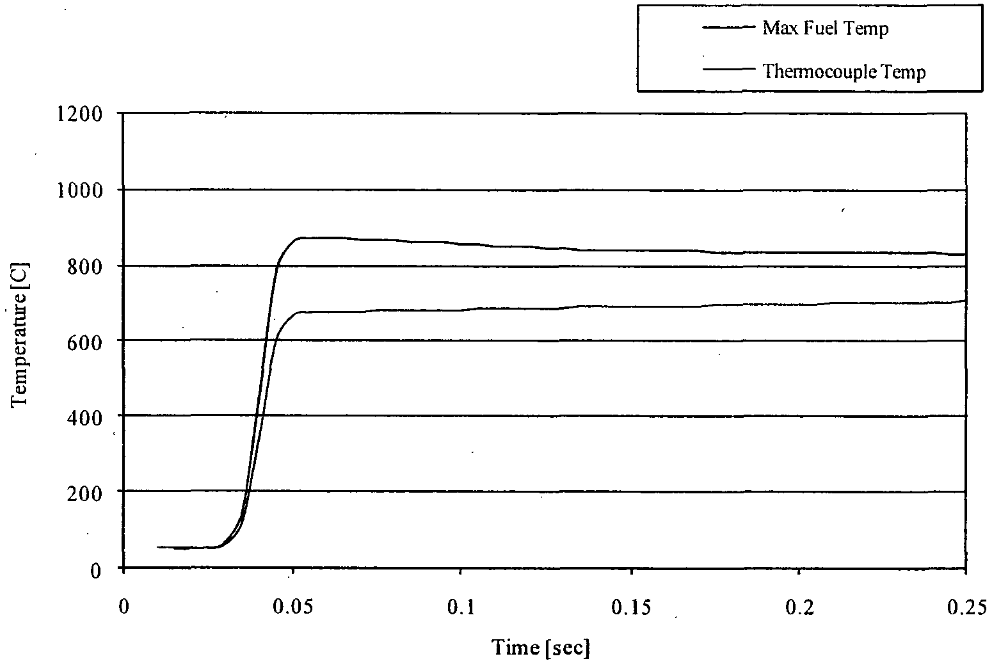

Figure 4-79 LEU MOL, Hot Channel Fuel Temperatures ($2.00 Pulse)

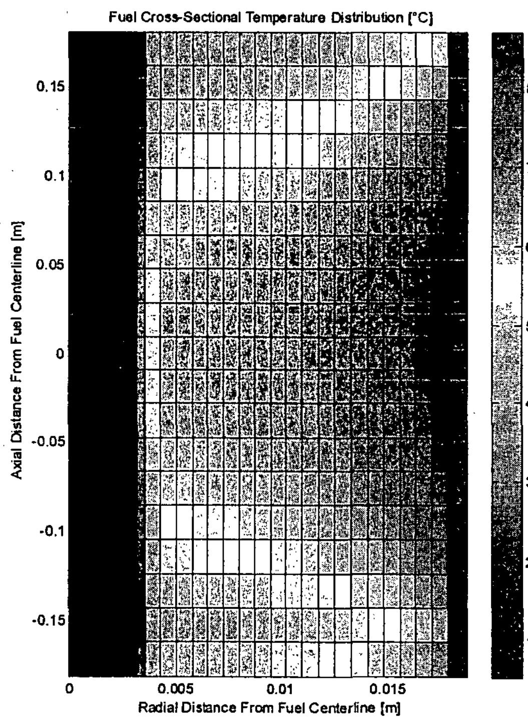

Figure 4-80 LEU MOL ICIT, Fuel Temperature Distribution at Time of Prompt Max Fuel Temperature ($2.00 Pulse)

Table 4-31 Summary of LEU MOL ICIT Pulse Behavior

LEU-MOL ICIT Core Configuration Pulse Results Summary					
Reactivity Insertion [$]	1.50	1.75	2.00	2.25	2.50
Peak Total Core Power [MW]	1393	2636	4460	7276	10017
Prompt Peak Fuel Temperature [°C]	591	743	870	982	1082
Max. Thermocouple Temperature [°C]	490	608	707	794	872

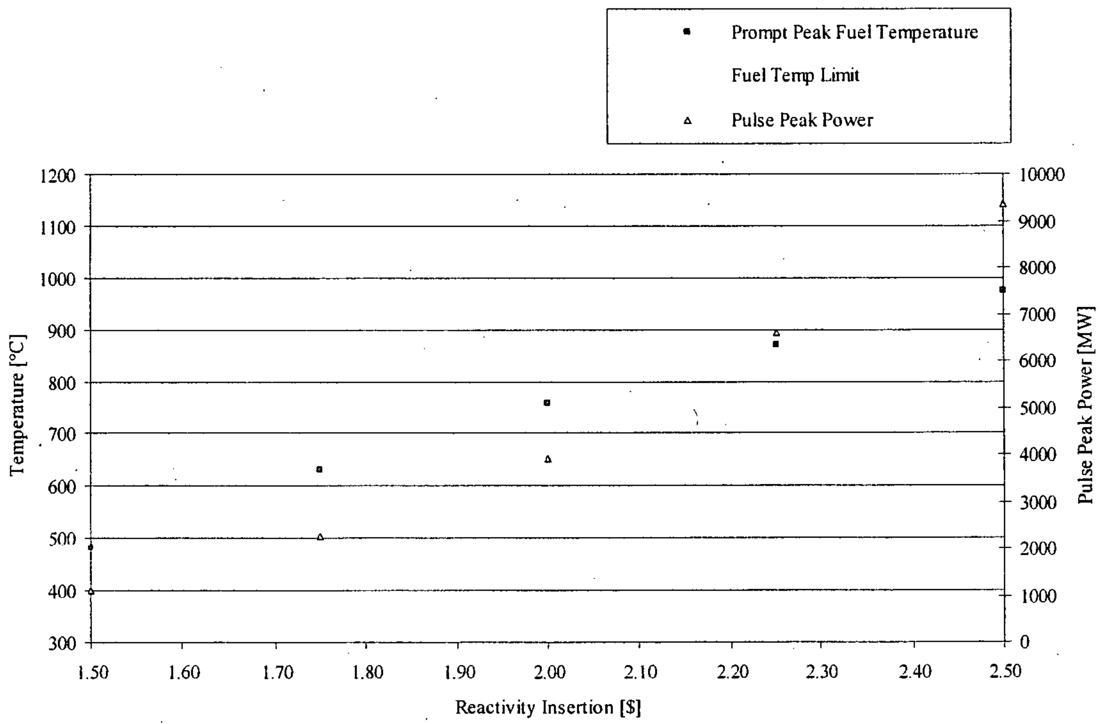

Figure 4-81 Pulse Summary (LEU EOL ICIT Core).

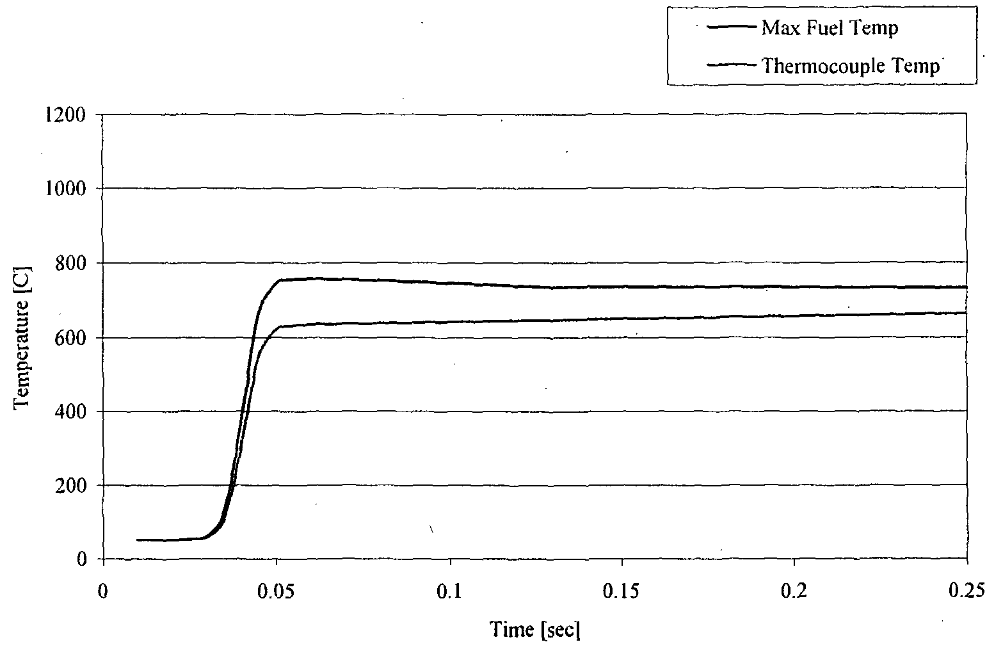

Figure 4-82 LEU EOL, Hot Channel Fuel Temperatures ($2.00 Pulse)

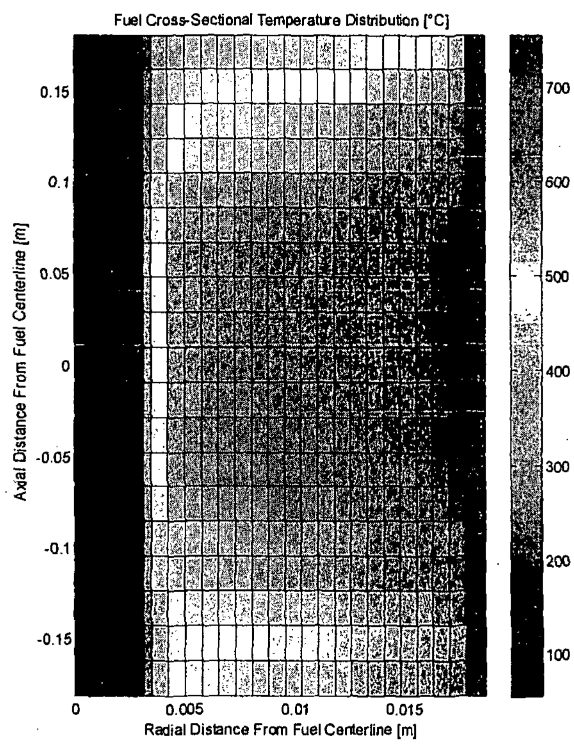

Figure 4-83 LEU EOL ICIT, Temperature Distribution at Time of Max Fuel Temperature ($2.00 Pulse)

Table 4-32 Summary of LEU EOL ICIT Pulse Behavior

LEU-EOL ICIT Core Configuration Pulse Results Summary					
Reactivity Insertion [$]	1.50	1.75	2.00	2.25	2.50
Peak Total Core Power [MW]	1120	2268	3909	6598	9340
Prompt Peak Fuel Temperature [°C]	484	630	757	870	972
Max. Thermocouple Temperature [°C]	438	560	665	759	845

Results presented in Tables 4-30, 4-31 and 4-32 show that the LEU MOL ICIT Core is the bounding ICIT core in terms of maximum fuel temperature produced for a given reactivity insertion.

Peak temperature observed during a pulse is linearly proportional to the prompt reactivity insertion. Linear extrapolation of the peak temperatures associated with the $2.00 and $2.25 pulses in the LEU MOL ICIT core indicate that a peak fuel temperature of 950°C due to the prompt maximum fuel temperature will be produced by the insertion of $2.18 is the most limiting case. A pulse reactivity insertion limit of $2.15 will ensure that at all times in core life, and in all core configurations, the maximum fuel temperature in the core will not exceed 950°C, providing a margin of 200°C from the Safety Limit.

5 REACTOR COOLANT SYSTEM

The reactor coolant system of the OSTR is described in the OSTR HEU SAR. The conversion from HEU to LEU fuel does not impact the reactor coolant system.

6 ENGINEERED SAFETY FEATURES

The engineered safety features of the OSTR are described in the OSTR HEU SAR. The conversion from HEU to LEU fuel does not impact the engineered safety features.

7 INSTRUMENTATION AND CONTROL SYSTEMS

The instrumentation and control systems of the OSTR are described in the OSTR HEU SAR. The conversion from HEU to LEU fuel does not impact the instrumentation and control systems.

8 ELECTRICAL POWER SYSTEMS

The electrical power systems of the OSTR are described in the OSTR HEU SAR. The conversion from HEU to LEU fuel does not impact the electrical power systems.

9 AUXILIARY SYSTEMS

The OSTR SAR lists the following as auxiliary systems: 1) heating, ventilation and air conditioning systems, 2) handling and storage of reactor fuel, 3) fire protection system, 4) communications and 5) possession and use of byproduct, source and special nuclear material. The conversion from HEU to LEU fuel impacts only the second item. Storage racks in the reactor tank have a multiplication factor (k_{eff}) that is less than 0.9.[20] A fuel handling tool and a fuel element inspection tool are present at the OSTR facility, and are described in Chapter 9.2 of the OSTR HEU SAR.

Existing approved procedures will be used for fuel handling, movement and storage for LEU and HEU fuel. Because the transfer into the bulk shield tank of both the LEU and HEU fuel can only happen one element at a time, the procedure for moving the fuel will be consistent with existing approved procedures. Prior to installation of the new LEU fuel, all HEU fuel will be removed from the reactor tank and stored in designated storage racks in the bulk shield tank. The storage racks will be placed directly on the bottom of the tank. Upon receipt, the new LEU fuel will be removed from its shipping casks and transferred to the storage racks in the bulk shield tank immediately after receipt inspection.

New fuel storage racks will be fabricated and installed in the Bulk Shield Tank (BST) prior to storage of any fuel. The racks will be constructed of stainless steel. Each rack will consist of a lower and an upper support plate, and two parallel rows of fuel element storage tubes. Multiple racks will be constructed, and bolted together in a rectangular assembly for stability. Each rack will be approximately eight feet long. When all racks are assembled, fuel will be stored in a square pitch array with pitch P = 8.0 cm. The 8.0 cm. pitch is sufficiently large to maintain k_{eff} <0.9 with all old HEU and new LEU fuel assemblies present simultaneously in the rack. Table 9-1 shows the values of k_{eff} with the storage rack filled with new LEU fuel, with the storage rack filled with FLIP fuel at its most reactive point in life, and with the rack filled with an equal mixture of the two fuel types.

To ensure a conservative analysis of BST criticality conditions, calculations involving FLIP fuel were performed under the assumption that the FLIP fuel is at its most reactive state in life. As shown in Figure 4-10, the core is in its most reactive state after ~1800 MWD. MCNP5-REBUS was used to determine the number density composition of the average fuel rod at this point in life.

To further enhance stability of the racks, and prevent movement of the racks into a more criticality-favorable configuration, the upper and lower support plates of each individual rack will incorporate 1 inch bumpers (see Figure 9-1). Each rack will have space for two rows of 20 elements. Five racks will be built, and the racks will be bolted together for additional stability. The rack footprint is smaller than the floor of the BST. For the purpose of the MCNP5 analysis, the rack / array is positioned in the south-east corner of the BST floor.

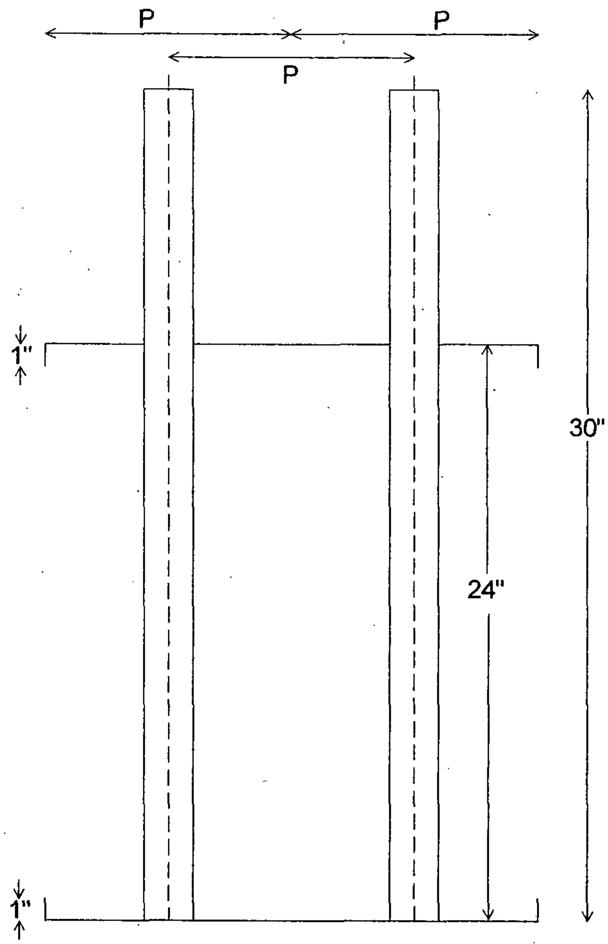

Figure 9-1 End View of Individual Storage Rack

Table 9-1 Summary of MCNP5 fuel rack scenarios.

Scenario	$k_{eff} \pm 1\sigma$
200 FLIP FE's at maximum reactivity	0.56429 +/- 0.00066
200 NEW LEU FE's	0.55572 +/- 0.00065
100 NEW LEU + 100 max reactivity FLIP FE's	0.57137 +/- 0.00067

An analysis was performed using MicroShield[21] to determine the radiation field generated above and next to the bulk shield tank containing the FLIP fuel. The source term used a photon rate of approximately 5E+13 γ s^{-1} for photons of energy 900 keV. Based on the dimensions of a typical fuel element, an exposure rate at 2-ft in water was calculated to be 41.15 R h^{-1}. In order to verify self-protection criteria, the OSTR has taken multiple measurements annually in this configuration over at least the last 25 years of FLIP fuel elements. This exposure rate corresponds to the measured exposure rate typically observed. This source term is conservative because measurements of these FLIP elements were typically performed after a cooling period of two days, and the fuel will be allowed to cool for longer than two days prior to moving it to storage. Using this source term and looking at the side of the tank, the calculated exposure rate for a single element through 1-ft of water and 36-in of concrete was 9.9E-5 R h^{-1}. Using this source term and looking at the top of the tank, the calculated exposure rate for a single element through 10-ft of water was 4.6E-9 R h^{-1}. Multiplying these two values by 100 to represent the entire FLIP core shows that these values are acceptable and will be consistent with our ALARA program.

As fuel is received at the OSTR facility, it will be stored in a physically secure location. Fuel will be handled and stored in accordance with criticality prevention requirements.

10 EXPERIMENTAL FACILITIES AND UTILIZATION

The experimental facilities of the OSTR are described in the OSTR HEU SAR. The conversion from HEU to LEU fuel does not impact the experimental facilities.

11 RADIATION PROTECTION PROGRAMS AND WASTE MANAGEMENT

As a result of the conversion, only Section 11.1.1.3 (specifically Table 11-3, included below) will have to be amended to show the FLIP fuel in cooling and the new 30/20 fuel in core. Upon receipt of the new 30/20 fuel, the FLIP fuel will be moved from the primary tank to the bulk shield tank for cooling until such time as it can be shipped off-site. The bulk shield tank, generally described in Section 10.2.3 of the HEU SAR, will provide adequate thermal cooling. The bulk shield tank has a gross filter and resin column purification system independent of the primary tank water purification system. The location of the fuel within the tank may vary, but will be consistent with our ALARA policy. The fuel shall be stored in a configuration that maintains a $k_{eff} < 0.9$.

Table 11-3 Representative Solid Radioactive Sources for the OSTR.

12 CONDUCT OF OPERATIONS

12.1 Organization and Staff Qualification

The HEU to LEU conversion does not require any changes to the organization and staff qualification of OSTR personnel.

12.2 Procedures

OSTR operating procedures (OSTROPs) will be revised to change all FLIP fuel references to LEU references. An OSTROP will be written to address receipt of new LEU fuel in accordance with applicable Quality Control requirements. An OSTROP will be written in accordance with the guidelines of section 12.6, Reload and Startup Plan, which will control the installation of the new fuel, initial approach to critical, initial startup to low power, initial startup to full power and all required testing and evaluation. New procedures and procedure changes shall be approved by facility staff per existing administrative requirements prior to implementation.

12.3 Operator Training and Requalification

The conversion from HEU to LEU fuel requires no changes to the OSTR requalification and training program with the exception of updating training materials to reflect the change to LEU fuel. Operators will be trained on SAR changes prior to implementation of the conversion SAR. Operators will be trained on the fuel receipt procedure prior to receiving the new LEU fuel. Operators will be trained on new fuel installation and initial startup prior to these evolutions.

12.4 Emergency Plan

The OSTR Emergency Plan refers to "70%-enriched uranium-zirconium hydride FLIP fuel elements" in section 1.0, Introduction. The Emergency Plan also references Design Basis Accident (DBA) consequences several times in sections 4.0, Emergency Classification System and 5.0, Emergency Action Levels (EAL). These references shall be updated to the appropriate values for LEU fuel and the DBA from this conversion document.

12.5 Physical Security Plan

Any changes to the facility physical security plan required by the conversion will be submitted separately and withheld from public disclosure.

12.6 Reload and Startup Plan

The OSTR was loaded with HEU FLIP fuel and restarted in 1976. Based on the results of Chapter 4 of this SAR, the new LEU core is expected to closely resemble the new HEU core in terms of the minimum number of fuel elements required for criticality, and the number of fuel elements required for an operational core configuration. The LEU refueling procedure will be adapted from the successful HEU refueling procedure used in 1976. The LEU refueling procedure and startup plan shall incorporate, at a minimum, all of the guidelines located in Appendix A, Reload and Startup Guidelines.

Comprehensive radiation surveys shall be performed at several power levels during acceptance testing. A startup report will be submitted to the NRC in accordance with the requirements of NUREG-1537 part 1, Chapter 12.6.

12.7 Startup Acceptance Criteria

Reactor parameters shall be measured as directed by the guidelines of section 12.6, Reload and Startup Plan. The acceptance criteria for measured values of reactor parameters are given in Appendix B, Startup Acceptance Criteria. The startup plan shall specify when and how measurements will be made in order to verify that the acceptance criteria are met.

13 ACCIDENT ANALYSIS

13.1 Introduction

In about 1980, the U.S. Nuclear Regulatory Commission requested an independent and fresh overview analysis of credible accidents for TRIGA® and TRIGA®-fueled reactors. Such an analysis was considered desirable since safety and licensing concepts had changed over the years. The study resulted in NUREG/CR-2387, Credible Accident Analysis for TRIGA® and TRIGA®-fueled Reactors.[22] The information developed by the TRIGA® experience base, plus appropriate information from NUREG/CR-2387, serve as a basis for some of the information presented in this chapter.

The reactor physics and thermal-hydraulic conditions in the OSTR at a power level of 1.1 MW are established in Chapter 4. In this chapter, the results of analyses of 30/20 LEU fuel with nominal 1.1 mass percent erbium are compared with analyses of FLIP fuel at 8.5 wt% with 70 % enrichment and 1.6 nominal mass percent erbium.

The fuel temperature is a limit on operation in both steady-state and pulse modes. This limit stems from the out-gassing of hydrogen from U-ZrH fuel and the subsequent stress produced in the fuel element cladding material. The strength of the stainless steel cladding as a function of temperature sets the upper limit on the fuel temperature. Fuel temperature limits of

1,150 °C (with clad < 500 °C) and 930 °C (with clad > 500 °C) for U-ZrH with a H/Zr ratio less than 1.70 have been set to preclude the loss of clad integrity.

Nine credible accidents for research reactors were identified in NUREG-1537[23] as follows:

- the maximum hypothetical accident (MHA);
- insertion of excess reactivity;
- loss of coolant accident (LOCA);
- loss of coolant flow;
- mishandling or malfunction of fuel;
- experiment malfunction;
- loss of normal electrical power;
- external events; and
- mishandling or malfunction of equipment.

This chapter contains analyses of postulated accidents that have been categorized into one of the above nine groups. Some categories contain accidents that do not appear applicable or credible for the OSTR, but this is acknowledged in a brief discussion of the category. Some categories contain an analysis of more than one accident even though one is usually limiting in terms of impact. Any accident having significant radiological consequences was included.

For those events that do not result in the release of radioactive materials from the fuel, only a qualitative evaluation of the event is presented. Events leading to the release of radioactive material from a fuel element were analyzed to the point where it was possible to reach the conclusion that a particular event was, or was not, the limiting event in that accident category. The MHA for TRIGA® reactors is the cladding failure of a single irradiated fuel element in air with no radioactive decay of the contained fission products taking place prior to the release.

13.2 Accident Initiating Events and Scenarios, Accident Analysis and Determination of Consequences

13.2.1 Maximum Hypothetical Accident (MHA)

For the OSTR, the MHA has been defined as the cladding rupture of one highly irradiated fuel element with no radioactive decay followed by the instantaneous release of the noble gas and halogen fission products into the air. Based on this MHA, three different scenarios have been chosen for analysis:

Scenario A: In this scenario, the entire north wall of the reactor room instantly vanishes. No credible cause for this occurrence can be imagined. The noble gas and halogen fission products that have been released to the reactor room air are assumed to mix instantly and uniformly with the room air. This reactor room air then moves out through the missing wall at the mean wind speed (1 m sec^{-1}). This is assumed to be a ground level release. It takes 8.52 seconds for the entire volume of the reactor room air to be evacuated. Thus, individuals outside the reactor room will be exposed to a radioactive cloud for a period of 8.52 seconds;

Scenario B: This scenario again assumes that the noble gas and halogen fission products instantly and uniformly mix with the reactor room air. The fission products that have been released to the reactor room air are then exhausted at the stack ventilation rate (4.39×10^6 $cm^3 sec^{-1}$). The path for this release is not specified. It could possibly be through the small door on the NE corner of the building, or it could be through the stack if the vent fans didn't shut down and the dampers did not close. The air is assumed to be discharged at ground level, and no credit is taken for an elevated release. The time to evacuate the entire volume of the reactor room is 14.7 minutes, and this is, therefore, the exposure time for individuals outside the reactor room; and

Scenario C: This scenario also assumes that the noble gas and halogen fission products instantly and uniformly mix with the reactor room air. The reactor room air then leaks from the room at the leak rate of 1.69×10^4 $cm^3 sec^{-1}$ as specified in the original OSTR SAR. In this case, it would take 63.7 hours for the entire volume of the reactor room air to be evacuated, and this is the exposure time for individuals outside the reactor room. This is also assumed to be a ground level release.

In the analysis, it is assumed that the OSTR has operated continuously at 1.1 MW for a period of one year. Thus, all halogens and all noble gases (except Kr-85) are at their saturation activity. However, the OSTR SAR assumes that all fission events occur in U-235. Because the LEU fuel will contain a significant amount of U-238, it is reasonable to assume that there will be more Pu-239 present at the fuel's end-of-life. Depletion calculations in fact show that the percentage of fission events originating from Pu-239 at the end-of-life will be 13.3% and 4.5% for the LEU and FLIP cores, respectively. Therefore, because the fission yield curves are different between Pu-239 and U-235, a difference in the source term inventory of halogens and noble gases might also exist.

Using the methodology described in section 13.2.1.2 of the HEU SAR, the source term inventory was calculated for both the original 1976 HEU FLIP core and the proposed LEU core. However, for these calculations, the following assumptions were used:

- HEU MOL NORMAL core maximum power per element is 18.37 kW
- LEU MOL ICIT maximum power per element is 18.52 kW
- Reactor power for both cores is 1.1 MW
- Five percent (5%) of the fissions from the FLIP core at EOL are due to Pu-239
- Fifteen percent (15%) of the fissions from the LEU core at EOL are due to Pu-239

Table 13-1 Saturated Activities for Highest Power Density FLIP Fuel Element

Isotope	Half life (s)	U-235 Cumulative Fission Yield	Pu-239 Cumulative Fission Yield	FLIP Saturated Activity (mCi)	LEU Saturated Activity (mCi)	FLIP Reactor Room Air Activity Without Water (mCi)	LEU Reactor Room Air Activity Without Water (mCi)
Br-82	127080	6.10E-07	1.27E-05	1.90E+01	3.90E+01	0.00	0.00
Br-83	8640	5.38E-03	2.97E-03	8.20E+04	8.04E+04	2.55	2.45
Br-84m	360	3.18E-04	4.85E-04	5.09E+03	5.50E+03	0.16	0.17
Br-84	1908	1.00E-02	4.29E-03	1.52E+05	1.47E+05	4.72	4.48
Br-85	172.2	1.26E-02	5.62E-03	1.91E+05	1.86E+05	5.95	5.66
Br-86	55.5	1.82E-02	4.89E-03	2.73E+05	2.59E+05	8.48	7.90
Br-87	55.9	2.02E-02	6.91E-03	3.04E+05	2.91E+05	9.46	8.89
I-131	692928	2.88E-02	2.89E-02	4.50E+05	4.62E+05	13.98	14.10
I-132	8208	4.30E-02	5.39E-02	6.79E+05	7.15E+05	21.10	21.81
I-133	74880	6.70E-02	6.97E-02	1.05E+06	1.08E+06	32.54	32.94
I-134	3156	7.74E-02	7.41E-02	1.20E+06	1.23E+06	37.42	37.56
I-135	23652	6.29E-02	6.54E-02	9.83E+05	1.01E+06	30.55	30.92
I-136	83.4	2.47E-02	1.75E-02	3.80E+05	3.79E+05	11.81	11.55
Kr-83m	6696	5.38E-03	2.97E-03	8.20E+04	8.04E+04	2.55	2.45
Kr-85m	16128	1.26E-02	5.64E-03	1.91E+05	1.85E+05	5.95	5.66
Kr-85	3.39E+08	2.74E-03	1.23E-03	4.16E+04	4.03E+04	1.29	1.23
Kr-87	4572	2.51E-02	9.89E-03	3.80E+05	3.66E+05	11.82	11.17
Kr-88	10224	3.57E-02	1.27E-02	5.38E+05	5.16E+05	16.74	15.75
Kr-89	189	4.61E-02	1.45E-02	6.94E+05	6.63E+05	21.59	20.22
Xe-131m	1028160	3.17E-04	5.40E-04	5.12E+03	5.62E+03	0.16	0.17
Xe-133m	189216	1.95E-03	2.35E-03	3.07E+04	3.22E+04	0.95	0.98
Xe-133	452736	6.70E-02	7.02E-02	1.05E+06	1.08E+06	32.56	32.98
Xe-135m	918	1.21E-02	1.71E-02	1.93E+05	2.06E+05	6.00	6.30
Xe-135	32760	6.53E-02	7.61E-02	1.03E+06	1.07E+06	31.92	32.71
Xe-137	229.2	6.11E-02	6.01E-02	9.52E+05	9.77E+05	29.60	29.79
Xe-138	846	6.37E-02	5.17E-02	9.84E+05	9.92E+05	30.60	30.26

This source term inventory for the LEU core was then used to calculate doses to occupational workers and members of the general public using the same methodology described in section 13.2.1. For a single element failure in air, the results for scenarios A, B, and C are found in Table 13-2 through Table 13-5 below. A comparison with Tables 13-5 through 13-10 in the HEU SAR show that the LEU core consistently results in doses that are within 5% of the values from the analysis of the FLIP HEU core.

Table 13-2 Occupational Radiation Doses in the Reactor Room Following a Single Element Failure in Air.

Reactor Room Occupancy (min)	Scenario	FLIP $CDE_{Thyroid}$ + $DDE_{Thyroid}$ (mrem)	LEU $CDE_{Thyroid}$ + $DDE_{Thyroid}$ (mrem)	FLIP TEDE (mrem)	LEU TEDE (mrem)
2	A	32	32	1	1
5	A	32	32	1	1
2	B	215	217	8	8
5	B	488	492	18	18
2	C	230	232	9	9
5	C	575	580	22	22

Table 13-3 Radiation Doses to Members of the General Public Following a Single Element Failure in Air – Scenario A.

Distance (m)	FLIP $CDE_{Thyroid}$ + $DDE_{Thyroid}$ (mrem)	LEU $CDE_{Thyroid}$ + $DDE_{Thyroid}$ (mrem)	FLIP TEDE (mrem)	LEU TEDE (mrem)
10	442	446	17	17
50	202	204	8	8
100	69	70	3	3
150	30	30	1	1
200	17	18	1	1
250	12	12	<1	<1
267	10	10	<1	<1

Table 13-4 Radiation Doses to Members of the General Public Following a Single Element Failure in Air – Scenario B.

Distance (m)	FLIP $CDE_{Thyroid}$ + $DDE_{Thyroid}$ (mrem)	LEU $CDE_{Thyroid}$ + $DDE_{Thyroid}$ (mrem)	FLIP TEDE (mrem)	LEU TEDE (mrem)
10	440	444	16	16
50	201	203	7	7
100	69	69	3	3
150	30	30	1	1
200	17	18	1	1
250	12	12	<1	<1
267	10	10	<1	<1

Table 13-5 Radiation Doses to Members of the General Public Following a Single Element Failure in Air – Scenario C.

Distance (m)	FLIP $CDE_{Thyroid}$ + $DDE_{Thyroid}$ (mrem)	LEU $CDE_{Thyroid}$ + $DDE_{Thyroid}$ (mrem)	FLIP TEDE (mrem)	LEU TEDE (mrem)
10	320	323	10	10
50	146	147	4	4
100	50	50	2	2
150	22	22	1	1
200	13	13	<1	<1
250	8	9	<1	<1
267	7	8	<1	<1

Based on these results, the LEU core should be essentially equal (i.e., within 5%) to the original 1976 FLIP core in all scenarios involving either radiation exposure or releases described in chapter 13 of the SAR.

13.2.2 Insertion of Excess Reactivity

Pulse reactivity limits are determined in section 4 of this SAR. Reactivity insertions due to control rod withdrawals under various circumstances are considered in section 13.2.2 of the HEU SAR. In each case, reactivity insertion due to control rod withdrawal is shown to be less than the pulse reactivity limit for the HEU core. The same approach is used for the LEU core. Reactivity insertion due to beam port flooding, and metal-water reactions that could occur due to high temperatures resulting from reactivity insertion accidents are also considered in the HEU SAR. Conversion from HEU to LEU fuel does not change the analysis of beam port flooding or metal-water reactions.

Uncontrolled withdrawal of a control rod may be caused by operator error or equipment malfunction. Interlocks prohibit the simultaneous manual or automatic withdrawal of more than one control rod. The same approach is used to analyze this type of accident as was used for the

HEU core. For a single delayed neutron group model with the prompt jump approximation, a linear (ramp) reactivity increase results in the following equation for power as a function of time:

$$\frac{P(t)}{P_0} = \left(e^{-\lambda t}\right)\left[\frac{\beta}{\beta - \gamma t}\right]^{(1+\lambda\beta/\gamma)}$$

where: $P(t)$ = power at time t

P_0 = initial power level

β = total delayed neutron fraction = 0.0076

λ = one group decay constant = 0.405 (sec^{-1})

t = time (sec)

γ = linear insertion rate of reactivity (Δk/k-sec^{-1})

Control rod data for the NORMAL core is shown in Table 13-6. The same values for total rod withdrawal times for the HEU core are used. Calculations, measurements and operating experience indicate that the NORMAL core gives the highest control rod worths.

Table 13-6 Control Rod Data for NORMAL configuration LEU core.

Rod	Total Worth	Total Withdrawal time (sec)	Average insertion rate ($/sec)	Total reactivity at SCRAM ($)
Transient	2.86	33.81	0.0846	$0.95
Safety	2.60	48.09	0.0541	$0.87
Shim	2.55	48.20	0.0529	$0.86
Regulating	3.36	36.18	0.0929	$0.96

For the LEU core, the regulating control rod has the highest total worth, and also the highest reactivity insertion rate. For the reactivity insertion accident, starting power levels of 100W and 1.0 MW were considered. The SCRAM setpoint was assumed to be 1.06 MW, and 0.5 seconds delay time was assumed between reaching the SCRAM setpoint and actual release of the control rods.

For the case with initial power of 100W, the reactor power was calculated to reach the trip setpoint in 9.86 seconds, and the peak reactivity insertion was $0.96. For the case with initial power of 1.0 MW, the reactor power was calculated to reach the trip setpoint in 0.55 seconds, and the peak reactivity insertion was \$0.10. In both cases, the peak reactivity insertion is well below the pulse reactivity insertion limit, and thus would produce no adverse safety effects.

The very unlikely accident involving the simultaneous withdrawal of all four control rods was also considered. An initial power of 100W is assumed, with a scram setpoint of 1.06 MW and a 0.5 second delay time. The reactivity insertion rate for four control rods is 0.2844 \$/sec. The trip setpoint is reached in 3.47 seconds and the total amount of reactivity inserted is \$1.13. This is still well below the pulse reactivity insertion limit. Note that the HEU SAR analysis was also conducted with the same assumption that the SCRAM setpoint is 1.06 MW, even though licensed power is 1.1 MW. If the SCRAM is assumed to occur at 1.1 MW, the values calculated for total reactivity at SCRAM will be slightly higher. In the bounding case of simultaneous withdrawal of four rods, the reactivity inserted for a SCRAM at 1.06 MW is \$1.129987 and the reactivity inserted for a SCRAM at 1.1 MW is \$1.130174.

13.2.3 Loss of Cooling Accident (LOCA)

The scenarios leading to a LOCA are not affected by the type of fuel present in the reactor. The significant consequences of a LOCA are removal of core cooling and removal of radiation shielding.

The loss of coolant accident was examined in NUREG/CR-2387. For a reactor such as the OSTR, this type of accident was not credible. The OSTR does have a piercing beam port, thus making a LOCA possible, but the likelihood of such an accident is deemed to be very low probability. Even if such an accident was to occur, all prior analyses conclude that natural convective air cooling of the fuel will keep the maximum fuel temperature well below the temperature for cladding failure if the reactor operates at a maximum power level of 1.5 MW or below.[24, 25, 26, 27, 28]

Analysis of radiation levels from the uncovered core were performed in section 13.2.3 of the HEU SAR. These analyses were based upon a fission product activity source term calculated using the standard equation:

$$A(t) = 1.4x10^6 P[t^{-0.2} - (t+T)^{-0.2}]$$

where: $A(t)$ is activity in curies

P is power in MW
t is time after shutdown (days)
T is time operating at power prior to shutdown (days)

This equation calculates fission product inventory following shutdown, and is insensitive to the fission product source (uranium or plutonium). Although the LEU core will produce more fissions from plutonium than the HEU core at end of life, the above equation still applies.[29] The HEU analysis very conservatively assumes operation at full power for 365 days prior to shutdown, and calculates dose rates at five different times after shutdown. Using the same assumptions, the source term and resultant dose rates will be the same for the LEU fuel. Dose rates directly above the core, in the reactor room, and at the facility fence line were calculated in the HEU SAR and found to be acceptable.

13.2.4 Loss of Coolant Flow

Loss of coolant flow scenarios are discussed in section 13.2.4 of the HEU SAR. This event is considered to be very unlikely, but even if it did occur, the consequences of a fuel element failure with no coolant would be bounded by the MHA. Conversion from HEU to LEU fuel does not change the assumptions, analyses or consequences of this accident class.

13.2.5 Mishandling or Malfunction of Fuel

Events which could cause accidents at the OSTR in this category include (1) fuel handling accidents where an element is dropped underwater and damaged severely enough to breach the cladding, (2) failure of the fuel cladding due to a manufacturing defect or corrosion and (3) overheating of the fuel with subsequent cladding failure during steady-state or pulsing operation. Each scenario is assumed to result in a single fuel element failure while submerged in water.

For HEU fuel, comparison between sections 13.2.1 and 13.2.5 of the HEU SAR clearly shows that the dose consequences from a fuel failure in water are less than the dose consequences from a fuel failure in air (the MHA) by a factor of approximately 3 or more, depending on the scenario. This is principally due to the absorption of halogens in the water. Section 13.2.1 of this conversion SAR shows that the source term (fission product inventory) for LEU fuel will be very similar to the source term for HEU fuel. Therefore, the dose consequences from an LEU fuel failure in water are assumed to be significantly less than the dose consequences from an LEU failure in air. An accident due to fuel mishandling or malfunction is thus bounded by the MHA.

Once the LEU core is installed, the frequency of fuel handling will be similar to the frequency of HEU fuel handling. During the HEU fuel offload, all elements will be moved, but a significant cooling period will be provided before HEU fuel is removed from the reactor pool. If an element is damaged during handling, fuel movement will be terminated until damage is assessed and resolved.

Fuel malfunction in the HEU core due to an improper combination of FLIP and standard fuel is also considered. This accident will no longer be possible since only LEU fuel will be present in the reactor tank after conversion is complete.

13.2.6 Experiment Malfunction

Improperly controlled experiments could potentially result in damage to the reactor fuel. Credible mechanisms for damage are explosive forces, corrosion and large reactivity changes. Limits on corrosive and explosive material do not need to be changed as a result of conversion, but reactivity limits must be updated.

For the HEU core, the sum of the absolute values of the reactivity worths of all moveable experiments is limited to less than $0.50. This limit ensures that the reactor can be made subcritical even if the most reactive rod is fully withdrawn from the core, the core is in its reference condition and all non-secured experiments are in their most reactive state. This limit does not need to be changed.

For the HEU core, the sum of the absolute values of the reactivity worths of all experiments is limited to less than $2.55. This specification ensures that a pulse caused by the insertion of reactivity due to an experiment failure will result in peak fuel temperature below the safety limit. The LEU core has a pulse reactivity limit of $2.15. Therefore, the sum of the absolute values of the reactivity worths of all experiments shall be limited to no more than $2.15 for the LEU core.

13.2.7 Loss of NORMAL Electrical Power

The OSTR does not require emergency backup systems to safely maintain core cooling. Conversion from HEU to LEU fuel does not change the assumptions, analyses or consequences of this accident class.

13.2.8 External Events

Hurricanes, tornadoes, floods and seismic activity are briefly discussed in section 13.2.8 of the HEU SAR. Conversion from HEU to LEU fuel does not change the assumptions, analyses or consequences of this accident class.

13.2.9 Mishandling or Malfunction of Equipment

No credible accident initiating events were previously identified in section 13.2.9 of the OSU SAR for this type of accident. Conversion from HEU to LEU fuel does not change the assumptions, analyses or consequences of this accident class.

14 TECHNICAL SPECIFICATIONS

The Technical Specifications establish an operating envelope, within which the integrity of the fuel is maintained. Conversion from HEU to LEU requires limited changes to the previously approved HEU specifications. Significant changes to the Technical Specifications include (1) replacement of all references to HEU fuel with references to LEU fuel, and (2) replacement of all pulse reactivity limits, and all reactivity limits based on pulse reactivity limits with the LEU based limits. Each section requiring any change should be replaced in its entirety with the sections listed below.

1.12 Fuel Element: A fuel element is a single TRIGA® fuel rod of low enriched uranium (LEU) type.

1.18 Operational Core: An operational core shall be a fuel element core which operates within the licensed power level and satisfies all the requirements of the Technical Specifications.

2 SAFETY LIMTS AND LIMITING SAFETY LIMIT SETTING

2.1 Safety Limit – Fuel Element Temperature

Applicability. This specification applies to the temperature of the reactor fuel.

Objective. The objective is to define the maximum fuel element temperature that can be permitted with confidence that no damage to the fuel element cladding shall result.

Specifications. The temperature in a TRIGA® fuel element shall not exceed 2,100°F (1,150°C) under any mode of operation.

Basis. The important parameter for a TRIGA® reactor is the fuel element temperature. This parameter is well suited as a single specification especially since it can be measured. A loss of the integrity of the fuel element cladding could arise from a build-up of excessive pressure between the fuel-moderator and the cladding if the fuel temperature exceeds the safety limit. The pressure is caused by the presence of air, fission product gases, and hydrogen from the dissociation of the hydrogen and zirconium in the fuel-moderator. The magnitude of this pressure is determined by the fuel-moderator temperature and the ratio of hydrogen to zirconium in the alloy.

The safety limit for the TRIGA® fuel element is based on data which indicate that the stress in the cladding due to the hydrogen pressure from the dissociation of zirconium hydride will remain below the ultimate stress, provided the temperature of the fuel does not exceed 2100°F (1150°C) and the fuel cladding is water cooled.

2.2 Limiting Safety Limit Setting (LSSS)

Applicability. This specification applies to the scram settings which prevent the safety limit from being reached.

Objective. The objective is to prevent the safety limits from being reached.

Specifications The limiting safety system setting shall be equal to or less than 510°C (950°F) as measured in an instrumented fuel element. The instrumented fuel element shall be located in the B-ring.

Basis. The value of the LSSS is designed to protect the fuel elements from exceeding the maximum fuel temperature safety limit (SL) of 1,150°C for fuel elements during non-pulsing reactor operation. It is not applicable to pulsing operations. The value of the LSSS at 510°C was conservatively chosen to be slightly lower than half the SL to account for instrument uncertainties and peaking factors.

MCNP5 based analysis shows that largest hot rod power to IFE power ratio occurs for the BOL ICIT core. The peak power in the B ring occurs at position B-6, and is approximately 8.5% higher than the power in the B-4 IFE position. The IFE is calibrated annually. Experience has shown that true temperature differs from indicated temperature by no more than 5%.

Axial flux measurements made in the HEU ICIT core configuration indicate that the difference between peak axial flux and the minimum flux at any of the three thermocouple elevations is no more than 18%. This should be limiting for the LEU core as well.

Typical fuel temperatures observed at full power are approximately 350°C. The analysis in the SAR section 13.2.2 shows that an uncontrolled withdrawal of the most reactive control rod at an initial power level of 1 MW would result in a trip signal being initiated within 1.05 seconds resulting in a reactivity insertion of $0.10. For an uncontrolled withdrawal of the most reactive control rod at an initial power level of 100 W, the trip signal would be initiated in 10.36 seconds resulting in a reactivity insertion of $0.96. Because fuel temperature lags behind power and the power is so low, each of these scenarios would result in high power trips before the fuel temperature trip is reached. This is confirmed by our experience of observed instrument behavior after a pulse. For the loss of coolant accidents described in section 13.2.3, the primary water temperature would trip the reactor or the low level alarm would annunciate and alert the operator long before enough water is lost to initiate a high fuel element temperature trip. Regardless, the SAR clearly shows that natural convective air cooling of the fuel will keep the maximum fuel temperature well below the SL even after an instantaneous complete loss of primary water at 1.5MW or below.

The thermocouple is located 0.300 inches from the fuel centerline. Radial temperature distributions for the BOL ICIT core show a peak to thermocouple location ratio of 5.9%.

Calculation of maximum fuel temperature for an indicated IFE temperature shows that given all the uncertainties and peaking factors, the LSSS is sufficiently conservative to guarantee that the SL is never exceeded. The calculation is as follows:

(nominal IFE temperature) x (max reactor power / nominal reactor power) x (max power per element in the B-ring / nominal IFE power) x (peak radial temperature / radial temperature at the TC) x (temperature measurement uncertainty factor) x (peak axial flux / axial flux at the TC) = maximum fuel temperature

$$(350°C) \times (1.10) \times (1.085) \times (1.059) \times (1.05) \times (1.18) = 548°C$$
$$(510°C) \times (1.10) \times (1.085) \times (1.059) \times (1.05) \times (1.18) = 798°C$$

For an indicated IFE temperature of 510°C (i.e., the LSSS), the calculated maximum fuel temperature is 798°C. This value is significantly less than the SL of 1150°C. This assures that the LSSS of 510°C as measured at the IFE maintains fuel temperature below the SL during steady-state operations.

3.1.4 Pulse Mode Operation

Applicability. This specification applies to the energy generated in the reactor as a result of a pulse insertion of reactivity.

Objective. The objective is to assure that the fuel temperature safety limit shall not be exceeded.

Specifications. The reactivity to be inserted for pulse operation shall be determined and limited by a mechanical block and electrical interlock on the transient rod, such that the reactivity insertion shall not exceed $2.15.

Basis. The fuel temperature rise during a pulse transient has been estimated by RELAP5-3D. LEU cores were analyzed at Beginning of Life, Middle of Life and End of Life. At each stage of core life, the ICIT core is shown to have the highest effective peak factor. As input, the RELAP5-3D pulse models used reactor kinetic behavior predicted by the point reactor kinetics equations. The models also used radial, axial and hot channel peak factors, as well as thermal and neutronic characteristics of the LEU fuel elements. A reactivity insertion of $2.15 is shown to produce a peak fuel temperature less than 950 °C for all cores at all times in core life. There is a safety margin of at least 200°C between maximum attainable fuel temperature and the fuel temperature safety limit under the worst case scenario. At all other times, the safety margin is greater than 200°C.

3.2.3 Reactor Safety System

Applicability. This specification applies to the reactor safety system channels.

Objective. The objective is to specify the minimum number of reactor safety system channels that shall be available to the operator to assure safe operation of the reactor.

Specifications. The reactor shall not be operated unless the minimum number of safety channels described in Table 2 and interlocks described in Table 3 are operable.

Table 2 - Minimum Reactor Safety Channels

Safety Channel	Function	Effective Mode		
		S. S.	Pulse	S. W.
Fuel Element Temperature	SCRAM @ 510°C	1	-	1
Power Level	SCRAM @ 1.1 MW(t) or less	2	-	2
Console Scram Button	SCRAM	1	-	1
Preset Timer	Transient rod SCRAM @ 15 sec or less after a pulse	-	1	-
High Voltage	SCRAM @ 25% of nominal operating voltage	1	1	1

Table 3 - Minimum Interlocks				
Interlock	Function	Effective Mode		
		S.S.	Pulse	S.W.
Wide-Range Log Power Level Channel	Prevents control rod withdrawal @ less than 2 cps	1	-	-
Transient Rod Cylinder	Prevents application of air unless fully-inserted	1	-	-
1 kW Pulse Interlock	Prevents pulsing above 1 kW	-	1	-
Shim, Safety, and Regulating Rod Drive Circuit	Prevents simultaneous manual withdrawal of two rods	1	-	1
Shim, Safety, and Regulating Rod Drive Circuit	Prevents movement of any rod except transient rod	-	1	-
Transient Rod Cylinder Position	Prevents pulse insertion of reactivity greater than $2.15	-	1	1

(1) Any single required safety channel or interlock may be inoperable while the reactor is operating for the purpose of performing a channel check, test, or calibration.

(2) If any required safety channel or interlock becomes inoperable while the reactor is operating for reasons other than that identified in Technical Specification 3.2.3 (1) above, the reactor shall be immediately (not to exceed 5 minutes upon discovery) shutdown.

Basis.

Fuel Element Temperature Scram: The fuel element temperature scram is set to cause a scram at or below the LSSS, which is 510°C. The supporting arguments for the safely limit of 1150°C are given in 4.5.3.1 of the HEU SAR. The LSSS is set to less than half for the safety limit. This is more than adequate to account for uncertainties in instrument response and core position of the instrumented fuel element.

Power Level Scram: The set point for both the safety and percent power channels are normally set to 106% of 1 MW(t), which is below the licensed power of 1.1 MW(t). The 6% difference allows for expected and observed instrument fluctuations at the normal full operating power of 1 MW(t) to occur without scramming the reactor unnecessarily. Section 13.2.2 of the conversion SAR shows that this set point is more than sufficient to prevent exceeding the reactivity insertion limit during non-pulsing operations and prevent the operator from inadvertently exceeding the licensed power.

Manual Scram: The manual scram must be functional at all times the reactor is in operation. It has no specified value for a scram set point. It is initiated by the reactor operator manually.

Preset Timer Scram: The preset timer ensures that the reactor power level will reduce to a low level after pulsing and preclude an unintentional restart or ramped increase to some equilibrium power.

High Voltage Scram: The high voltage scram must be set to initiate a scram before the high voltage for any of the three detectors reaches 25% or less of the nominal operating voltage. The loss of operating voltage down to this level is an indication of detector failure. Many measuring channels and safety systems are fundamentally based upon accurate response of the detectors.

Wide-Range Log Power Level Channel Interlock: The rod withdrawal prohibit interlock prevents the operator from adding reactivity in the following situations:

a) When the count rate on the wide-range log power channel falls below 2 cps, the count rate is insufficient to produce meaningful instrumentation response. If the operator were to insert reactivity under this condition, the period could quickly become very short and result in an inadvertent power excursion. A neutron source is added to the core to create sufficient instrument response that the operator can recognize and respond to changing conditions.
b) When the period/log test switch is out of the operate position, a false signal is fed into the signal chain for the wide-range log and wide-range linear channels, effectively rendering those technical specification required measuring channels inoperable.
c) When the detector current selector switch is out of the operate position, the signal for the selected detector is diverted to an ammeter, effectively rendering the selected technical specification required measuring channels inoperable.
d) When the fuel temperature selector switch is in the fourth position and not one of the three positions to read the thermal couples in the instrumented fuel element, the technical specification required measuring channel is effectively rendered inoperable.

Transient Rod Cylinder Interlock: This interlock prevents the application of air to the transient rod unless the rod is fully inserted. This will prevent the operator from pulsing the reactor in steady-state mode.

1 kW Pulse Interlock: The 1-kW permissive interlock is designed to prevent pulsing when wide range log power is above 1-kW. Section 4.7.10 of the conversion SAR shows that the peak temperature reached during the maximum $2.15 pulse in the bounding middle-of-life ICIT core will be <950°C for a pulse starting with fuel at an initial temperature of 20°C. The methodology clearly shows that if the initial temperature was higher, the resulting peak temperature must be lower. However, there has not been analysis or experiment to examine the relationship between pulsing at low power (i.e., <1.0 kW) when the temperature profile of the fuel is essentially isothermal, and pulsing at high power when the temperature profile in the fuel is centrally peaked. This interlock therefore prevents the reactor from being pulsed at power levels which produce measurably significant increases in fuel temperature above ambient pool temperature.

Shim, Safety and Regulating Rod Drive Circuit: The single rod withdrawal interlock prevents the operator from removing multiple control rods simultaneously such that reactivity insertions from control rod manipulation is done in a controlled manner. The analysis in section 13.2.2 of the conversion SAR shows that the reactivity insertion due to the removal rate of the most reactive rod or all the control rods simultaneously is still well below the reactivity insertion design limit of $2.15.

Shim, Safety and Regulating Rod Drive Circuit: In pulse mode, it is necessary to limit the reactivity inserted to less than the design limit of $2.15 as shown in section 4.7.10 of the conversion SAR. This interlock ensures that all pulse reactivity is due to only the transient rod while in pulse mode. Otherwise, any control rod removal in pulse mode would add to the inserted reactivity of the transient rod and create an opportunity for exceeding the reactivity insertion limit.

Transient Rod Cylinder Position Interlock: For the transient rod cylinder interlock, section 4.7.10 of the conversion SAR shows that the designed limiting reactivity insertion for the fuel is $2.15. This interlock limits transient rod reactivity insertions below this value. Furthermore, this interlock is designed such that if the electrical (i.e., limit switch) portion fails, a mechanical (i.e., metal bracket) will still keep the reactivity insertion below the criterion.

3.8.1 Reactivity Limits

Applicability. This specification applies to experiments installed in the reactor and its irradiation facilities.

Objective. The objective is to prevent damage to the reactor or excessive release of radioactive materials in the event of an experiment failure.

Specifications. The reactor shall not be operated unless the following conditions governing experiments exist:

a. The sum of the absolute values of the reactivity worths of all moveable experiments shall be less than $0.50;

b. The sum of the absolute values of the reactivity worths of all experiments shall be less than $2.15;

Basis. The reactivity limit of \$0.50 for movable experiments is designed to prevent an inadvertent pulse from occurring and to maintain a value below the shutdown margin. Movable experiments are by their very nature experiments in a position where it is possible for a sample to be inserted or removed from the core while critical. This value is also below the analyzed pulse design limit of \$2.15.

The reactivity worth limit of \$2.15 for all experiments is designed to prevent an inadvertent pulse from exceeding the design limit of \$2.15. This limit applies to movable, unsecured and secured experiments. Regardless of any other administrative or physical requirements, this limit has been shown to protect the reactor during the fuel's entire lifetime.

5.2 Reactor Coolant System

Applicability. This specification applies to the tank containing the reactor and to the cooling of the core by the tank water.

Objective. The objective is to assure that coolant water shall be available to provide adequate cooling of the reactor core and adequate radiation shielding.

Specifications.

a. The reactor core shall be cooled by natural convective water flow.

b. The tank water inlet and outlet pipes to the heat exchanger and to the demineralizer shall be equipped with siphon breaks not less than 14 feet above the top of the core.

c. A tank water level alarm shall be provided to indicate loss of coolant if the tank level drops 6 inches below normal level.

d. A bulk tank water temperature alarm shall be provided to indicate high bulk water temperature if the temperature exceeds 120°F (49°C).

Basis.

a. This specification is based on thermal and hydraulic calculations which show that the TRIGA® fuel in operational cores can operate in a safe manner at power levels up to 1.9 MW with natural convection flow of the coolant water.

b. In the event of accidental siphoning of tank water through inlet and outlet pipes of the heat exchanger or demineralizer system, the tank water level will drop to a level no less than 14 feet from the top of the core.

c. Loss-of-coolant alarm caused by a water level drop of no more than 6 inches provides a timely warning so that corrective action can be initiated. This alarm is located in the control room.

d. The bulk water temperature alarm provides warning so that corrective action can be initiated in a timely manner to protect the quality of the reactor tank. The alarm is located in the control room.

5.3 Reactor Core and Fuel

5.3.1 Reactor Core

Applicability. This specification applies to the configuration of fuel and in-core experiments.

Objective. The objective is to assure that provisions are made to restrict the arrangement of fuel elements and experiments so as to provide assurance that excessive power densities shall not be produced.

Specifications.

a. The core shall be an arrangement of TRIGA® uranium-zirconium hydride fuel-moderator elements positioned in the reactor grid plate.

b. The TRIGA® core assembly may consist of fuel elements.

c. The fuel shall be arranged in a close-packed configuration except for single element positions occupied by in-core experiments, irradiation facilities, graphite dummies, aluminum dummies, stainless steel dummies, control rods, and startup sources.

d. The reactor shall not be operated at power levels exceeding 1 kW with a core lattice position water filled, except for positions on the periphery of the core assembly.

e. The reflector, excluding experiments and irradiation facilities, shall be water or a combination of graphite and water.

Basis.

a. TRIGA® ZrH fueled cores have been in use for years and their characteristics are well documented. The Puerto Rico Nuclear Center, the Gulf Mark III cores and the Texas A&M core are or were operational and characteristics are available. Gulf has also performed a series of experiments using mixed cores. Analytic studies performed at OSTR for a variety of operational core arrangements indicate that such cores would safely satisfy all operational requirements.

b. Only LEU fuel elements are anticipated to be used.

c. In-core water-filled experiment positions have been demonstrated to be safe in the Gulf Mark III reactor. The largest values of flux peaking will be experienced in hydrogenous in-core irradiation positions. Various non-hydrogenous experiments positioned in element positions have been demonstrated to be safe in cores up to 2-MW operation.

d. For cases where one in-core position is water filled, except in the core periphery, the maximum reactor power level is reduced to 1 kW to ensure safe peak power generation levels in adjacent element positions.

e. The core will be assembled in the reactor grid plate which is located in a tank of light water. Water in combination with graphite reflectors can be used for neutron economy and the enhancement of irradiation facility radiation requirements.

5.3.2 Control Rods

Applicability. This specification applies to the control rods used in the reactor core.

Objective. The objective is to assure that the control rods are of such a design as to permit their use with a high degree of reliability with respect to their physical and nuclear characteristics.

Specifications.

a. The shim, safety, and regulating control rods shall have scram capability and contain borated graphite, B_4C powder or boron, with its compounds in solid form as a poison, in aluminum or stainless steel cladding. These rods may incorporate fueled followers which have the same characteristics as the fuel region in which they are used.

b. The transient control rod shall have scram capability and contain borated graphite or boron, with its compounds in a solid form as a poison in an aluminum or stainless steel cladding. The transient rod shall have an adjustable upper limit to allow a variation of reactivity insertions. This rod may incorporate an aluminum- or air-follower.

Basis. The poison requirements for the control rods are satisfied by using neutron absorbing borated graphite, B_4C powder or boron as its compounds. These materials must be contained in a suitable clad material such as aluminum or stainless steel to ensure mechanical stability during movement and to isolate the poison from the tank water environment. Control rods that are fuel-followed provide additional reactivity to the core and increase the worth of the control rod. The use of fueled-followers in the fueled region has the additional advantage of reducing flux peaking in the water-filled regions vacated by the withdrawal of the control rods. Scram capabilities are provided for rapid insertion of the control rods which is the primary safety feature of the reactor. The transient control rod is designed for rapid withdrawal from the reactor core which results in a reactor pulse. The nuclear behavior of the air- or aluminum-follower, which may be incorporated into the transient rod, is similar to a void.

5.3.3 Reactor Fuel

Applicability. This specification applies to the fuel elements used in the reactor core.

Objective. The objective is to assure that the fuel elements are of such a design and fabricated in such a manner as to permit their use with a high degree of reliability with respect to their physical and nuclear characteristics.

Specifications. TRIGA® Fuel Elements

The individual fuel elements shall have the following characteristics:

1. Uranium content: nominal 30 wt% enriched to a nominal 20% ^{235}U;
2. Hydrogen-to-zirconium atom ratio (in the ZrH_x): between 1.5 and 1.65;
3. Natural erbium content (homogeneously distributed): nominal 1.1 wt%;
4. Cladding: 304 stainless steel, nominal 0.020 inches thick; and
5. Identification: top pieces of fuel elements will have characteristic markings to allow visual identification of fuel elements.

Basis. The specifications for uranium wt% and enrichment represent maximum values for the fuel specification. The difference between these requirements and the fuel specification represent increases in power density of less than 5% which is well within the safety margin established for the safety limit.

The fuel specification for a single fuel element permits a minimum erbium content of about 5.6% less than the design value of 1.1 wt%. However, the quantity of erbium in the full core must not deviate from the design value by more than 3.3%. This variation for a single fuel element would result in an increase in fuel element power density of about 2%. Such a small increase in local power density would reduce the safety margin by approximately 2%.

The maximum hydrogen-to-zirconium ratio of 1.65 could result in a maximum stress under accident conditions in the fuel element cladding of about a factor of two greater than the value resulting from a hydrogen-to-zirconium ratio of 1.60. However, this increase in the cladding stress during an accident would not exceed the rupture strength of the cladding.

15 OTHER LICENSE CONSIDERATIONS

15.1 Prior Utilization of Reactor Components

The conversion of the OSTR from HEU FLIP fuel to LEU fuel will be accomplished using new, unirradiated, recently fabricated LEU fuel that has been previously approved by the NRC.

15.2 License Conditions

For the conversion, there are two anticipated stages. The first requires receipt of the new LEU fuel until such time as it is appropriate to issue the order for conversion. The second requires possession and use of the LEU fuel and possession only for the HEU fuel (i.e., the conversion). For the first stage, the order to possess, but not use, the new LEU fuel will require an amendment to the license by May 1, 2008. Specifically:

amend (new) section 2.b(5) of the license to read:

> Pursuant to the Act and 10 CFR Part 70, "Domestic Licensing of Special Nuclear Material," to receive and possess up to 16.30 kilograms of contained uranium-235 at enrichment less than 20 percent in the form of non-power reactor fuel in connection with operation of the reactor; and to possess, but not separate, such special nuclear material as may be produced by the operation of the facility.

For the second stage, the order for conversion from HEU to LEU will require three amendments to the license by September 1, 2008. These amendments are for possession and use of the new LEU fuel (i.e. 100 LEU fuel elements), possession only of the current HEU fuel and a new value for the maximum reactivity insertion. Specifically:

amend section 2.b(2) of License R-106 to read:

> Pursuant to the Act and 10 CFR Part 70, "Domestic Licensing of Special Nuclear Material," to receive, possess and use up to 16.30 kilograms of contained uranium-235 at enrichment less than 20 percent in the form of non-power reactor fuel in connection with operation of the reactor; and to possess, but not separate, such special nuclear material as may be produced by the operation of the facility.

amend section 2.b(5) of the license to read:

> Pursuant to the Act and 10 CFR Part 70, "Domestic Licensing of Special Nuclear Material," to receive and possess up to 12.83 kilograms of contained uranium-235

at equal to or greater than 20 percent enrichment and other special nuclear material produced by operation of the facility in the form of non-power reactor fuel until this fuel is removed from the facility.

amend section 2.c(1) of the license to read:

The licensee may operate the facility at steady state power levels not in excess of 1100 kilowatts (thermal) and, in the pulse mode, with reactivity insertions not to exceed $2.15.

15.3 Decommissioning

The conversion of the OSTR from HEU FLIP fuel to LEU fuel has no effect on the OSTR decommissioning plan.

APPENDIX A, RELOAD AND STARTUP GUIDELINES

The LEU refueling procedure and startup plan shall incorporate, at a minimum, all of the following guidelines.

- All HEU fuel, including in-core fuel elements, control rod followers, instrumented fuel element(s) and fuel elements stored in the in-tank storage racks shall be removed from the reactor tank prior to insertion of any LEU fuel elements into the reactor tank.
- Prior to loading any LEU fuel in the reactor core, a neutron source and all required graphite reflector elements shall be installed in the core.
- The criticality state of the new core shall be monitored using standard 1/M plots where M is the ratio of the count rate with n fuel elements in the core divided by the initial count rate. The count rate shall be obtained from an installed fission chamber via a counter-scaler. Count rates for the 1/M plot shall be obtained with all four control rods fully withdrawn.
- The initial count rate shall be obtained when the neutron source, three fuel-followed control rods and one air-followed control rod are installed in the core. Satisfactory control rod motion and control rod scram times shall be obtained after the control rods are installed in the core and before any additional fuel is installed in the core.
- After the initial count rate has been obtained, install the IFE in the B-ring. Then install five fuel elements in the remaining B-ring positions. Then install ten fuel elements in the vacant C-ring positions. Obtain a count rate and update the 1/M plot.
- Install eight fuel elements in positions D-2 through D-9. Obtain a count rate and update the 1/M plot.
- Install eight fuel elements in the positions D-11 through D-18. Obtain a count rate and update the 1/M plot.
- Continue adding fuel elements to the E-ring, and then to the F-ring once the E-ring is full. When adding fuel to the F-ring, load the first element in position F-1, and then proceed by filling adjacent positions in a clockwise manner. Add fuel elements in groups of no more than four fuel elements at a time until the 1/M plot indicates that the reactor is sub-critical by about ten fuel elements (with all rods withdrawn). Obtain a count rate and update the 1/M plot after each group addition of fuel elements. After filling the E-ring

and before proceeding to fill the F-ring, re-verify satisfactory control rod motion and control rod scram times.

- Once the 1/M plot indicates the reactor is subcritical by about ten fuel elements, continue adding fuel elements to the E-ring, and then the F-ring in groups of no more than two fuel elements at a time until the 1/M plot indicates that the reactor is sub-critical by about five fuel elements. Obtain a count rate and update the 1/M plot after each addition of two fuel elements.
- Continue adding fuel elements to the E-ring, and then the F-ring one at a time until the 1/M plot indicates that the reactor will be supercritical after addition of the next fuel element. Obtain a count rate and update the 1/M plot after addition of each fuel element.
- Add a fuel element and verify the reactor is supercritical with all control rods withdrawn. Calculate the core excess with all control rods withdrawn using the period method.
- Perform a rough calibration of the control rods using the rod drop method.
- Add fuel elements in groups of four or less. After the addition of each group, perform a rough calibration of the control rods using the rod drop method. Check shutdown margin after the addition of each group. Continue loading the core until the shutdown margin is approximately $1.00.
- Calibrate all four control rods using the period method.
- Measure the reactivity worth of fuel elements in the F-ring. Add additional fuel elements to achieve the operational core which has the desired excess reactivity and shutdown margin conditions.
- Re-calibrate all control rods using the period method. Re-calculate excess reactivity and shutdown margin.
- Measure the reactivity worth of at least two elements per ring.
- Calibrate the fuel element temperature measurement channel.
- Perform channel tests of all safety channels and interlocks listed in the Technical Specifications which can be performed without operating at full power.
- Perform a power calibration at or near 500 kW.
- Perform the initial increase to 100% power. Increase power in stepwise increments. Record all flux channels and fuel temperature indications at each step.

- Repeat the stepwise increase to full power and record the same indications as above. Due to clad deformation during the initial increase to full power and the resultant fuel to clad gap increase, fuel temperatures are expected to be higher than during the initial increase to 100% power.
- Calculate the power coefficient of reactivity and fuel element temperature coefficient of reactivity.
- Perform channel tests of the remainder of all safety channels and interlocks listed in the Technical Specifications.
- Perform a power calibration at 1000 kW
- Perform pulse mode operational tests.

APPENDIX B, STARTUP ACCEPTANCE CRITERIA

B.1 Initial Criticality

The minimum critical mass shall be defined as the minimum number of fuel elements required for the reactor to have an effective multiplication factor greater than or equal to 1.0 with all four control rods fully withdrawn. The MCNP5 model predicts the minimum critical core configuration will have 69 fuel elements (section 4.5.2) with the F-Ring being loaded counterclockwise starting from the F-1 position. With all control rods withdrawn, this configuration is expected to be supercritical by $0.10. The erbium content of the fuel is specified to be 1.1 +0.0/-0.3 mass percent, so the actual minimum critical core is expected to have less than 69 total fuel elements.

Acceptance Criteria: The minimum critical mass is expected with a fuel loading between 60 and 70 fuel elements.

B.2 Control Rod Worth by Rod Drop Method

Control rod worth is first estimated by the rod drop method immediately after initial criticality is reached, before additional fuel is added.

Acceptance Criteria: The worth of the control rods is expected to be between $1.50 and $4.00, depending on the type of rod and its location in the core.

B.3 Control Rod Worth by Period Method

Control rod worth is first estimated by the period method when the core is loaded to a shutdown margin of approximately $1.00. Control rod worth is again measured by the period method when the operational core is installed.

Acceptance Criteria: For the operational core, the worth of the control rods is expected to be between $1.50 and $4.00, depending on the type of rod and its location in the core.

B.4 Shutdown Margin and Excess Reactivity

Excess reactivity is the amount of positive reactivity the core would have if all control rods were withdrawn. Shutdown margin is the amount of negative reactivity in the core with the highest worth rod fully withdrawn and all other rods fully inserted.

Acceptance Criteria: Excess reactivity and shutdown margin shall be calculated for an operational core in all allowed operating modes. Calculations shall be based on measurements taken on a cold, clean core. Excess reactivity and shutdown margin shall be within the allowed values of the Technical Specifications.

B.5 Power and Temperature Coefficient

The power coefficient is the net change in reactivity between some low power and some higher power divided by the net change in power. The temperature coefficient is the net change in reactivity between some low power and some higher power divided by the net change in temperature corresponding to the low and higher power. Power and temperature coefficients shall be determined over several different power intervals. Power and temperature coefficients shall be determined during power changes subsequent to the initial power increase to 100 percent.

Acceptance Criteria: The power and temperature coefficients shall be verified to be negative over all operating ranges. The power defect (the reactivity change between power sufficiently low that no fuel heating is occurring and full power) shall be between $1.50 and $3.00.

B.6 Reactor Power Calorimetric Calibration

A reactor power calorimetric calibration shall be performed subsequent to the initial power increase to 100 percent. The calorimetric calibration shall be performed using the existing OSTROP.

Acceptance Criteria: After completion of the power calibration, including instrument adjustment, the linear, safety and percent power channels shall indicate between 99.0 and 101.0 percent at full reactor power of 1.0 MW.

B.7 SCRAM Tests

SCRAM limits are set at 106% of full power to allow flexibility to operate up to 1.0 MW, but to prevent exceeding licensed power of 1.1 MW.

Acceptance Criteria: The Safety Channel SCRAM shall be activated at an indicated power no greater than 106 percent on the Safety channel. The Percent Power channel SCRAM shall be activated at an indicated power no greater than 106 percent on the Percent channel.

B.8 Pulse Mode Tests

To characterize pulse behavior, a series of pulses starting at about $1.10 and proceeding in increments of about $0.10 shall be performed. The maximum pulse reactivity insertion limit of \$2.15 shall not be exceeded. Peak power, peak temperature and integrated power data shall be recorded from console instruments. Additionally, power and temperature data should be digitally recorded at high speed in order to confirm console data, and to allow determination of pulse width. Note that the graphs specified in the acceptance criteria may depart from linearity at higher reactivity insertions due to the fact that longer rod ejection times are experienced during the larger reactivity insertions because of the increased travel distances.

Acceptance Criteria: The graph of peak temperature vs. prompt reactivity should show a linear dependence. The graph of integrated power vs. prompt reactivity should show a linear dependence. The graph of peak power vs. (prompt reactivity)^2 should show a linear dependence.

REFERENCES

1. HEU Safety Analysis Report for the Oregon State TRIGA® Reactor, submitted in conjunction with the OSU license renewal application of October 5, 2004, as supplemented.
2. NUREG-1282, "Safety Evaluation Report on High-Uranium Content Low-Enriched Uranium-Zirconium Hydride Fuels for TRIGA® Reactors," USNRC, August 1987
3. Ibid.
4. M. T. Simnad, "The U-ZrH_x Alloy: Its Properties and Use in TRIGA® Fuel," Nuclear Engineering and Design **64** (November 1980), 403-422.
5. NUREG -1282, op. cit.
6. Ibid.
7. Ibid.
8. Ibid.
9. "MCNP—A General Monte Carlo N-Particle Transport Code, Version 5," LA-CP-03-0245, F. B. Brown, Ed., Los Alamos National Laboratory (2003).
10. "The REBUS-MCNP Linkage," J. G. Stevens, Argonne National Laboratory (Draft).
11. Bretscher, M., "β_{eff}/l_p for Water-Reflected Fresh Critical Cores of the Oak Ridge Research Reactor Reflected by Water," RERTR Program, Argonne National Laboratory, July 31, 1986.
12. M. T. Simnad, F. C. Foushee, and G. B. West, "Fuel Elements for Pulsed TRIGA® Research Reactors," *Nuclear Technology* **28** (1976) 31-56.
13. RELAP5-3D Code Development Team, "Volume 1: code structure, system models, and solution methods, in RELAP5-3D code manual'" 2005, Idaho National Laboratory: Idaho Falls, Idaho. p. 600.
14. Bene, J. V. D., "TRIGA® Reactor Thermal-Hydraulics Study, STAT-RELAP Comparison," General Atomics Report, to be published.
15. Top Gridplate, TRIGA® Mark III, General Atomics Drawing T13S210J106 rev. C.
16. Todreas, N. E., Kazimi, M. S., "Nuclear Systems II: Elements of Thermal Hydraulic Design," Vol. 2, 2001. Taylor and Francis Group LLC 506, New York.
17. Reflector Assembly, Oregon, General Atomics Drawing T2D210J110 rev. A.
18. Groeneveld, D. C., et. al., "The CHF Lookup Table," Nuclear Engineering and Design, 2007, p. 1-24.

19. Bernath, L., "A Theory of Local Boiling Burnout and its Application to Existing Data," Chemical Engineering Progress Symposium. Series No. 30, Volume 56, pp. 95-116 (1960).

20. OSTR HEU SAR, op. cit.

21 Grove Engineering, MicroShield version 5.05, March 2003.

22. Credible Accident Analyses for TRIGA® and TRIGA®-fueled Reactors, NUREG/CR-2387, PNL-4028, April 1982.

23. USNRC, "Guidelines for Preparing and Reviewing Applications for the Licensing of Non-Power Reactors, Standard Review Plan and Acceptance Criteria", NUREG 1537, Part 2, Section 13, February 1996.

24. M. T. Simnad, "The U-ZrH_x Alloy: Its Properties and Use in TRIGA® Fuel," E-117-833, GA Technologies, Inc., San Diego, CA, February 1980.

25. Regulatory Guide 1.145, "Atmospheric Dispersion Models for Potential Accident Consequence Assessments at Nuclear Power Plants," U.S. Nuclear Regulatory Commission, August 1979.

26. Stationary Neutron Radiography System, Final Safety Analysis Report, McClellan Air Force Base, Sacramento, CA, August 1990.

27. Safety Analysis Report for the Torrey Pines TRIGA® Mark III Reactor, GA-9064, General Atomics, January 5, 1970.

28. Safety Analysis Report for the TRIGA® Reactor Facility, University of Texas at Austin, May 1991.

29. Lamarsh, J. R., Introduction to Nuclear Engineering, 2nd Edition, Addison Wesley, 1983,. page 72.